Hungarian Academy of Sciences Doctoral Dissertation

TWO NOVEL NEUROPEPTIDES WITH MATERNAL FUNCTIONS

Dr. Árpád Dobolyi, PhD

Semmelweis University
Department of Anatomy, Histology and Embryology
Laboratory of Neuromorphology

Budapest, 2013

TABLE OF CONTENTS

1. ABSTRACT

The discovery and functional characterization of 2 neuropeptides are reported. Tuberoinfundibular peptide of 39 residues (TIP39) was previously purified as the endogenous ligand of the so far orphan parathyroid hormone 2 receptor (PTH2 receptor) but we first identified the gene that encodes TIP39, and discovered its maternal functions. The other neuropeptide is amylin, whose gene had been described previously and shown to be expressed in the pancreas. We first determined its expression in the brain, therefore, the status of amylin as a neuropeptide and provided strong evidence for its involvement in maternal regulations.

TIP39 is predominantly expressed in the brain, in 3 different sites. While the expression level of TIP39 is diminished postnatally, its expression is induced in mother rats in 2 of the 3 sites of its expression, the posterior intralaminar complex of the thalamus (PIL), and the medial paralemniscal nucleus (MPL). The distribution of TIP39 fibers is similar to that of PTH2 receptor in the brain. The PIL projects mostly to hypothalamic brain regions such as the preoptic area and the arcuate nucleus while the MPL provides TIP39 predominantly to brainstem auditory regions. We also showed that the PIL receives ascending input from the spinal cord while the MPL has afferent neuronal connections with auditory brain regions. TIP39 neurons in both the PIL and MPL were activated by pup-exposure in mother rats. Suckling-induced elevation of serum prolactin was reduced by a PTH2 receptor antagonist applied into the lateral ventricle or locally into the arcuate nucleus but not the preoptic area by means of focal virus infection. In turn, local PTH2 receptor antagonist in the preoptic area reduced maternal motivation without affecting prolactin levels. These findings are in agreement with literature data that the preoptic area is the central regulator of maternal behaviors while prolactin secretion required for lactation is regulated by neurons in the arcuate nucleus. The results also provide the long sought-after reflex arch how suckling information reaches the hypothalamus to affect maternal behaviors and hormonal changes. To find targets of TIP39 in the preoptic area, a microarray study was performed, which identified amylin as a novel neuropeptide expressed only in the maternal preoptic area. Amylin neurons are also activated by suckling. They have a distribution similar to that of TIP39 fibers within the preoptic area, and are closely apposed by TIP39 terminals. Furthermore, the maternal induction of amylin is reduced in mice lacking the PTH2 receptor.

The 2 newly identified maternal peptides in the brain are unique among neuropeptides in the high degree of induction in mothers. Together with their receptor, they represent important new mechanisms in the control of central maternal adaptation and future targets for the development of drugs affecting specific maternal disorders such as postpartum depression.

2. LIST OF ABBREVIATIONS

ac	anterior commissure
AcN	accumbens nucleus
AH	anterior hypothalamic area
AHi	amygdalo-hippocampal transition zone
al	ansa lenticularis
AM	anteromedial thalamic nucleus
AN	accumbens nucleus
AON	anterior olfactory nucleus
APT	anterior pretectal nucleus
aq	cerebral aqueduct
Arc	arcuate nucleus
Au1	primary auditory cortex
AuV	secondary auditory cortex, ventral area
AVPe	anteroventral periventricular nucleus
A7	A7 noradrenergic cell group
A11, A13	A11, A13 dopaminergic cell group
BDA	biotinylated dextran amine
BL	basolateral amygdaloid nucleus
BLA	basolateral amygdaloid nucleus, anterior part
BMA	basomedial amygdaloid nucleus, anterior part
BNST	bed nucleus of the stria terminalis
BNSTv	ventral subdivision of the BNST
BSTMPM	posteromedial part of the medial subdivision of the BNST
cAMP	cyclic adenosine 3 5'-monophosphate
ca	cerebral aqueduct
cc	corpus callosum
CeA	central amygdaloid nucleus
CG	periaqueductal central gray
CGRP	calcitonin gene-related peptide
CIC	central nucleus of the inferior colliculus
CM	central medial thalamic nucleus
CP	caudate putamen
Cu	cuneate nucleus
CuF	cuneiform nucleus
CoA	cortical amygdaloid nucleus
cp	cerebral peduncle
CRH	corticotropin-releasing hormone
CTB	cholera toxin β subunit
cu	cuneate fasciculus
DA	dopamine

DG	dentate gyrus
DH	dorsal horn
Dk	nucleus of Darkschewitsch
dlf	dorsolateral fasciculus
DM(H)	dorsomedial hypothalamic nucleus
DpMe	deep mesencephalic nucleus
DR	dorsal raphe nucleus
DTg	dorsal tegmental nucleus
ECIC	external cortex of the inferior colliculus
EGP	external globus pallidus
f	fornix
fr	fasciculus retroflexus
FS	fundus striati
GABA	γ-amino-butyric acid
GAD	glutamic acid decarboxylase
GAPDH	glyceraldehyde 3-phosphate dehydrogenase
GFP	green fluorescent protein
GnRH	gonadotropin-releasing hormone
Gr	gracile nucleus
Hipp	hippocampus
IC	inferior collicle
IGP	internal globus pallidus
ILL	intermediate nucleus of the lateral lemnsicus
Inf	infundibular nucleus
IPF	interpeduncular fossa
KF	Kölliker-Fuse nucleus
L2	lamina 2 of the dorsal horn
LG	lateral geniculate body
LH	lateral hypothalamic area
ll	lateral lemniscus
LPAG	periaqueductal gray, lateral subdivision
LS	lateral septal nucleus
LSv	ventral subdivision of the lateral septal nucleus
LV	lateral ventricle
mcp	middle cerebellar peduncle
MD	mediodorsal thalamic nucleus
me	median eminence
MeA	medial amgydaloid nucleus
mfb	medial forebrain bundle
MG	medial geniculate body
MGN	medial geniculate nucleus
ml	medial lemniscus

mlf	medial longitudinal fasciculus
MMG	medial nucleus of the medial geniculate body
MMN	medial mamillary nucleus
MPA	medial preoptic area
MPL	medial paralemniscal nucleus
MPN	medial preoptic nucleus
mt	mamillothalamic tract
M5	motor trigeminal nucleus
NAcc	nucleus accumbens
och, ox	optic chiasm
OT	olfactory tubercle
ot	optic tract
PAG	periaqueductal gray
PB	phosphate buffer
PBG	parabigeminal nucleus
PBL	lateral parabrachial nucleus
pc	posterior commissure
Pe	hypothalamic periventricular nucleus
PF	parafascicular thalamic nucleus
PH	posterior hypothalamic nucleus
PIL	posterior intralaminal complex of the thalamus
Pir	piriform cortex
Pn	pontine nuclei
PnO	pontine reticular nuclei
Po	posterior thalamic nucleus
POA	preoptic area
PoT	triangular subdivision of the posterior thalamic nucleus
PP(N)	peripeduncular nucleus
PPTg	pedunculopontine tegmental nucleus
PrC	precommissural nucleus
Prh	perirhinal cortex
PRL	prolactin
PTH	parathyroid hormone
PTHrP	parathyroid hormone-related peptide
Pu	putamen
Pul	pulvinar thalami
PVG	periventricular gray of thalamus
PVN	hypothalamic paraventricular nucleus
PVT	paraventricular thalamic nucleus
py	pyramidal tract
R	red nucleus
Re	reuninens thalamic nucleus

Reth	retroethmoid nucleus
rs	rubrospinal tract
RM	nucleus raphe magnus
RR	retrorubral nucleus
Rt	reticular thalamic nucleus
Sag	sagulum nucleus
SC	superior colliculus
SCh	suprachiasmatic nucleus
scp	superior cerebellar peduncle
SI	susbstantia innominata
sm	stria medullaris
SN	substantia nigra
SO	supraoptic nucleus
SOC	superior olivary complex
sod	supraoptic decussations
SPA	subparafascicular area
SPF	subparafascicular nucleus
SPFm	subparafascicular nucleus, magnocellular part
SPFp	subparafascicular nucleus, parvicellular part
Sp5	spinal trigeminal nucleus
STh	subthalamic nucleus
Sub	subiculum
TIP39	tuberoinfundibular peptide of 39 residues
TH	tyrosine hydroxylase
TIDA	tuberoinfundibular dopaminerg neurons
TRH	thyrotropin releasing hormone
VA	ventroanterior thalamic nucleus
VB	ventrobasal complex of the thalamus
VLL	ventral nucleus of the lateral lemiscus
VMG	ventral nucleus of the medial geniculate body
VMH	hypothalamic ventromedial nucleus
VPL	ventral posterolateral thalamic nucleus
VPM	ventral posteromedial thalamic nucleus
VPPC	ventral parvicellular posteromedial thalamic nucleus
VTA	ventral tegmental area
ZI	zona incerta
3V	third ventricle
4n	trochlear nerve
4V	fourth ventricle
5n	trigeminal nerve
5th	root of the trigeminal nerve
7n	facial nerve

3. INTRODUCTION

3.1. Significance of the topic

There are several reasons why studying the maternal nervous system is important. First, motherhood is an outstanding element of humanity, one that has attracted artists for centuries and has crucial significance in society. However, its scientific investigation lags behind its importance. Second, the maternal brain is a model of changes of the adult nervous system. The most remarkable adult physiological and behavioral changes take place during motherhood. Finally, a dam (rodent mother) represents an easily reproducible subject to model emotional motivation and social interactions. Maternal instinct to take care of the pups could also be considered as a model of love and self-sacrifice, feelings that are difficult to approach experimentally. Furthermore, the dysfunctions of maternal adaptations could also be studied in animal models, which could lead to the understanding of postpartum depression, the most frequent psychiatric disorder after childbirth with a prevalence rate of 10% to 15% (Abou-Samra et al., 1992; Mallikarjun and Oyebode, 2005). The high percentage of depression in the postpartum period and the deteriorated mother-infant communication as an early sign of maternal depression (Breese McCoy, 2011) suggest a causal relationship between dysfunctions of maternal adaptation and the onset of depression.

Neuropeptides are signaling molecules in the nervous system and typically have slow actions but play important neuromodulatory functions during adaptive processes. Therefore, they represent a group of regulatory molecules, which could have important maternal functions in the female brain. Indeed, this aspect of some peptides has been intensively investigated in the past but none of them has been shown to be selectively expressed in the maternal brain. Therefore, we focused our attention to peptides that – at least in some brain sites – demonstrate markedly enhanced expression in the postpartum period as they can reveal important mechanisms of regulations in the maternal brain.

3.2. Maternal alterations in brain physiology

Behavioral, endocrine, and psychological changes in mothers represent one of the most profound physiological alterations in the adult central nervous system (Fig.1). Experimental models of maternal behaviors are well established in rodents as control females avoid or even hurt pups while mothers take care of them: retrieve them in the nest, nurse them, perform anogenital licking of pups etc (Numan and Insel, 2003). Additional emotional changes include maternal aggression towards intruders, decreased anxiety in general, and reduced

responsiveness of the hypothalamo-pituitary-adrenal axis in stress situations (Carter et al., 2001; Neumann, 2003). Some other behavioral changes support the increased food and fluid intake required for lactation (Knobil and Neill, 2006). Major endocrine alterations include prolactin and oxytocin release to support lactation, and the suppression of gonadotropin-releasing hormone (GnRH) secretion leading to lactational anoestrous.

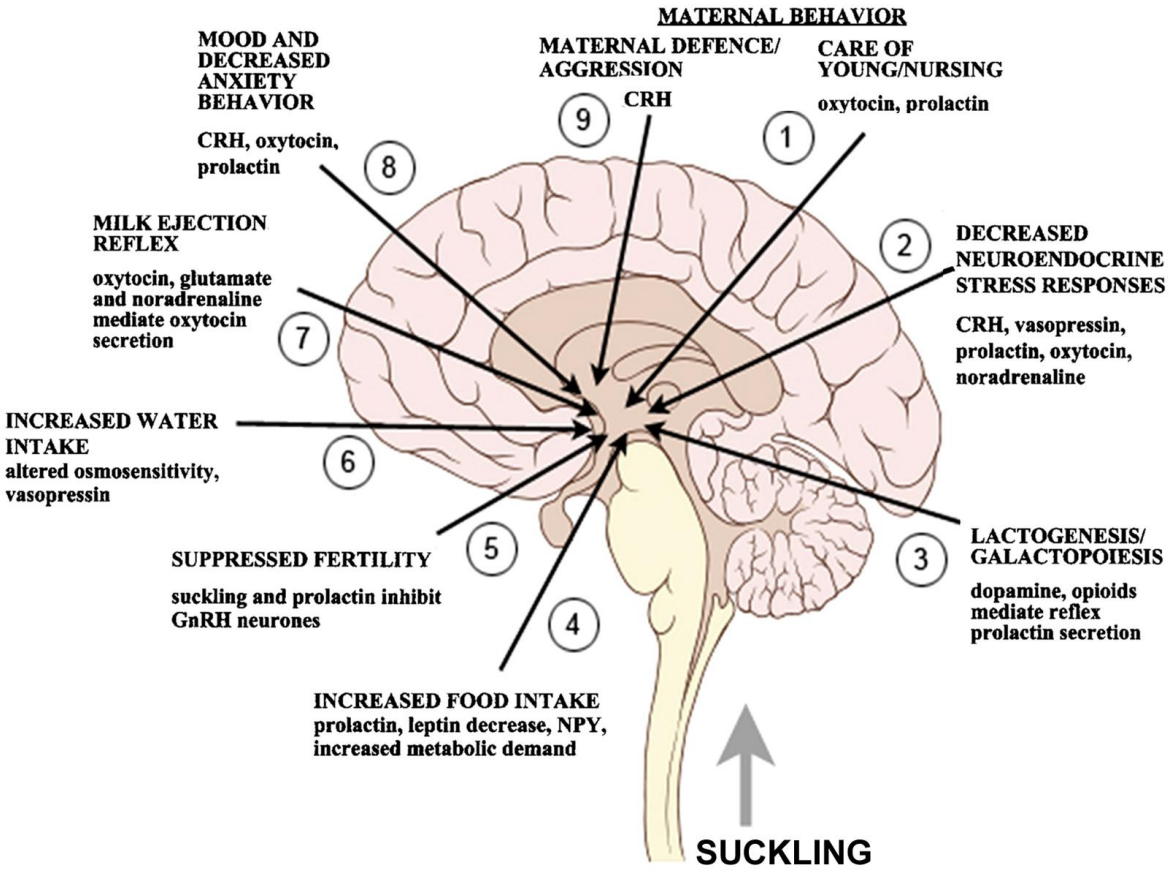

Fig. 1. The summary of adaptive responses to motherhood (Russell et al., 2001).

The mechanisms of maternal adaptations are not well established but are not likely to be simply mediated by hormonal changes. Although the behavioural changes are initiated by hormonal alterations in the last days of pregnancy (Bridges, 1996; Siegel, 1986) decreased levels of these hormones are detected during lactation (Lamming, 1994). In addition, the full range of maternal behaviors can be induced by prolonged pup exposure even in ovariectomized virgin females. These maternally sensitized rats do not lactate and provide a model to separate metabolic regulations from regulations of maternal behaviors (Rosenblatt,

1967). Somatosensory inputs derived from the pups play the most important role in sensitization (Stern, 1989). The same somatosensory inputs are thought to maintain maternal behaviours in dams after parturition (Febo et al., 2008). Lesion and microstimulation studies suggested that the reflex arch ascends conveying information from the nipples travels through the lateral mesencephalic tegmentum and enter the zona incerta ventromedial to the medial geniculate body (Dubois-Dauphin et al., 1985; Juss and Wakerley, 1981; Tindal and Knaggs, 1977; Wakerley et al., 1978). Excitotoxic lesions of this area blocked the milk-ejection reflex (Hansen and Kohler, 1984) and c-fos expression was detected here in lactating mothers (Lin et al., 1998) suggesting relay of the pathway in this position. It remained to be established if this pathway participates only in the neuroendocrine responses of prolactin and oxytocin release or also in more general maternal influences on brain adaptations.

The regulation and coordination of maternal adaptations take place in the central nervous system. A number of different approaches support that the preoptic area plays a crucial role in the initiation and maintenance of maternal behaviours. Large electrical as well as axon-sparing excitotoxic lesions of the MPOA eliminate all maternal behaviours without affecting other, e.g. feeding behaviours (Numan and Woodside, 2010) and similar effects were found following temporal pharmacological inactivation of MPOA (Arrati et al., 2006; Pereira and Morrell, 2009). In contrast to lesions, electrical stimulation of the MPOA increased maternal responsiveness (Morgan et al., 1997). In addition, brain activity is elevated in the MPOA in response to pup exposure based on c-fos (Li et al., 1999b; Lonstein et al., 1998b), 2-deoxyglucose (Del Cerro et al., 1995) and fMRI techniques (Febo et al., 2005). Subsequent lesion and activation studies suggest that other brain regions may also be involved in specific aspects of maternal behaviors including the lateral septum, the bed nucleus of the stria terminalis, the medial and cortical amygdaloid nuclei, the anteroventral periventricular nucleus, hypothalamic paraventricular nucleus, parts of the periaqueductal gray, the accumbens nucleus and the ventral tegmental area (Fig. 2).

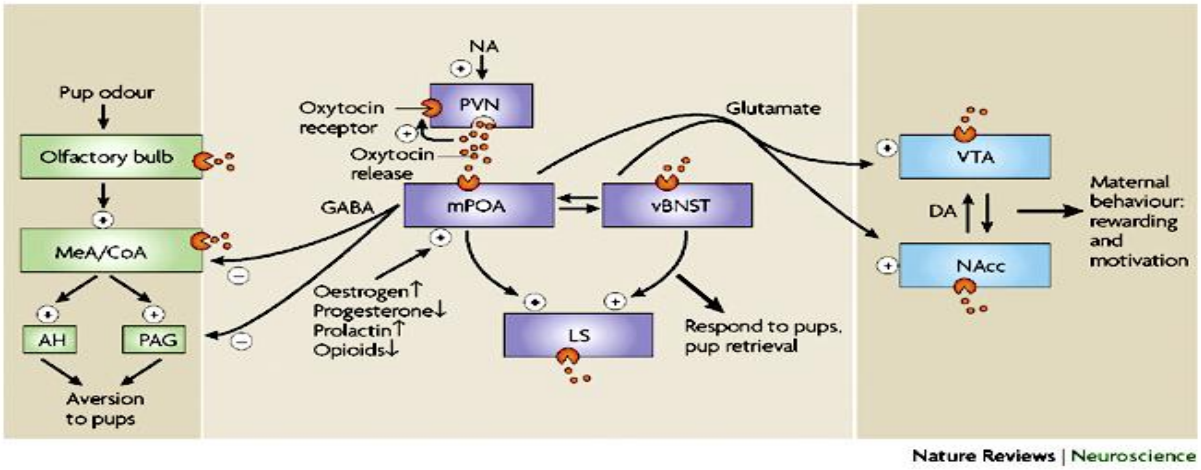

Fig. 2. Brain centers involved in maternal behaviors and motivation (Brunton and Russell, 2008). Abbreviations: AH – anterior hypothalamic area; CoA – cortical amygdaloid nucleus; DA – dopamine; MeA - medial amygdaloid nucleus; mPOA – medial preoptic area; NAcc – accumbens nucleus; PAG – periaqeductal gray; PVN – hypothalamic paraventricular nucleus; vBNST – ventral subdivision of the bed nucleus of the stria terminalis; VTA – ventral tegmental area.

3.3. Neuropeptides

Neuropeptides consist of 3-50 amino acids (aa) encoded by the genome. Neuropeptides are always cleaved enzymatically by prehormone convertases in the endoplasmic reticulum and the Golgi apparatus, and often undergo additional posttranslational modifications such as amidation, pyroglutamate formation, etc. (Hökfelt et al., 2000). Neuropeptides are then packed into so-called dense core vesicles and transported to the presynaptic terminals (Bean et al., 1994). Importantly, these vesicles are not released by single action potentials or low-frequency stimulation even though small vesicles containing neurotransmitters are released by this stimulus at the same synapse (Hökfelt et al., 1992). Thus, neuropeptides typically have no effect on the basal function of the network (Hökfelt et al., 1987). In turn, high-frequency stimulation leads to the secretion of a large amount of neuropeptides, which can act locally or more distantly by diffusion. Neuropeptides always act *via* high-affinity G-protein coupled receptors (Baraban and Tallent, 2004). There is not a single neuropeptide the receptor of which is a ligand-gated ion channel in vertebrates. Some proteins considered neuropeptides by some researchers, e.g. prolactin and leptin, have single transmembrane domain tyrosine-kinase receptors. However, it is more logical to not consider

these signal proteins as neuropeptides. Thus, all neuropeptides possess 7 transmembrane domain receptors, which belong to 2 subgroups (Fredholm et al., 2007). Typically, the receptors of small neuropeptides (3-30 aa) are class I, rhodopsin-like G-protein coupled receptors while larger neuropeptides (25-50 aa) possess class II, secretin-like G-proteins coupled receptors (Jacoby et al., 2006). Neuropeptides are eliminated from the extracellular space by proteolytic degradation. After neuropeptides are released from the presynaptic terminal, they are not taken back by the terminals and the large dense core vesicles cannot be replenished (Bean et al., 1994). Instead, newly synthesized neuropeptide packages arrive from the cell body, a process, which takes a significant amount of time, several hours or even days (van den Pol, 2012). These characteristics require a significant induction of neuropeptide expression during recruitment, e.g. in the postpartum period for maternal neuropeptides.

3.4. Neuropeptides in maternal regulations

A number of neuropeptides play important roles in different aspects of maternal regulations:

Prolactin secretion into the circulation is essential to the production of milk in the mammary gland of lactating mothers (Neville, 2006). Prolactin also stimulates maternal behaviors, reduces the stress response and anxiety, participates in the suppression of fertility, and the regulation of appetite and body weight (Grattan and Kokay, 2008). Prolactin release from anterior pituitary lactotrop cells is primarily regulated by inhibitory dopamine neurons in the hypothalamus (Freeman et al., 2000) but is also affected by several neuropeptides (Bodnar et al., 2009). The regulatory roles of *thyrotropin releasing hormone* (Lyons et al., 2010; Yamada et al., 2006) and *opioid peptides* (Arbogast and Voogt, 1998; Callahan et al., 2000; Selmanoff and Gregerson, 1986; Tavakoli-Nezhad and Arbogast, 2010) are best established. The expression level of thyrotropin releasing hormone is increased (Fjeldheim et al., 2005) while that of the opioid peptides are decreased during lactation (Kim et al., 1997).

Suckling also evokes the secretion of *oxytocin* synthesized in the paraventricular hypothalamic nucleus and secreted from the neural lobe of the pituitary to induce milk ejection (Burbach et al., 2006; Wakerley et al., 1978). However, oxytocin produced and released in different brain sites including the medial and central amygdaloid nuclei is an established regulator of emotional and social behaviors and also plays a role in the regulation of maternal behaviors and reduced responsiveness of the HPA axis (Neumann, 2008; Slattery and Neumann, 2008; Terenzi and Ingram, 2005).

The demand of milk production creates negative energy balance, which, however, does not account for the entire hyperphagia during lactation (Smith and Grove, 2002; Xu et al., 2009). Increased prolactin levels and the suckling stimulus may also play a role in the increased food intake (Chen and Smith, 2003; Woodside, 2007). Peptide products of proopiomelanocortin and other peptides involved in food intake regulation (Meister, 2007; Palkovits, 2003) may play a role in the elevated food intake during pregnancy and lactation (Crowley et al., 2007; Ladyman et al., 2010). *Neuropeptide Y* induced in the dorsomedial hypothalamic nucleus (Chen and Smith, 2003) may have a specific role in sustaining the chronic hyperphagia of lactation (Xu et al., 2009) and it might also participate in the suppression of *GnRH* secretion during lactation (Pralong, 2010; Wojcik-Gladysz and Polkowska, 2006).

The suppression of GnRH secretion leading to reduced estrogen serum level and lactational anoestrous is characteristic in mothers (McNeilly, 2006). The central common pathways for the regulation of GnRH neurons are kisspeptin neurons (Oakley et al., 2009) located in the anteroventral periventricular and arcuate nuclei (Lehman et al., 2010). All factors influencing estrogen levels, such as stress, suckling, body weight, estrogen itself, etc. are proposed to act via the kisspeptin system (Pineda et al., 2011). Lactational anoestrus is primarily driven by the suckling stimulus during the first half of lactation and by negative energy balance during its second half (Tsukamura and Maeda, 2001). The kisspeptin system was suggested to mediate both actions (Smith et al., 2010; Topaloglu et al., 2010)) at least partially through reduced kisspeptin expression in the postpartum period (Yamada et al., 2007).

Stress coping strategies are also altered during late pregnancy and postpartum: mother rats demonstrate decreased anxiety and reduced responsiveness of the hypothalamo-pituitary-adrenal (HPA) axis including diminished synthesis and release of *corticotropin releasing hormone* (Carter et al., 2001; Neumann, 2001; 2003). Suckling was suggested to drive the hyporesponsiveness of the HPA axis in the postpartum period (Brunton et al., 2008) even though suckling itself rapidly increases *adrenocorticotropin* and corticosterone secretion (Walker et al., 1992).

Postpartum behavioral changes in females are also critically important parts of mammalian reproduction (Knobil and Neill, 2006). Although sexual steroid may contribute to the development of maternal behaviors by reducing inhibition of olfactory origin (Numan and Insel, 2003), decreased levels of these hormones are detected during lactation (Lamming, 1994) and the full range of maternal behaviors can be induced by prolonged pup exposure

even in ovariectomized virgin females (Fleming and Rosenblatt, 1974; Rosenblatt, 1967) suggesting that suckling or at least the presence of pups is necessary for maintaining maternal behaviors (Numan and Woodside, 2010). The preoptic area of hypothalamus plays a pivotal role in the regulation of maternal behaviors based on their absence following preoptic lesions (Gray and Brooks, 1984; Numan, 1986) and the large number of neurons in the preoptic area exhibiting Fos activation in postpartum dams (Lonstein et al., 1998b; Stack and Numan, 2000). Other brain regions connected to the preoptic area also participate in the regulation of different aspects of maternal behaviors. For example, the ventrolateral subdivision of the caudal periaqueductal grey has been shown to regulate kyphosis, the most effective body posture in rats for suckling pups, and maternal aggression (Lonstein et al., 1998a). *Prolactin, oxytocin and opioids* have been implicated in the control of maternal behaviors (Numan, 2006). More recently, the role of *vasopressin* (Bosch et al., 2010) and *melanin-concentrating hormone* (Rondini et al., 2010) have also been proposed.

In summary, it is established that reduced kisspeptin expression and consequently low gonadotropin-releasing hormone secretion are responsible for lactational anoeastrus and that profoundly elevated prolactin and oxytocin secretion lead to milk production and ejection, respectively. What we do not know how these signals are regulated in mothers, whether and how they are driven by the suckling stimulus. Furthermore, the control of other aspects of maternal adaptations including maternal motivation and behaviors are less well understood.

3.5. Tuberoinfundibular peptide of 39 residues

Tuberoinfundibular peptide of 39 residues (TIP39) was purified on the basis of its activation of the parathyroid hormone 2 receptor (PTH2 receptor), a seven transmembrane domain G-protein coupled receptor (Usdin et al., 1999b). The distribution of TIP39 containing fibers and terminals is very similar to the distribution of PTH2 receptor-containing neurons and neuronal fibers throughout the brain (Dobolyi et al., 2003b; Faber et al., 2007), and TIP39 is a potent and selective PTH2 receptor agonist (Usdin, 2000). These functional and anatomical matches suggest that TIP39 is the endogenous ligand of the PTH2 receptor in the brain, and that they form a neuromodulator system. TIP39 neurons have a highly restricted localization. This pattern of synthesis by cells in a few discrete areas and widespread, but still topographically organized, projections to several distant brain areas resembles several other recently developed neuropeptide systems including, for example, relaxins (Ma and Gundlach, 2007), orexins (Baumann and Bassetti, 2005), calcitonin-gene related peptide (van Rossum et al., 1997), prolactin-releasing peptide (Roland et al., 1999), kisspeptin (Mikkelsen and

Simonneaux, 2009), and urocortins (Pan and Kastin, 2008). Based on the available data, however, the TIP39-PTH2 receptor system is a unique neuropeptide-receptor system whose localization and functions in the central nervous system are different from any other neuropeptides (Dobolyi et al., 2010).

TIP39 is a member of a small peptide family comprised of parathyroid hormone (PTH), parathyroid hormone-related peptide (PTHrP) and TIP39 (Usdin et al., 1999b). Mature PTH and PTHrP are polypeptides of about 100 residues. They are products of separate genes but they activate the parathyroid hormone 1 receptor (PTH1 receptor) with equal potency (Gensure et al., 2005; Muff et al., 1994). Their first 34 or 36 residues are sufficient for high-affinity binding and full efficacy at the PTH1 receptor, and they share 12 of these amino acids (Gillespie and Martin, 1994; Martin et al., 1991). TIP39 contains only four of the residues that are common to PTH(1–34) and PTHrP(1–36), and several additional similar residues (Usdin et al., 1999b). However, TIP39 has a backbone structure that can be nearly superimposed on that of PTH (Piserchio et al., 2000). Based on the similarity of TIP39 to PTH and its activation of the PTH2 receptor, TIP39 is referred to as parathyroid hormone 2 in the UniGene database at http://www.ncbi.nlm.nih.gov/sites/entrez (Mm.207078 for the mouse and Hs.339845 for the human gene). However, this name is also used for a second form of PTH found in fish that more closely resembles mammalian PTH than does TIP39 (Gensure et al., 2004). PTH, produced by the parathyroid gland, is the most important regulator of calcium homeostasis. It increases plasma calcium ion concentration *via* direct actions in the kidney and the skeleton (Hurwitz, 1996; Rizzoli et al., 1992). PTHrP is a paracrine factor that functions in a number of organs and plays a critical role in skeletal development (Law et al., 1994; Martin et al., 1997). TIP39 and the PTH2 receptor are expressed at very low levels in kidney and bone (Usdin et al., 1996; Usdin et al., 1999a). In the periphery, they may play a role in the cardiovascular system (Eichinger et al., 2002; Ross et al., 2005; Ross et al., 2007) and in gonadal function (Usdin et al., 2008). However, TIP39 and the PTH2 receptor are most abundant in the central nervous system (Dobolyi et al., 2002; Usdin et al., 1995).

3.6. Amylin

Amylin, a peptide of 37 amino acids, belongs to the calcitonin gene-related peptide (CGRP) family, which also includes calcitonin, CGRPα, CGRPβ, adrenomedullin, and intermedin / adrenomedullin 2 (Wimalawansa, 1997). This family of peptides has a unique pharmacology. The binding specificity of 2 ´family B´ G-protein-coupled receptors, the calcitonin receptor and the calcitonin receptor-like receptor depends on additional proteins,

the 3 receptor activity-modifying proteins (RAMP1-3), which are single transmembrane domain accessory proteins (Oliver et al., 2001; Poyner et al., 2002). Each RAMP has different distribution in the brain (Oliver et al., 2001), and form 3 pharmacologically distinct amylin receptors with the calcitonin receptor (Hay et al., 2004). RAMPs also form CGRP and adrenomedullin receptors in association with the calcitonin receptor-like receptor (Poyner et al., 2002).

In early distributional studies, amylin expression had only been detected in the pancreatic B-cells and not in the brain (Leffert et al., 1989; Lutz, 2006). More recently, the expression of amylin has also been reported in neurons of sensory ganglia (Mulder et al., 1995) where it might have a role in nociception (Gebre-Medhin et al., 1998). Plasma amylin derived from co-secretion with insulin from pancreatic B-cells contributes to meal-ending satiation (Lutz, 2010; Osto et al., 2007; Rushing et al., 2000) via its action on the region of the area postrema and the nucleus of the solitary tract (Potes and Lutz, 2010). In addition, amylin might also act as an adiposity signal (Lutz, 2010; Rushing et al., 2001).

4. OBJECTIVES

Several aspects of motherhood has been investigated and recognized in the past. Hormonal changes in mothers have long been examined by reproductive endocrinologist, e.g. we have significant knowledge on the dopaminergic control of prolactin release. Obstetricians and gynecologist have of course always catered for mothers. Psychological aspects of motherhood have also been addressed in appropriate scientific fields. However, despite the recent progress in the field, the regulatory mechanisms within the maternal brain regions remained largely obscure. In particular, we do not have sufficient information on the neuropeptides related to motherhood and their specific actions. Apart from neurohypophyseal oxytocin, there are no peptides known to dramatically increase their expression during motherhood. In addition, the neuronal circuitry that regulates maternal responses is not known, the anatomical pathways and neurochemical characteristics of the reflex arch that mediates the effect of suckling to forebrain centers remain to be elucidated. Therefore, the general objectives of these studies were to identify maternally expressed neuropeptides and describe the neuronal circuitry that regulates maternal responsiveness. This novel approach to understand maternal adaptations was to be performed using a wide array of advanced methodological repertoire.

4.1. The specific objectives of the study

- ***Identify the gene encoding TIP39 and describe the distribution of its expression***

  The gene and mRNA encoding TIP39 was to be analyzed followed by the distribution of the mRNA in different organs as well as in different brain regions using RT-PCR and in situ hybridization. After characterizing a newly developed antibody against TIP49, the distribution of the peptide in cell bodies as well as neuronal fibers was also addressed.

- ***Determine TIP39 expression levels during ontogenic development and the reproductive cycle***

  TIP39 mRNA as well as peptide levels were to be assessed in all 3 regions of expression of TIP39, the periventricular gray of the thalamus (PVG), the posterior intralaminar complex of the thalamus (PIL), and the medial paralemniscal nucleus (MPL) in the lateral pons, during embryonic and postnatal development, puberty, pregnancy and the postpartum period.

- ***Describe the afferent and efferent neuronal connections of TIP39 neurons activated in mothers in the PIL and MPL***

  The activation of TIP39 neurons in mother rats was to be investigated by the Fos technique. The neuronal connections of activated TIP39 neurons in the PIL and MPL were to be examined using retrograde neuronal tracers as well as pathway transection methods. Most experiments were designed to be performed in mothers in order to visualize otherwise not visible TIP39 neurons and fibers.

- ***Map the distribution of the receptor of TIP39, the PTH2 receptor in the brain of rodents, macaque and human***

  The distribution of PTH2 receptor expression in the brain was to be determined by *in situ* hybridization histochemistry in macaque and mouse, and X-gal histochemistry in mice expressing β-galactosidase driven by the promoter of the PTH2 receptor. The protein was to be visualized by immunohistochemistry both in rodents and postmortem human brain samples. The distribution of the PTH2 receptor is compared between different species as well as to the distribution of TIP39 fibers and fiber terminals.

- ***Measure the effects of antagonizing the PTH2 receptor in mothers on prolactin secretion and maternal motivation***

  A PTH2 receptor antagonist was to be delivered into the brain by 2 different means: 1) acute injection into the lateral ventricle, 2) infection of a localized group of cells by a virus that codes the PTH2 receptor antagonist. Serum prolactin levels were to be measured in response to suckling. Maternal motivation was evaluated in mothers with infected cells in the preoptic area using a conditioned place preference test when the mothers can choose between a pup-associated and a control cage.

- ***Identify maternally changing peptides in the preoptic area of hypothalamus and characterize their interaction with the TIP39-PTH2 receptor system***

  A microarray experiment was designed to determine genes whose mRNA level is increased 9 days postpartum in lactating mother rats as compared to mothers deprived of their litter on the day of delivery. The highest, over 25 times increase was found for amylin, a novel neuropeptide. Therefore, the distribution of amylin-expressing cells, their innervation by TIP39, and their activation in response to suckling were addressed.

5. MATERIALS AND METHODS

5.1. Experimental subjects and tissues

5.1.1. Rodents

Some procedures were performed according to approved National Institutes of Mental Health (Bethesda, MD, USA) animal care protocols, and in accordance with the National Institutes of Health Guide for the Care and Use of Laboratory Animals. Other experiments were approved by the Semmelweis University, Budapest, and Animal Examination Ethical Council of the Animal Protection Advisory Board. Procedures involving rats were carried out in accordance with the Hungarian Ministry of Agriculture's Animal Hygiene and Food Control Department guidelines for experimental protocols and with EU Directive 2010/63/EU for animal experiments. Female and male Wistar rats and C57Bl/6 mice (Charles Rivers Laboratories, Hungary) were used in this study. All efforts were made to minimize the number of animals used and their suffering. Animals were kept on standard laboratory conditions with 12-h light, 12-h dark periods (lights on at 6.00 a.m.), and supplied with dry rat food and drinking water *ad libitum*. Animals were housed 3 per cage at a temperature of 22±1 °C before experiments. For mating, 2 female and a male rat were kept in a cage for 5 days. After that, potentially pregnant females as well as dams with litter and their pup-deprived and control experimental counterparts were kept in cages individually. Mother rats delivered their pups on day 22 of pregnancy. Mothers who delivered fewer than 8 pups or whose pups died were excluded from the study. The number of pups was adjusted to 8 within 2 days of delivery. For surgery, perfusions, and dissections, the animals were anesthetized with an intramuscular injection of anesthetic mix containing 0.2ml/300g body weight ketamine (100 mg/ml) and 0.2ml/300g body weight xylazine (20 mg/ml).

5.1.2. Knock-in mice expressing β-galactosidase driven by the PTH2 receptor promoter

The first protein coding exon of the mouse PTH2 receptor gene was replaced by the bacterial lacZ coding sequence by homologous recombination in F1 (129Sv/Ev x c57Bl/6) hybrid mouse ES cells, as previously described (Valenzuela et al., 2003). Following identification of ES cells with appropriate recombination by the Regeneron group, the cells were expanded and introduced into c57Bl/6 blastocysts in the NIMH transgenic mouse core facility. Resulting mice were back-crossed with C57Bl/6 mice. Heterozygous animals were used for the experiments. Knock-in mice were identified by PCR based genotyping on DNA from tail biopsies using primers for lacZ or one primer in the inserted sequence and one

primer in the flanking gene sequence (Faber et al., 2007). The primer sequences were: 5'-GCGCTGGTTGATTAGATACC, P2R_HDR2-B; 5'-GCTTCCTCGTGCTTTACGGTATC, Neo_3'b; and 5'-GAGAGGCTGTTTGTAGAAGGCTGA, P2R_64264U which produced bands of 260 base pairs from the wild-type allele and 700 from the knock-in allele.

5.1.3. PTH2 receptor knock-out mice

Mice with a null mutation of the PTH2 receptor were generated and characterized in a previous study (Coutellier et al., 2011). Briefly, loxP sites were introduced into intronic sequence flanking exon 5 of the receptor in 129S6 X C57BL6/N F1 ES cells. The 'floxed exon 5' mice were then bred with a 'Cre deleter' line [that expresses Cre recombinase in germ cells; Tg(Prm-cre)58Og]. Mice with permanent deletion of exon 5 were identified by a polymerase chain reaction and then bred with C57Bl/6J mice, producing heterozygous exon 5 deleted mice. No gross abnormality or defect was found in the PTH2 receptor knock-out mice in an observational battery measuring general health and neurological functions (Coutellier et al., 2011). Animals used in this study were backcrossed to C57Bl/6J for four generations.

5.1.4. Macaque tissue

Tissue collection and all procedures were performed according to protocols approved by the Animal Care and Use Committee of the National Institute of Mental Health following ethical review, and in accordance with the Institute for Laboratory Animal Research Guide for the Care and Use of Laboratory Animals. The authors further attest that all efforts were made to minimize the number of animals used and their suffering. A 3 male macaque monkey (Macaca mulatta) was sedated with ketamine and then euthanized by i.v. administration of an overdose of pentobarbital. The testis was dissected for the preparation of hybridization probes and the brainstem was dissected for *in situ* hybridization histochemistry. Tissues were frozen and stored at -80 ^{o}C until sectioning.

5.1.5. Human tissue

Human brain samples were collected in accordance with the Ethical Rules for Using Human Tissues for Medical Research in Hungary (HM 34/1999) and the Code of Ethics of the World Medical Association (Declaration of Helsinki). Tissue samples were taken during brain autopsy at the Department of Forensic Medicine of Semmelweis University in the framework of the Human Brain Tissue Bank, Budapest, or at the Department of Pathology of the

University of Pécs, as approved by institutional ethics committees of the Semmelweis University or the University of Pécs. Prior written informed consent was obtained from the next of kin, which included the request to consult the medical chart and to conduct neurochemical analyses. The study reported in the manuscript was performed according to animal care protocols approved by the Committee of Science and Research Ethics, Semmelweis University (TUKEB 34-1/2002). The medical history of the subjects was obtained from medical or clinical records, interviews with family members and relatives, as well as from pathological and neuropathological reports (Table 1). All personal identifiers had been removed and samples coded before the analyses of tissue.

Brains were removed from the skull with a post-mortem delay of 2–6 h. For microdissection, the brains were cut into 5 large parts (cerebral lobes, diencephalon, brainstem, cerebellum), and frozen immediately at -80 ^{o}C. For immunocytochemistry, brains were cut into 5-10 mm thick coronal slices and immersion fixed in 4% paraformaldehyde in 0.1 M phosphate buffer (PB) for 6-10 days. Then, the slices were postfixed in the same solution with addition of 15% saturated picric acid.

Table 1. Information on human tissue used in the study.

Brain Number	**Gender**	**Age (years)**	**Clinical Diagnosis**	**Tissue**	**Detection method**
1	female	89	Alzheimer disease	fresh frozen micropunched samples	RT-PCR
2	male	56	Cardiac failure	fresh frozen micropunched samples	RT-PCR
3	female	8	Leukemia	immersion fixed hypothalamus	immunolabeling
4	male	10	Leukemia	immersion fixed insula, diencephalon, brainstem	immunolabeling
5	male	62	Unknown	immersion fixed medulla and spinal cord (C1,2)	immunolabeling

5.2. Microdissection of brain tissue

5.2.1. Microdissection of human brain tissue samples

Brain nuclei and areas including the frontal cortex, hippocampus, septum, caudate nucleus, amygdala, ventral thalamus, mediodorsal thalamic nucleus, pulvinar, lateral and medial geniculate bodies, subthalamic nucleus, medial hypothalamus, pretectal area, substantia nigra, ventral tegmental area, pontine nuclei, tegmentum and reticular formation, ventrolateral medulla, dorsal vagal complex, inferior olive, spinal trigeminal nucleus, and cerebellar cortex were individually microdissected from the brains of an 89 year old woman and a 56 year old man using the micropunch technique (Palkovits, 1973; Palkovits et al., 2008) guided by human brain atlases (Mai et al., 1997; Paxinos and Huang, 1995). Briefly, the large parts of the frozen brains were cut into 1.0-1.5 mm thick coronal sections by an electric slicer at about –5-10 ^{o}C, and individual brain regions and nuclei were removed from the slides by special punch needles with an inside diameter of 1.0-3.5 mm visualized using either a head magnifier, or a stereomicroscope. The slices were kept on dry-ice during the whole procedure. The microdissected samples were collected in 2.0 mm airtight plastic (Eppendorf) tubes and stored at -80 °C until further use.

5.2.2. Microdissection of rat brain tissue samples

Thick coronal brain sections were prepared around the preoptic area with a razor blade cut immediately rostral to the optic chiasm and 2 mm caudal to this level (Fig. 3). A horizontal cut immediately above the anterior commissure, and sagittal cuts on both sides of the brain 2 mm lateral to the midline were used to dissect tissue blocks that contained the preoptic area of the hypothalamus as well as small parts of adjacent brain structures including parts of the diagonal band of Broca, the anterior commissure, the optic tract, the ventral pallidum (Fig. 3). The dissected tissue samples were quickly frozen on dry ice, and stored at -80^{o}C.

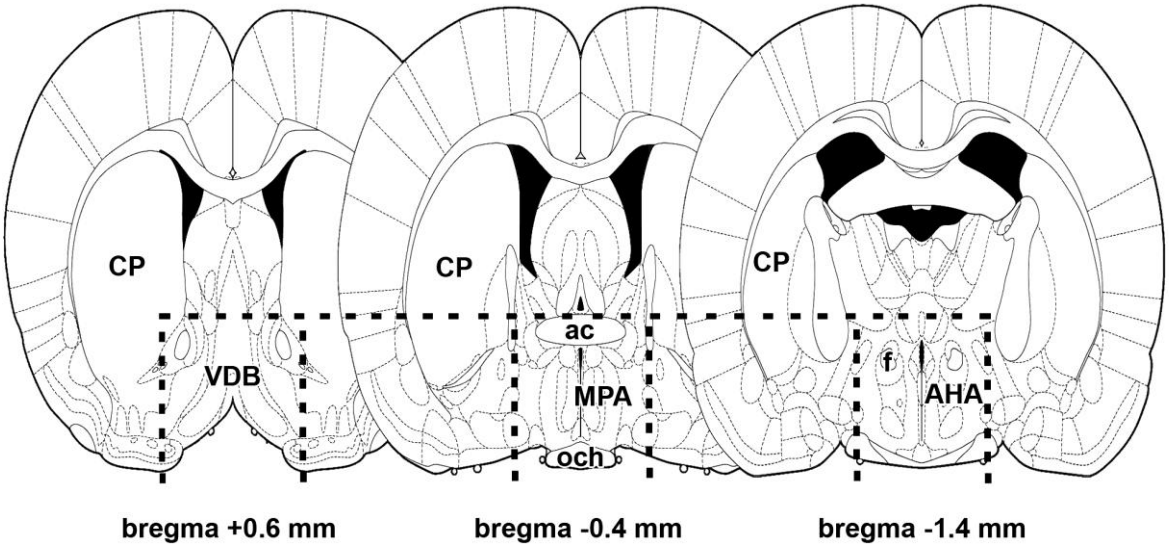

Fig. 3. Schematic figures demonstrate the brain region dissected for microarray and RT-PCR experiments. The rostral cut of coronally oriented tissue blocks was performed at bregma level +0.6 mm. The caudal surface of the microdissection was at bregma level -1.4 mm. Dorsally, the dissection was made with a horizontal cut immediately above the anterior commissure (ac) as indicated by dashed line. Vertical dashed lines indicate the lateral border of the microdissection 2 mm lateral from the midline. The figure is from our previous publication (Dobolyi, 2009).

5.3. Microarray

RNA was purified from microdissected preoptic area 9 days after delivery from 4 primiparous lactating mothers and 4 mothers separated from pups immediately after parturition. Microarray measurements were performed in the Microarray Core Facility of the Semmelweis University using Agilent methods (Agilent Technologies, Palo Alto, CA). Quality-checked total RNA of 500 ng was reverse transcribed by the Low-input RNA Linear Amplification Kit (Agilent Technologies) and then transcribed to either Cy5 or Cy3-labeled cRNA. The labeled cRNA was purified (RNeasy kit, Qiagen, Valencia, CA), the dye content (>8.0 pmol dye / μg cRNA) and concentration of cRNA measured. For fluorescent microarray experiments, 4 pairs of mRNAs were arbitrarily formed. Each pair consisted of Cy5-labeled cRNA derived from a lactating mother and Cy3-labeled cRNA derived from a mother deprived of her pups. 1 μg of labeled cRNA was hybridized to Agilent Rat Oligonucleotide 4x44K microarrays overnight at 60 ^{o}C and washed by the ozone-safe SSPE method. The

slides were treated with Stabilizing and Drying Solution (Agilent Technologies) and scanned by Agilent Microarray Scanner according to the instructions of the manufacturer. Data were normalized by the Feature Extraction software version 7.5 with default parameter settings for oligonucleotide microarrays and then transferred to GeneSpring 7.3 program (Agilent Technologies), with which normalization and data transformation steps were performed. The oligonucleotid sequence for amylin on the microarray chip corresponded to 354-413 bps of GenBank accession number NM_012586. This sequence shows about 47% sequence identity to the corresponding part of calcitonin, and 52-53% to other members of the CGRP peptide family.

5.4. RT-PCR

5.4.1. RT-PCR of the PTH2 receptor from human

Total mRNA was isolated using Trizol^{R} Reagent (Invitrogen, Carlsbad, CA) from 50-100 mg of brain tissue according to the manufacturer's instructions. The degradation of RNA was assessed by running the purified RNAs on denaturing formaldehyde gels. Samples, in which the amount of 28S rRNA was at least equal to that of 18S rRNA, were processed further for RT-PCR. After diluting total RNA to 2 μg / μl, RNA was treated with Amplification Grade DNase I (Invitrogen) and cDNA was synthesized with a Superscript II reverse transcriptase kit (Invitrogen) according to the manufacturer's instructions. After 10-fold dilution, 2.5 μl of the resulting cDNA was used as template in PCR reactions. The primer pair for PTH2 receptor was 5′-CAATTGCTTGGCTGTAGCTTT-3′ and 5′-ACAAAATCAATTTGCAGACACAA-3′ resulting in a PCR product of 440 bp that corresponds to bp 2162-2601 of the human PTH2 receptor (GenBank accession number NM_005048). The PCR product using this PTH2 receptor primer pair has been verified by sequencing to result in a product specific for the PTH2 receptor (Bagó et al., 2008). The primer pair for the housekeeping gene glyceraldehyde-3-phosphate dehydrogenase (GAPDH) was 5′-CCACCCAGAAGACTGTGGAT-3′ and 5′-CCCTGTTGCTGTAGCCAAAT-3′ resulting in a PCR product of 423 bp that corresponds to bp 650-1072 of human GAPDH (GenBank accession number NM_002046). The PCR reactions were performed with iTaq DNA polymerase (Bio-Rad Laboratories, Hercules, CA) in total volumes of 12.5 μl using primers at 300 nM final concentration under the following conditions: 95 ^{o}C for 3 min, followed by cycles of 95 ^{o}C for 0.5 min, 60 ^{o}C for 0.5 min and 72 ^{o}C for 1 min. The presence the PTH2 receptor was evaluated after 38 cycles while the presence of GAPDH after 33 cycles. Equal amounts (10 μl) of PCR products were run on gels and pictures taken with a

digital camera. Primers for PTH2 receptor are specific to sequences in different exons to allow recognition of potential genomic DNA contamination by the larger size of the product.

5.4.2. Real-time RT-PCR for TIP39 and amylin measurement in rat samples

Total RNA was isolated from the microdissected PVG, MPL, PIL, or preoptic area using Trizol^{R} Reagent (Invitrogen, Carlsbad, CA) according to the manufacturer's instructions. After diluting RNA to 2 μg/μl, it was treated with Amplification Grade DNase I (Invitrogen) and cDNA was synthesized with a Superscript II reverse transcriptase kit (Invitrogen) according to the manufacturer's instructions. After 10-fold dilution, 2.5 μl of the resulting cDNA was used as template in PCR reactions. For TIP39, multiplex PCR was used with dual-fluorescence labeled TAQMAN probes (6-FAM-CGCTAGCTGACGACGCGGCCT-TAMRA for TIP39), and glyceraldehyde-3-phosphate-dehydrogenase (GAPDH) probe (JOE-ATGGCCTTCCGTGTTCCTACCCCC-TAMRA). The primers for TIP39 (CTGCCTCAGGTGTTGCCCT and TGTAAGAGTCCAGCCAGCGG) were used at 300 nM whereas the primers for GAPDH (CTGAACGGGAAGCTCACTGG and CGGCATGTCAGATCCACAAC) were used at 150 nM concentration. For amylin and corresponding GAPDH, PCR reactions were performed using SYBR Green dye (Sigma, St. Louis, MO). The primers for amylin (ACATGTGCCACACAACGTCT and ACAAACACAGCAAGCACAGG corresponding to 222-241 and 493-512 bps of GenBank accession number NM_012586) and GAPDH (TGCCACTCAGAAGACTGTGG and GTCCTCAGTGTAGCCCAGGA corresponding to 540-559 and 812-831 bps of GenBank accession number M17701) were used at 300 nM final concentration. All PCR reactions were performed with iTaq DNA polymerase (Bio-Rad Laboratories, Hercules, CA) in total volumes of 12.5 μl under the following conditions: 95 ^{o}C for 3 min, followed by 35 cycles of 95 ^{o}C for 0.5 min, 60 ^{o}C for 0.5 min and 72 ^{o}C for 1 min. Cycle threshold values (C_T values) were obtained from the linear region of baseline adjusted amplification curves. Standard curves obtained by measuring dilution series were used to calculate the amount of cDNA in the samples. Statistical analyses (Prism 4 for Windows, GraphPad Software, Inc.) were performed by one-way analysis of variance for the comparison of the 3 different groups followed by Bonferroni posttests for post hoc comparisons.

5.5. In situ hybridization histochemistry

5.5.1. Production of rat in situ hybridization probes for amylin, TIP39, and PTH2 receptor

PCR products were produced from maternal preoptic cDNA using 2 different primer pairs for amylin corresponding to 222-241 and 493-512 bps, and to 54-73 and 243-262 bps of GenBank accession number NM_012586. For TIP39 and the PTH2 receptor, cDNA from diencephalon was used as a template for PCR reactions. Three regions of the rat TIP39 cDNA sequence were used to generate probes, corresponding to amino acids –55 to 17; –18 to 37, and –55 to 37, where amino acid 1 is the first residue of mature TIP39. Similarly, regions of the rat PTH2 receptor cDNA sequence corresponding to bases 482-864 and bases 1274-1828 was used to generate probes. The PCR products were purified from gel, inserted into TOPO TA cloning vectors (Invitrogen) and transformed chemically into competent bacteria. Selected plasmids were applied as templates in PCR reactions, using the specific primer pairs with the forward primers also containing a T3 for sense probes, while the reverse primers a T7 RNA polymerase recognition site for antisense probes. At the end, the identities of the cDNA probes were verified by sequencing. The different probes for the same genes produced equivalent hybridization patterns in all 3 cases. Comparisons between signals from antisense and sense (control) riboprobes were made on serial sections hybridized simultaneously and processed together. Sense probes did not result in specific labeling.

5.5.2. Macaque probe preparation for in situ hybridization

Template cDNA was prepared from macaque testis by an RT reaction, as described above. PCR reactions were also performed essentially as described above using primers with human TIP39 (5′-GGGGACTGTGCGGGAAGC-3′ and 5′-GCATGTACGAGTTCAGCCAGTGG-3′) and PTH2 receptor (5′-TGTGGGGCTTCATCTTGATAGG-3′ and 5′-ATGGCGGTGTCCTTTTCCAGTC-3′) sequences. The PCR products were cloned into plasmid vectors, and their identities were confirmed by DNA sequencing. A plasmid for each probe was used as template in PCR reactions, using primers that appended a T7 RNA polymerase recognition sequence (5′-GCGCGTAATACGACTCACTATAGGG-3′) into the 5’ end of the antisense primer. The TIP39 probe was a 372 base amplicon, which differed from the predicted human sequence (GenBank accession number NM_178449) at 16 scattered base positions. It also lacked codons for two amino acid residues in the predicted leader sequence. The PTH2-R probe was a 500 base amplicon. It differed from the predicted human sequence (GenBank accession number NM_005048) at 14 bases. It also contained a 49 base insertion that corresponds to

predicted intronic sequence. The small number of differences between the macaque probes and predicted human sequences may reflect PCR error or artifacts that do not affect their use as probes, or genuine species differences.

5.5.3. In situ hybridization protocol

The freshly dissected tissue was quickly frozen on dry ice. Serial coronal sections (12 μm) were cut using a cryostat, mounted on positively charged slides (SuperfrostPlus®, Fisher Scientific, Pittsburgh, PA), dried, and stored at -80°C until use. Antisense [^{35}S]UTP-labeled riboprobes were generated using T7 RNA polymerase of the MAXIscript transcription kit (Ambion, Austin, TX) from polymerase chain reaction-amplified fragments of the amylin or TIP39 cDNA subcloned into TOPO TA vectors. For hybridization, we used 80 μl hybridization buffer and 1 million DPM of labeled probe per slide. Washing procedures included a 30 min incubation in RNase A, followed by decreasing concentrations of sodium-citrate buffer (pH = 7.4) at room temperature, and then at 65°C. After drying, the slides were dipped in NTB2 nuclear track emulsion (Eastman Kodak) and stored at 4°C for 3 weeks for autoradiography. Then, the slides were developed and fixed with Kodak Dektol developer and Kodak fixer, respectively, counterstained with Giemsa and coverslipped with Cytoseal 60 (Stephens Scientific, Riverdale, NJ).

5.5.4. Quantitation of in situ hybridization data by counting autoradiography grains

Amylin mRNA-expressing neurons, above which more than 9 autoradiography grains (3 times the average background) were detected, were typically present in 3 coronal sections cut at 216 μm distances. The total number of these cells was counted on 21st day of pregnancy, 1, 9, and 23 days after parturition. In addition, the number of autoradiography grains were counted in 20-20 evenly distributed but otherwise randomly selected amylin mRNA-expressing neurons in each of the 3-3 brains on 21st day of pregnancy, 1, 9, and 23 days after parturition. Both the total number of amylin mRNA-expressing neurons in the 3 consecutive sections and the average number of autoradiography grains per cell were calculated on one side of the 3-3 brain sections. Statistical analyses were performed using Prism 5 for Windows (GraphPad Software Inc.). Both cell numbers and the number of autoradiography grains in the 4 groups (21st day of pregnancy, 1, 9, and 23 days after parturition) were compared using one-way ANOVA followed by Tukey´s multiple comparison post-hoc test.

5.5.5. Densitometric analysis of in situ hybridization histochemistry

Dark-field photomicrographs were taken of the sections where the TIP39 signal was the highest in the PIL using a 10x objective. Each image was divided into 2 halves with identical size, such that one half contained all the observed TIP39 autoradiography signals, while the other half served as background control. The pixel number of white area (lighter than an arbitrary grayness used for all the images) was calculated for both halves of the images using ImageJ 1.47v (National Institutes of Health, USA) software. The difference between the 2 values (the half picture containing TIP39-expressing cells – the half picture containing only background autoradiography signal) was used to quantify the TIP39 mRNA level. TIP39 mRNA levels at the 5 different time points were compared using one-way ANOVA followed by Bonferroni´s multiple comparison test.

5.6. Histology

5.6.1. Tissue collection

Rats were deeply anesthetized and perfused transcardially with 150 ml saline followed by 300 ml of ice-cold 4% paraformaldehyde prepared in phosphate buffer (PB, 100 mM, pH=7.4). Brains were removed and postfixed in 4% paraformaldehyde for 24h and then transferred to PB containing 20% sucrose for 2 days. Serial coronal sections were cut at 50 μm on a sliding microtome (SM 2000R, Leica Microsystems, Nussloch, Germany). Sections were collected in PB containing 0.05% sodium-azide and stored at 4°C.

5.6.2. Cresyl-violet staining

Sections were mounted consecutively on gelatin-coated slides and dried. Sections were stained in 0.1% cresyl-violet dissolved in PB, then differentiated in 96% ethanol containing acetic acid. Sections were then dehydrated and coverslipped with Cytoseal 60 (Stephens Scientific, Riverdale, NJ).

5.6.3. Luxol fast blue staining

Sections were collected and mounted consecutively on gelatin-coated slides and dried. Myelinated fibers were visualized with the sulphonated copper ohthalocyanine Luxol Fast Blue with a modification of the Kluver-Barrera method as described before (McIlmoyl, 1965). Briefly, 25 μm thick sections were stained in 0.1% Luxol fast blue dissolved in 96% ethanol containing 0.05% acetic acid, and differentiated in 0.05% lithium-chloride followed by 70%

ethanol. Subsequently, sections were then stained in 0.1% cresyl-violet. At the end, sections were dehydrated and coverslipped as described above.

5.6.4. X-gal labeling

PTH2 receptor knock-in mice as well as wild type control littermates were used to visualize the β-galactosidase marker enzyme histochemically. Mice were anesthetized and perfused transcardially with 10 ml phosphate-buffered saline (PBS; pH 7.4) followed by 30 ml of cold 2% paraformaldehyde – 0.2% glutaraldehyde mixture dissolved in PBS. Brains were removed, postfixed in 0.2% glutaraldehyde in PBS overnight, and coronal sections of 50 μm thickness were cut on a vibrating microtome from bregma level of 3 mm to -8 mm. Sections were washed twice for 10 minutes each in wash buffer (100 mM phosphate buffer at pH 7.4, 2 mM $MgCl_2$, 0.01% Na-deoxycholate, and 0.02% octylphenol-ethylene oxide condensate [Nonidet P-40]). Then, the sections were incubated in freshly made staining solution containing 5 mM potassium ferricyanide, 5 mM potassium ferrocyanide, and 1 mg/ml X-gal (5-bromo-4-chloro-3-indolyl--D-galactopyranoside) dissolved in wash buffer at room temperature in darkness overnight. Sections were then washed twice in 50 mM Tris buffer (pH=8.0), mounted on positively charged slides, and coverslipped with mounting medium (Cytoseal^{TM} 60; Stephens Scientific, Kalamazoo, MI).

5.6.5. Immunohistochemistry

5.6.5.1. TIP39 antiserum

TIP39 was detected with an affinity-purified antiserum from a rabbit immunized with rat (r) TIP39 coupled to keyhole limpet hemocyanin by 1-ethyl-3-(3-dimethylaminopropyl)carbodiimide. The titer (50% maximum binding to immobilized peptide) of the affinity-purified anti-rTIP39 antiserum against rTIP39 was 3 ng / ml. Immunolabeling with the affinity-purified anti-rTIP39 was abolished by pre-incubation with 1 μM synthetic rTIP39. The anti-rTIP39 antiserum exhibited less than 1% cross-reactivity with parathyroid hormone and no detectable cross-reactivity with other peptides tested including parathyroid hormone related peptide, calcitonin, substance P, vasoactive intestinal peptide, glucagon, and calcitonin gene-related peptide (Dobolyi et al., 2002). The anti-rTIP39 antiserum labels cell bodies in rat with exactly the same distribution as observed by *in situ* hybridization histochemistry with probes directed against TIP39 mRNA (Dobolyi et al., 2003b). In addition, TIP39 immunolabeling disappears from fibers following lesion of the distant TIP39 cell bodies (Dobolyi et al., 2003a).

5.6.5.2. PTH2 receptor antiserum

PTH2 receptor was detected with an affinity-purified antiserum from a rabbit immunized with the synthetic peptide RQIDSHVTLPGYVWSSSEQDC, corresponding to residues 480–500 of the rat PTH2 receptor (GenBank Entry U55836), conjugated to keyhole limpet hemocyanin. Antiserum from two rabbits immunized with this peptide produce strong immunolabeling of HEK293 cells stably expressing the human PTH2 receptor (Usdin et al., 1999a; Wang et al., 2000). Preimmune serum does not label the PTH2 receptor-expressing cells, and no labeling of either the parent HEK293 cells or HEK293 cells stably expressing the human PTH1 receptor is detected. Similarly, there was intense labeling of 20–30% of COS-7 cells transfected with PTH2 receptor cDNA but no labeling of cells in mock transfected cultures. Several bands were labeled in Western blots of PTH2 receptor-enriched membranes, probably representing a combination of multiple glycosylation states and aggregation or oligomerization of the receptor. The highest mobility major band migrated with an apparent molecular weight of 84K, consistent with the size seen following western blotting of a C-terminal epitope labeled PTH2 receptor, and labeling of the receptor with a radioactive photoaffinity ligand. Following digestion with PNGase F, the mobility of the high mobility major band increased to an apparent molecular weight of 63K, consistent with the predicted size of the protein based on its cDNA sequence. No signal is seen in membranes prepared from the parent HEK293 cells or ones expressing the PTH1 receptor. Only 4 out of the 21 residues are the same as those in the human, mouse or rat PTH1 receptor and no significant labeling is detected in rat kidney tubules. Absorption of the antibody with the peptide used to generate it eliminated tissue labeling, and specific staining was absent when pre-immune serum is used to label tissue (Usdin et al., 1999a; Wang et al., 2000).

5.6.5.3. Amylin antiserum

An anti-amylin antiserum (rabbit anti-amylin (rat), catalog No. T-4146.0050, Bachem, Bubendorf, Switzerland) was used for the study. The specificity of this antiserum for amylin in the preoptic area was suggested by the same distribution of immunolabeled cells in lactating mother rats as for in situ hybridization for amylin and the lack of immunolabeling in the same location in control females. In addition, we also performed preabsorption experiments. The anti-amylin antiserum was incubated for 2 days at room temperature with synthetic rat amylin (United States Biological, Swampscott, MA). The concentrations of amylin were 5, and 0.5 μM, and an aliquot of anti-amylin antiserum without amylin was also

kept at room temperature for 2 days. Holding anti-amylin antiserum at room temperature for 2 days did not alter the immunolabeling. However, immunolabeling was markedly reduced when we used antiserum absorbed with 0.5 μM synthetic rat amylin. Furthermore, immunolabeling was not detectable in the brain following preabsorption with 5 μM amylin.

5.6.5.4. Additional antibodies used in immunohistochemistry

Commercially available and characterized mouse anti-calbindin D-28k (1:5,000; product #C9848, clone CB-955, lot #031M4859, Sigma, St. Louis, MO), mouse anti-parvalbumin (1:3,000; product #P3088, clone PARV-19, lot #100M4797, Sigma), and goat anti-rat calcitonin gene-related peptide antisera (CGRP; 1:500; Biogenesis, Kingston, NH) were used in the study.

5.6.5.5. Immunohistochemistry protocol

Rats and mice were perfusion fixed and their brains sectioned as described above. Immunohistochemistry was performed on 50 μm thick free-floating sections. The sections were pretreated in PB containing 0.5% Triton X-100 and 3% bovine serum albumin for 1 hour. Sections were then incubated in anti-amylin antiserum (1:2000) at room temperature for 2 days. Following the application of the primary antibody, sections were incubated in biotin-conjugated goat anti-rabbit secondary antibody (1:800, Vector Laboratories, Burlingame, CA) for 2 hours, and then in ABC reagent (1:400, Vectastain ABC Elite kit, Vector Laboratories) for 2 hours. Subsequently, the labeling was visualized by incubation in 0.02% 3,3-diaminobenzidine (DAB; Sigma), 0.08% nickel (II) sulfate and 0.001% hydrogen peroxide in PB for 4 minutes. Sections were mounted, dehydrated and coverslipped with Cytoseal 60 (Stephens Scientific, Riverdale, NJ).

5.6.5.6. Immunolabeling of PTH2 receptor in human tissue

For immunocytochemistry, coronally oriented tissue blocks of about 10x10x20 mm from 3 human brains were sectioned in the coronal plane. One tissue block containing insular cortex and continuous tissue blocks from the rostral end of the diencephalon (from 1 mm rostral to the anterior commissure) to the caudal end of the brainstem from a 10 year old male was sectioned. Another tissue block comprising the entire hypothalamus from the brain of an 8 year old female was sectioned. In addition, 2 tissue blocks from a 62 year old male containing the caudal part of the medulla oblongata (from the level of the obex) to the rostral part of the cervical spinal cord were also sectioned.

Two days before sectioning, the tissue blocks were transferred to PB for 2 days to remove the excess paraformaldehyde. Subsequently, the blocks were placed in PB containing 20% sucrose for 2 days for cryoprotection. Then, the blocks were frozen, and cut into 50 μm thick serial coronal sections on a sliding microtome. Immunolabeling was performed on every 10th section. Briefly, the free-floating sections were pretreated with 3% bovine serum albumin in PB containing 0.5% Triton X-100 for 30 min at room temperature. The sections were then placed in anti-PTH2 receptor primary antiserum (1:20000 dilution) for 48 h at room temperature. Then, the sections were placed in biotinylated anti-rabbit secondary antibody (1:600 dilution; Vector Laboratories, Burlingame, CA) for 2 h followed by incubation in a solution containing avidin–biotin–peroxidase complex (1:300 dilution; Vector Laboratories) for 2 h. The sections were then treated with fluorescein isothiocyanate (FITC)-tyramide (1:8000 dilution) and H_2O_2 (0.003%) in Tris hydrochloride buffer (0.05 M, pH 8.2) for 6 min. The sections were then mounted, dried, and coverslipped in antifade mounting medium (Prolong Antifade Kit, Molecular Probes, Eugene, OR).

5.6.5.7. Double labeling TIP39 with calbindin and parvalbumin

Sections were double labeled for TIP39 and calbindin or parvalbumin. Every fourth free-floating section was first stained for TIP39 by using FITC-tyramide amplification fluorescent immunocytochemistry, as described above for the PTH2 receptor immunolabeling in human. Sections were then incubated overnight in mouse anti-calbindin D-28k, or mouse anti-parvalbumin antisera Following application of the primary antibody, sections were incubated in donkey Alexa Fluor 594 anti-goat or anti-mouse secondary antibodies (Life Technologies, Grand Island, NY) for 2 hours and coverslipped as described above for fluorescent labeling.

5.6.6. Microscopy and image processing

Sections were examined using an Olympus BX60 light microscope equipped with fluorescent epi-illumination and a dark-field condenser. Images were captured at 2048 X 2048 pixel resolution with a SPOT Xplorer digital CCD camera (Diagnostic Instruments, Sterling Heights, MI) using 4-40 X objectives. Confocal images were acquired with a Nikon Eclipse E800 confocal microscope equipped with a BioRad Radiance 2100 Laser Scanninig System using a 20-60 X objectives at an optical thickness of 1-3 μm. Images were adjusted using the "levels" and "sharpness" commands in Adobe Photoshop CS 8.0. Full resolution of the

images was maintained until the final versions, which were adjusted to a resolution of 300 dpi.

5.7. Fos activation study

5.7.1. Pup exposure of mother rats

Rat dams were deprived of pups on postpartum day 8-9 at 13:00. During separation, the litter was held together in a cage that was kept warm by a lamp. The following day at 9:00, pups were returned to the cages of one group of mother rats. All mothers accepted the pups and suckling started within 5 min. Pups were returned to another group of mothers in a way that prevented physical contact but allowed the dams to see, hear, and smell the litter through metal bars (about 3 cm distance). Control dams were not united with their litters. All rat dams were sacrificed 22h after the pups had been removed, which in relevant cases was 2h after pups were returned to their mothers. Animals were perfused transcardially and processed for Fos and TIP39 immunohistochemistry.

5.7.2. Fos immunohistochemistry

In each group of brains, every fourth free-floating section was immunolabeled for Fos with DAB immunoperoxidase labeling using a rabbit anti-Fos primary antiserum (1:30000; c-Fos (4) sc-52; Santa Cruz Biotechnology, Delaware, CA). The sections were incubated in biotin-conjugated donkey anti-rabbit secondary antibody at 1:1000 (Jackson ImmunoResearch, West Grove, PA) for 1h and then in ABC complex (1:500; Vector Laboratories) for 2h and incubated in 0.02% 3,3-diaminobenzidine (DAB; Sigma), 0.08% nickel (II) sulfate, and 0.003% hydrogen peroxide in PB. Finally, the sections were mounted, dehydrated and coverslipped with Cytoseal 60 (Stephens Scientific, Riverdale, *NJ).*

5.7.3. Double immunolabeling of Fos and TIP39

One set of every fourth free-floating section from the rat dams used for single-labeling of Fos was immunolabeled for TIP39 using FITC-tyramide amplification immunofluorescence, as described above. Sections were then placed in rabbit anti-Fos primary antiserum (1:10000) for 48h at room temperature and visualized with Alexa Fluor 594 donkey anti-rabbit secondary antibody, as described above. Amplification allowed the use of a dilution of the TIP39 antibody (1:3000) that could not be visualized with the Alexa Fluor 594 donkey anti-rabbit secondary antibody, as previously described for double labeling with antibodies raised in the same species (Hunyady et al., 1996).

5.7.4. Analysis of double immunolabeling for TIP39 and Fos

After identifying the PIL section with the most TIP39-ir neurons in each of the animals double-labeled for TIP39 and Fos, we counted all TIP39-ir neurons with an identifiable cell nucleus and all double-labeled cells. Counts were obtained using an Olympus BX60 light microscope with a 20x objective, fluorescent epi-illumination, and a filter that allows for simultaneous green and red visualization. The number of single-labeled Fos-ir cells was subsequently calculated in the area of the TIP39 neurons.

For the statistical analysis of neuronal activation in the PIL, the number of Fos-ir neurons, the number of TIP39 neurons, and the number of double labeled neurons were compared between the 3 groups (suckled dams, dams exposed to pups without physical contact, control dams not exposed to pups) using one-way ANOVA tests followed by Bonferroni Post-Tests for posthoc comparisons.

5.7.5. Triple-immunolabeling of Fos, TIP39, and Kv2.1

Preoptic area sections from suckling mothers were double-immunolabeled for Fos and TIP39 as described above, then incubated in mouse anti-rat Kv2.1 α-subunit (1:300; catalog #75-014C9848, clone K89/34, lot #444-1LC-27, NeuroMab, Davis, CA). Then, these sections were incubated in Cy5 anti-mouse secondary antibody, mounted, and coverslipped.

5.7.6. The analysis of TIP39 innervation of preoptic neurons

Sections triple labeled for Fos, TIP39, and Kv2.1 potassium channel from 3 mothers were used for the analysis. Analysis was performed on serial confocal images collected at an optical thickness of 1 μm were analyzed for 32 neurons in the medial preoptic nucleus and 32 neurons in the ventral subdivision of the bed nucleus of the stria terminalis that were labeled by Kv2.1. The fraction of Fos-expressing neurons that were closely apposed by TIP39 fibers were assessed in both the medial preoptic nucleus and the ventral subdivision of the bed nucleus of the stria terminalis.

5.7.7. Double labeling of Fos immunoreactivity and amylin mRNA

Perfusion fixed, cryoprotected brains of 3 pup exposed mothers were frozen and sectioned at a thickness of 20 μm using a cryostat. Slide attached sections were processed for *in situ* hybridization, as described above. Immunolabeling for Fos was performed before dipping the slides into autoradiographic emulsion. The immunolabeling protocol was the

same as that used for single labeling Fos immunocytochemistry, except for the use of the rabbit anti-Fos primary antiserum at a dilution of 1:7000. Fos was visualized using nickel intensified DAB reactions, after which the *in situ* hybridization procedure was continued by dipping the slides into emulsion.

5.7.8. Analysis of amylin and Fos double labeling

All sections containing amylin neurons (typically 3 sections per brain) were analyzed. The numbers of amylin-ir neurons as well as the number of cells labeled for both amylin and Fos were counted in the medial preoptic nucleus (MPN), the medial preoptic area (MPA), and the ventral subdivision of the bed nucleus of the stria terminalis (BNSTv) using the 20x objective of an Olympus BX60 light microscope equipped with fluorescent epi-illumination and a filter that allowed us to see both green and red colors.

5.8. Electrolytic lesions

Holes of about 2 mm diameter were drilled into the skull above the coordinates (Paxinos and Watson, 1997) of the PVG (AP: -4.2, L: 0.4, V: -6.5 mm), the PIL: AP: -4.7, L: 2.1, V: -6.5 mm), and the MPL (AP: -8.5, L: 2.6, V: -7 mm). Monopolar stainless steel electrodes (0.25 mm in diameter) insulated except for 0.5 mm of the tip (A-M systems, Carlsborg, WA) were introduced. A constant 3 mA DC anodal current produced by a lesion producing device (Stoelting, Wood Dale, Ill) was applied for 10 seconds to produce bilateral or unilateral lesions in the subparafascicular area, and the medial paralemniscal nucleus. Approximately 5 minutes after the current application, the electrodes were removed and the skin sutured. Animals were allowed to survive for 6-7 days.

5.9. Transection of the supraoptic decussations

Holes of about 1x3 mm diameter were drilled into the right side of the skull above the target coordinate (AP= -2.6, L= 3.0, V= 8.6 mm) 75° to the antero-posterior axis. Transections were performed with 2-mm-wide glass knives targeted to cut the supraoptic decussations perpendicularly. Animals were allowed to survive for 6 days following transections.

5.10. Retrograde tracer experiments

5.10.1. Iontophoretic targeting of cholera toxin B subunit (CTB)

Injections of the retrograde tracer cholera toxin B subunit (CTB; List Biological Laboratories, Campbell, CA) were targeted to the PIL (n = 23), the medial preoptic area (n = 6), the arcuate nucleus (n=6), and the MPL (n=29). The relation of injection sites to the position of TIP39 neurons was evaluated by double labeling. Some of the misplaced injections were used as controls. For stereotaxic injections, rats were positioned in a stereotaxic apparatus with the incisor bar set at -3.3 mm. Holes of about 2-mm diameter were drilled into the skull above the target coordinates. Glass micropipettes of 15–20-μm internal diameter were filled with 0.25% CTB dissolved in 0.1 M PB and lowered to the following stereotaxic coordinates (Paxinos and Watson, 2007): AP= -4.7, L= 2.1, V= 6.5 for the PIL, AP = -0.5 mm, L = 0.5 mm, V = 7.8 mm for the medial preoptic area, AP = -2.8 mm, L = 0.2 mm, V = 9.3 mm for the arcuate nucleus, and AP= -8.3, L= 2.4, V: 6.8 mm for the MPL. Once the pipette was in place, the CTB was injected by iontophoresis using a constant current source (51413 Precision Current Source, Stoelting, Wood Dale, IL) that delivered of +6 μA current, which was pulsed on for 7 seconds and off for 7 seconds for 15 minutes. Following injection, the pipette was left in place for 10 minutes with no current, was then withdrawn under negative current. Animals were sacrificed 7 days following tracer injection.

5.10.2. CTB immunolabeling

Every fourth free-floating section was stained for CTB as described above for immunohistochemistry. Sections were incubated overnight in goat anti-CTB (1:10,000; product #703, lot #7032AA, List Biological Laboratories) antiserum at room temperature. Following the application of the primary antibody, sections were incubated in biotin-conjugated horse anti-goat secondary antibody (1:1000, Vector Laboratories) for 1 hour, and then in ABC reagent (1:500, Vectastain ABC Elite kit, Vector Laboratories) for 2 hours. Subsequently, the labeling was visualized by incubation in 0.02% 3,3-diaminobenzidine (DAB; Sigma), 0.08% nickel (II) sulfate and 0.001% hydrogen peroxide in PB for 4 minutes. Sections were mounted, dehydrated and coverslipped with Cytoseal 60 (Stephens Scientific, Riverdale, NJ).

5.10.3. Double labeling TIP39 with CTB

Brain sections of animals injected with CTB were processed for double labeling with CTB and TIP39. Every fourth free-floating section was first stained for TIP39 by using FITC-

tyramide amplification fluorescent immunocytochemistry as described above. Sections were then incubated overnight in goat anti-CTB (1:5,000) at room temperature. Following application of the primary antibody, sections were incubated in donkey Alexa Fluor 594 anti-goat secondary antibody (Life Technologies, Grand Island, NY) for 2h. After washes, sections were mounted and coverslipped with antifade medium (Prolong Antifade Kit; Molecular Probes, Eugene, OR).

5.11. Experiments using PTH2 receptor-expressing viruses

5.11.1. Virus preparation

Two lentiviral vectors were prepared: a HYWH-GFP virus was designed to express a secreted form of histidine[4], tyrosine[5], tryptophan[6], histidine[7]-TIP39 (HYWH-TIP39) an antagonist of the PTH2 receptor (Kuo and Usdin, 2007), plus GFP that remained within infected cells and allowed their visualization, while a control virus expressed GFP only. To produce th HYWH-GFP lentiviral vector, we used a combination of oligonucleotide synthesis, PCR, and conventional subcloning techniques. In the resulting construct, the fibronectin signal sequence was fused to the sequence of the PTH2 receptor antagonist HYWH-TIP39 (Kuo and Usdin, 2007) followed by an IRES sequence and then the sequence of GFP within a lentiviral vector as described previously (Dimitrov et al., 2013). In brief, two oligonucleotides (ATGCTCAGGGGTCCGGGACCCGGGCGGCTGCTGCTGCTGGCAGTCCTGTGCCTG GGGACC and AGGACACGGACCCCTGGAGCCACGCGACGTGGCTTCGGCCCTTCTCGTTCTCCTC GGACCGCGTAATGACC GTAC) were annealed and extended to generate the fibronectin signal sequence and the 5' end of HYWH-TIP39. A PCR reaction containing this product, plus the two following oligonucleotides: GCATGAGCTCGCCGCCACCATGCTCAGGGGTCCGGGA and GCATGGATCCTCAGGGCGCGTCCAGCA, plus a plasmid encoding HYWH-TIP39 produced a fibronectin signal sequence/HYWH-TIP39 fusion sequence that we then cloned into the PmeI site of the lentiviral vector pWPI (Addgene plasmid 12254, contributed by D. Trono, École Polytechnique Fédérale de Lausanne). Following sequencing in the NINDS intramural sequencing facility to determine correct sequence and orientation, viral particles were produced by calcium phosphate-mediated co-transfection of HEK293T cells with this plasmid, psPAX2 (Addgene plasmid 12260; D. Trono), and pMD2.G (Addgene plasmid 12259; D. Trono). A concentrated virus stock was produced by polyethylene glycol precipitation of tissue culture media followed by ultracentrifugation (Kutner et al., 2009). A

titer of approximately 10e10 transducing units/ml was estimated by counting fluorescent cells 72h following infection of HEK293 cells. To produce virus encoding only GFP we processed the plasmid pFUGW-GFP (Addgene # 14883, contributed by D. Baltimore, California Inst Technology) and helper plasmids using the procedures described above for the production of HYWH-encoding virus (Lois et al., 2002).

5.11.2. Virus injection

Using stereotaxic injections (as described below for tracer injections), we targeted these viral vectors bilaterally into the mediobasal hypothalamus immediately lateral to the arcuate nucleus and also into the medial preoptic area, of female rats. Glass micropipettes of 15–20-μm internal diameter were backfilled with virus suspended in sterile saline. Once the pipette was in place, 300 nl of the virus was pressure injected. Pipettes were left in place for 10 min. After virus injections, animals were allowed to recover for 2 weeks before the start of mating.

5.11.3. Validation of the virus injection

After the experiments, the animals were perfused and the position of the virus injection was determined based on the fluorescent visualization of GFP in the infected cells. Based on the design of the virus, it expresses the PTH2 receptor antagonist HYWH-TIP39 and GFP as long es the infected cell is viable. Functional evidence for the *in vivo* effectiveness of the virus has also been recently provided (Dimitrov et al., 2013).

5.12. Measurement of suckling-induced prolactin release

5.12.1. Implantation of jugular cannulae

Jugular catheters were placed on days 9-10 postpartum under gas anesthesia, one day before blood sampling began. Dams received 25-mm-long sterile polyethylene jugular cannulae (Plastics One). The right common jugular vein was exposed, a cannula was inserted into the vessel, secured in place with suture, and pulled through incisions on the skin between the scapulae. The inserted cannulae were filled with heparinized saline and sealed with metal pins.

5.12.2. Blood sampling

Each rat was handled before the blood sampling for 5 m per day for 3 days before the procedure. On the day of the experiment (postpartum days 10-11) at 08.00 h, a first blood

sample was taken, then dams were separated from their pups for 4 hours. After 4 h separation, a second blood sample was obtained 5 min before the pups were returned to their mothers. Suckling usually started immediately, and never longer than 10 m after the return of the pups. Blood samples were taken at 5, 15, 30, and 60 min after pups were reunited with their mother. At each time point, 200 µl blood was obtained and an equal amount of sterile saline was injected into the circulation through the same canullas. Plasma was separated and stored at -20°C until assayed for prolactin.

5.12.3. Prolactin assay

Prolactin was measured with radioimmunoassay kits kindly provided by Dr. Alfred F. Parlow (National Hormone and Peptide Program, Harbor UCLA Medical Center, Torrance, CA, USA). As described previously, our procedure differed slightly from instructions supplied with the kit (Bodnar et al., 2005). The chloramine-T method was used for iodination, and protein A (BactASorb, Human Rt, Gödöllő, Hungary) was used to separate bound and free hormone. LKB Clinigamma software was used for data collection and calculations for curve fitting. Within-assay variance was 10%. Between-assay variance was 14%. The sensitivity of the prolactin assay was 0.5 ng/ml rat plasma (or 25 pg prolactin). All samples were analyzed in duplicate using 50 µl of plasma for each measurement.

5.12.4. Statistical analysis of the prolactin assay data

Statistical analyses were performed using Prism 5 for Windows (GraphPad Software, Inc., La Jolla, CA). Basal plasma prolactin levels between the 2 groups (rats injected with PTH2 receptor antagonist expressing virus and rats injected with control virus) before taking away the pups were compared using Student´s t-test. For the suckling experiment, plasma prolactin levels of the 2 groups were compared using two-way repeated measures ANOVA to evaluate whether the expression of the antagonist had an effect on the prolactin level. To determine at which time points the antagonist injection was effective, Bonferroni Post-Tests for posthoc comparisons were used.

5.13. Conditioned place preference test

The procedure applied is a modification of previously described conditioned place preference tests used to investigate maternal motivation (Mattson et al., 2003; Seip and Morrell, 2009).

5.13.1. Conditioning

On or about the 16th day of pregnancy, 13 control virus and 13 PTH2 receptor antagonist expressing virus injected pregnant rats were moved from their standard white cages to similar size blue cages. As an additional contextual clue for conditioning to pup association, a thick-walled oval orange tray (15 and 20 cm diameters) was placed permanently, with the litter, in the mother's blue cage on postpartum day 6-7.

5.13.2. Testing of preference

Three days later, the mothers were deprived of their pups for 2h and then tested. The experimental apparatus consisted of freshly washed white and blue cages connected by a 20 cm-long tube 12 cm in diameter (Fig. 4). The rat mothers were free to move about within the apparatus. A tray similar to the orange one used for conditioning was placed in the blue cage while a thin-walled black triangular tray (13 x 15 cm) was placed in the white cage. The illumination was the same in the 2 cages, but the tube was considerably darker. The position of the dams was monitored for 1h and the time spent in each compartment calculated.

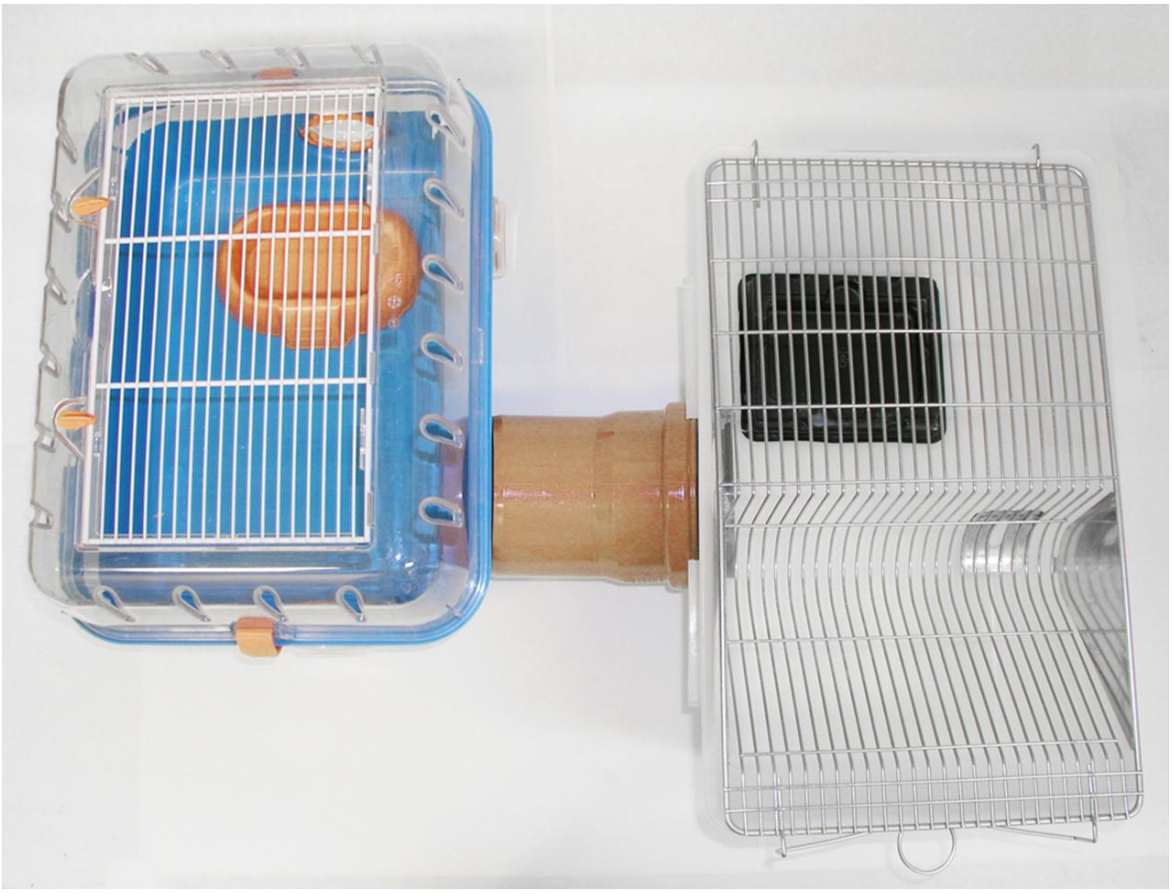

Fig. 4. The apparatus used for conditioned place preference test

5.13.3. Control conditioned place preference test with non-maternal virgin females

A similar experiment was performed with non-maternal virgin female rats (5 control virus and 5 PTH2 receptor antagonist expressing virus injected) to evaluate their preference for the 2 different cages. The rats were moved from their standard white cages into the blue cages with the contextual clue for 3 days (without pups), after which they were tested with the same experimental apparatus as the mothers.

5.13.4. Statistical analysis of the conditioned place preference test data

First, the test was validated with the analysis of time that the control virus injected animals spent in the different compartments using one-way repeated measures ANOVA followed by Bonferroni Post-Tests for posthoc comparisons. To evaluate the time the rats spent in the pup-associated *vs.* control cage, a time preference index was calculated as 100 * (time spent in the pup associated cage – time spent in the control cage) / (time spent in the pup associated cage + time spent in the control cage). The time index is zero if the rats spend the same amount of time in the two cages. The time preference indices of the 2 groups (rats injected with PTH2 receptor antagonist expressing virus and rats injected with control virus) were compared using Student´s t-test. In an additional analysis that focused on the preference of individual animals, spending greater than 20% more time in one cage than the other was used as the cutoff for identifying cage preference. Between-group cage preference comparisons were examined using Chi-square test of independence and Fisher´s exact test.

6. RESULTS

6.1. The gene encoding TIP39

6.1.1. Identification of the gene encoding TIP39

We searched genomic databases with use of the determined partial sequence of purified TIP39 and identified homologous human and mouse sequences (Dobolyi et al., 2002). From these, we predicted sequences for TIP39's precursor: MET**C(R)**Q**M(V)**SRSPR**E(V)**RLLLLLLLLL**L(V)**VPWG**T(V)G(R)P(T)***ASGVALP**L(P)A(V)**GV**F(L)**SLR**A(P)**PGRAWA**G(D)L(P)G(A)S(T)**P**L(R)(P)**RRSLALADDAAFRERARLL AALERR**R(H)**WL**D(N)**-SYM**Q(H)**KLL**L(V)**LDAP. [Bold letters indicate residues that differ between the mouse and human sequences, with the human residue in parentheses after the mouse residue. An asterisk indicates a predicted signal peptide cleavage site and the dash indicates the location of an intron in the genomic sequences. Residues corresponding to the purified peptide are underlined.]

We amplified cDNAs corresponding to this mRNA from mouse and rat hypothalamus, and isolated a clone containing this sequence from a human hypothalamic cDNA library (Dobolyi et al., 2002). The deduced human TIP39 peptide sequence was identical with purified bovine TIP39, whereas the predicted mouse peptide differs at 4 of the 39 residues. Sequences corresponding to the purified peptide were followed by a stop codon and preceded by nucleotides encoding two arginine residues. The entire predicted TIP39 precursor is 100 residues and includes a predicted signal peptide of 30 residues (Fig. 5).

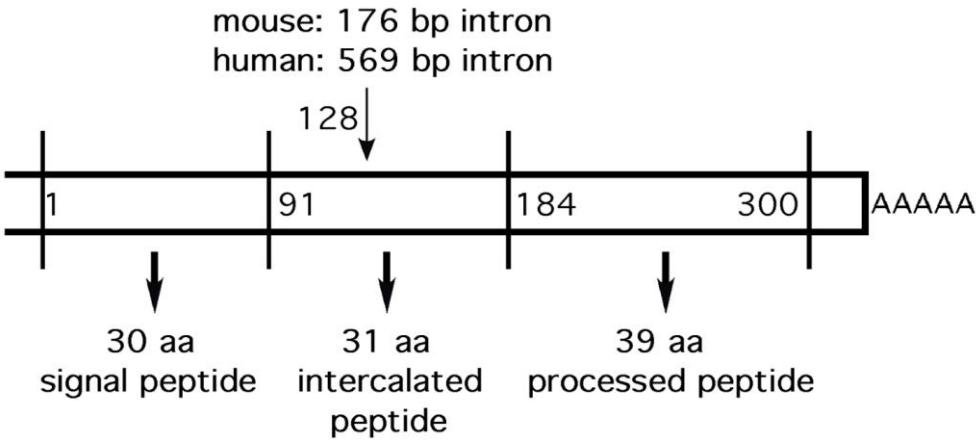

Fig. 5. Structure of mRNA encoding TIP39.

6.1.2. The distribution of TIP39 expression in different organs

With reverse transcription–PCR we found abundant TIP39 mRNA in rat brain (Dobolyi et al., 2002). In addition, testis also expressed TIP39 mRNA but it was not detected in several other different tissues (Fig. 6).

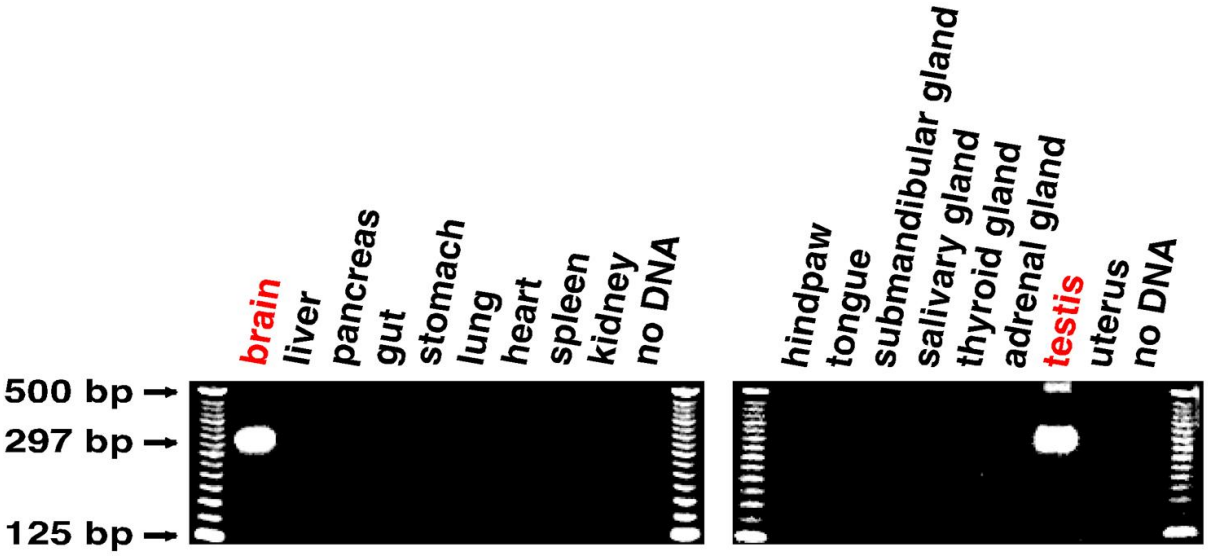

Fig. 6. PCR amplification of TIP39 cDNA from several different rat tissues. The predicted size of the product amplified from cDNA is 297 bp; from genomic DNA it is 594 bp. The figure is from our previously published figure with a slight modification (Dobolyi et al., 2002).

6.2. The distribution of TIP39 neurons in the brain

6.2.1. TIP39-expressing neurons in young adult male rat

TIP39 mRNA-expressing neurons were found by in situ hybridization histochemistry in 2 brain sites in adult male rats (Dobolyi et al., 2003b; Dobolyi et al., 2002). These areas include the medial paralemniscal nucleus in the lateral pons and the periventricular gray of the thalamus (Fig. 7). The latter area may also be referred to as the subparafascicular area because it includes the subparafascicular thalamic nucleus. To visualize the peptide TIP39, an antibody was developed, which labeled neuronal cell bodies with the same distribution as TIP39 mRNA expression (Fig. 7).

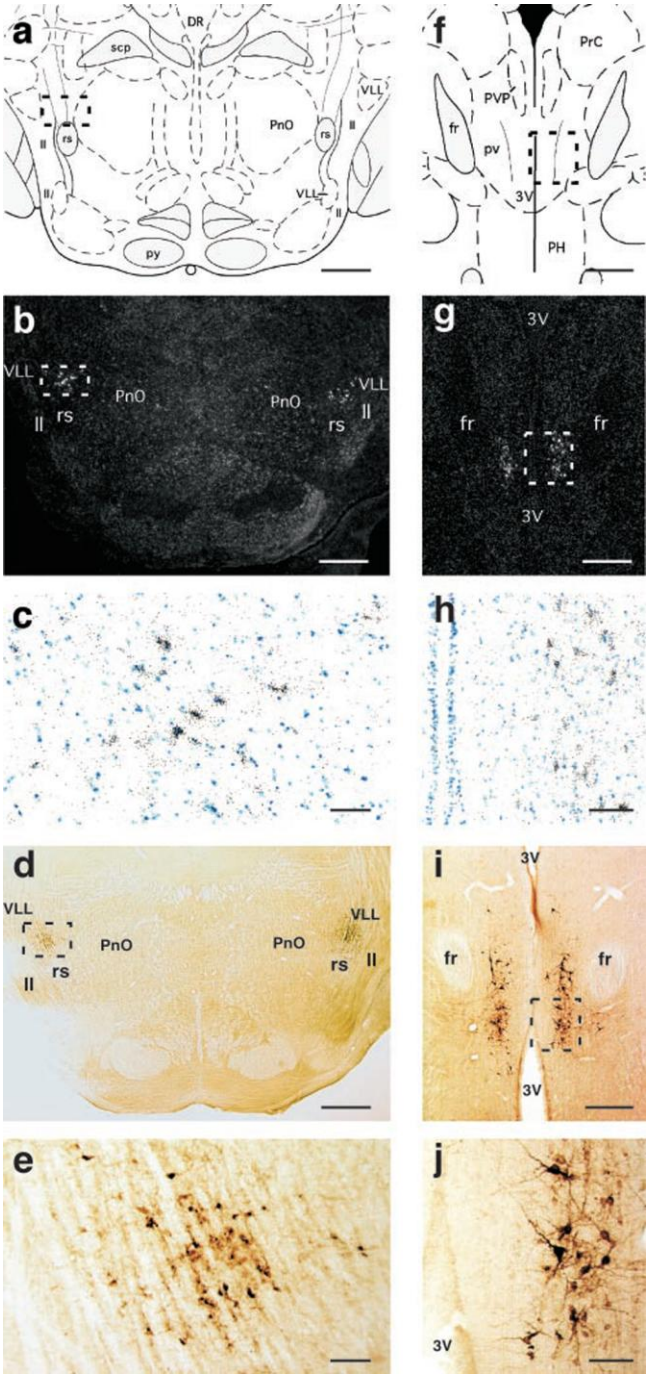

Fig. 7. Brain localization of TIP39-containing cells. (*a*–*e*) medial paralemniscal nucleus at 8.7 mm from the bregma level. (*f*–*j*) periventricular gray of the thalamus at 4.4 mm from the bregma. Drawings indicate the location of the micrographs (*a*, *f*). The localization of TIP39 mRNA detected by *in situ* hybridization histochemistry is shown at low magnification in dark-field micrographs (*b*, *g*) and at greater magnification of the framed areas in bright field (*c*, *h*). The localization of TIP39 protein is demonstrated by peroxidase immunocytochemistry in colchicine-treated animals, shown at low magnification (*d*, *i*) and at greater magnification

of the framed areas (*e*, *j*). Scale bars = 1 mm for *a, b* and *d*, 100 μm for *c*, *e*, *h*, *j*, and 500 μm for *g*, *h*, and *i*. The figure is taken from our previous publication (Dobolyi et al., 2002).

6.2.2. The distribution of TIP39 neurons in the periventricular gray of the thalamus (PVG)

Periventricular thalamic TIP39 neurons constitute the largest TIP39 cell group in the brain of young adult rats and mice (Dobolyi et al., 2003b; Faber et al., 2007). TIP39 neurons in the PVG appear rostrally first above the third ventricle, close to the midline at bregma level -3.8 mm (Fig. 8A1). These TIP39 neurons are located ventral to the central median nucleus of the thalamus, dorsal to the posterior hypothalamic nucleus and medial to the parvicellular ventral posterior nucleus of the thalamus and mostly medial to the magnocellular subparafascicular nucleus. More caudal TIP39 neurons are located more and more dorsally between the midline and the fasciculus retroflexus (Fig. 8A2). Midway through the rostro-caudal extent of the PVG, a few cells appear ventrally to the main cell group and are aligned immediately next to the caudal end of the third ventricle. Additional TIP39 neurons are situated more laterally, ventral to the fasciculus retroflexus. Caudally, the density of TIP39 cells sharply decreases and the cells disappear as the PVG becomes the periaqueductal gray of the midbrain at the level of the posterior commissure without apparent cytoarchitectonic change (Fig. 8A3). In sagittal sections, the distribution of the periventricular TIP39 neurons has a sigmoid shape with a rostro-ventral to postero-dorsal orientation (Fig. 2B,C). These TIP39 neurons in the PVG are intermingled with tyrosine hydroxylase (TH)-containing neurons corresponding to the A11 dopaminergic cell group. Although the distributions of TIP39 and dopaminergic cell bodies largely overlap, the dopaminergic cells are situated somewhat more laterally than the TIP39 cells. Furthermore, we did not detect any TIP39/tyrosine hydroxylase double-labeled cells in the area (Dobolyi et al., 2010).

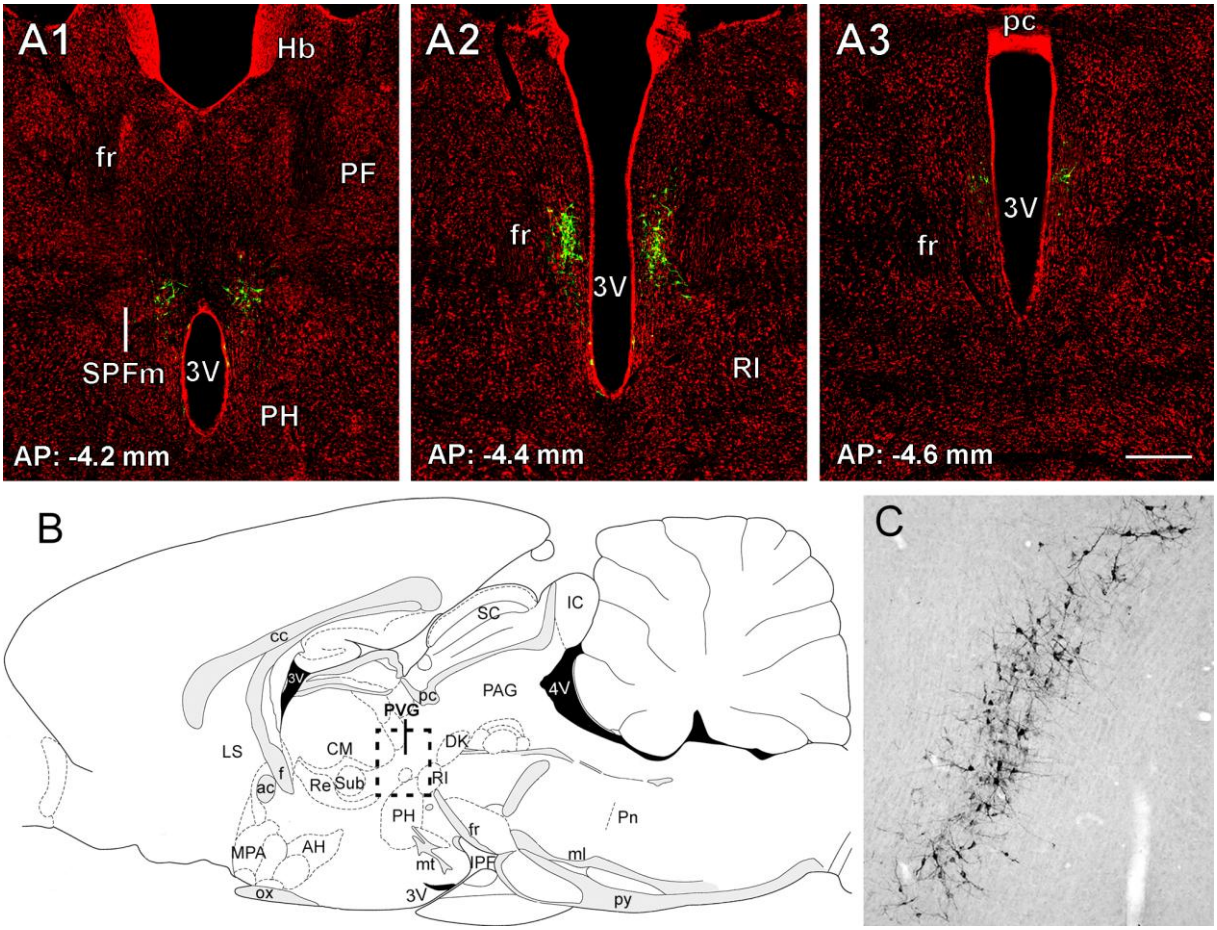

Fig. 8. TIP39 neurons in the periventricular gray of the thalamus. A: TIP39-ir neurons (green) are shown in the PVG in coronal sections labeled with a fluorescent Nissl dye (red) at antero-posterior (AP) coordinates -4.2, -4.4, and -4.6 mm from the bregma level. B: The position of the PVG is shown in a drawing of a sagittal section of the rat brain at 0.4 mm lateral from the midline (Paxinos and Watson, 2007). C: A photomicrograph of a sagittal section corresponding to panel B shows the location of TIP39-ir neurons in the PVG. Scale bar = 500 µm for A and D, and 300 µm for C. Panel A, panels B, C are from our 2 different previous publications, respectively (Dobolyi et al., 2010; Wang et al., 2006a).

6.2.3. The distribution of TIP39 neurons in the medial paralemniscal nucleus (MPL)

Cells of the MPL are distinguished from those in adjacent areas by their organization into dorsolaterally oriented cell columns separated by 20–50-µm wide cell-free zones, probably occupied by fibers of the lateral lemniscus that pass through the region (Varga et al., 2008). The ventral border of the MPL is the rubrospinal tract, which is easily distinguished and clearly separated by the abrupt end of the cell columns. However, lateral to the rubrospinal tract, the MPL extends somewhat ventrally, which gives the nucleus a triangular

shape with ventral, dorsal, and medial angles. In addition, in the rostral half of the MPL, a small group of large acetylcholinesterase-positive cells of the epirubrospinal nucleus is located between the medial part of the rubrospinal tract and the medial part of the MPL. The rostral part of the MPL is embedded between the pedunculopontine tegmental and the retrorubral nuclei, from which the MPL is separated by a zone of lower cell density (Fig. 9E). Medially, the MPL borders on the oral part of the pontine reticular formation and the pedunculopontine tegmental nucleus (Fig. 9B,E). The MPL narrows dorsally between the caudal part of the pedunculopontine tegmental nucleus and the dorsal nucleus of the lateral lemniscus, giving the nucleus a cone shape (Fig. 9B). The lateral border of the MPL is the intermediate nucleus of the lateral lemniscus (Fig. 9B). The caudal borders of the MPL are the region of the A7 noradrenaline cell group medially and the Kölliker-Fuse nucleus laterally (Fig. 9E,F).

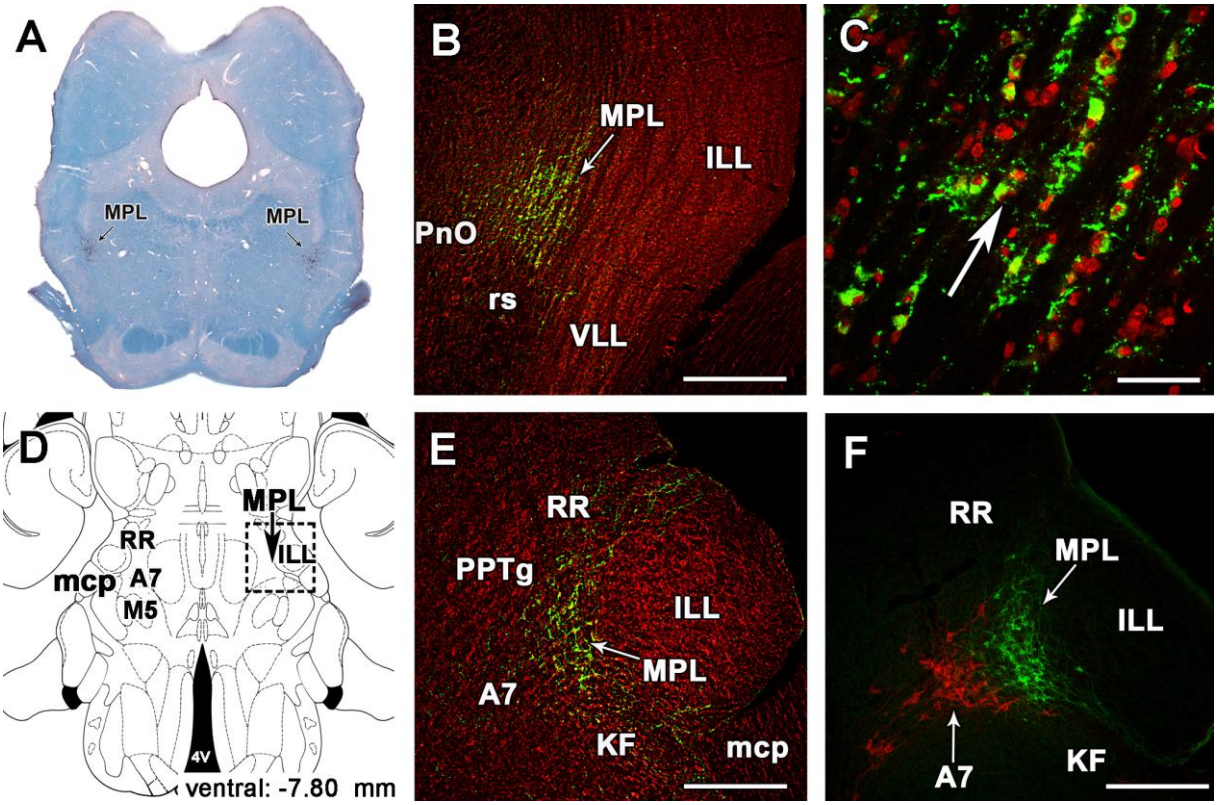

Fig. 9. The medial paralemniscal nucleus (MPL) in the rat. A: The position of TIP39 neurons (black arrows) is shown in a coronal section stained with a combination of Luxol dye to visualize myelinated fibers in blue and cresyl-violet to label cell bodies. B: The MPL is delineated by the distribution of TIP39 neurons (green) in a section labeled with fluorescent Nissl dye (red) at 8.3 mm caudal to the bregma level. C: A high magnification photomicrograph demonstrates the dorsolaterally oriented columnar organization of the MPL.

D: A schematic drawing of a horizontal section 7.8 mm ventral to the surface of the brain (Paxinos and Watson, 1998) shows the position of the MPL by a black arrow. E: A photomicrograph of a horizontal section corresponding to the position of the framed area in D demonstrated the position of the MPL by TIP39-ir (green). F: The same area in a double immunolabeled section shows the relation of TIP39 neurons (green) in the MPL and TH (red) neurons belonging to the A7 noradrenergic cell group. Scale bar = 500 μm for B, E, and F, and 100 μm for C. The panels are modifications of our previously published figures (Varga et al., 2008).

6.2.4. Identification of a third group of TIP39 neurons, the posterior intralaminar complex of the thalamus (PIL)

6.2.4.1. TIP39 expression during ontogenic development

TIP39 expression was investigated during ontogeny, which allowed the identification of a third group of cells in the posterior intralaminar complex of the thalamus (Brenner et al., 2008; Dobolyi et al., 2006b). TIP39 neurons are abundant in this brain region by embyonic day 16.5, and disappear by postnatal day 5 (Fig. 10A). This in sharp contrast to the development of TIP39 neurons in the other thalamic brain region, the periventricular gray of the thalamus, where TIP39 immunioreactivity appears only in the early postnatal period (Fig. 10B), even though TIP39 levels also decrease in the PVG and MPL during the peroid of pubertal development (Dobolyi et al., 2006b).

TIP39 neurons in the PIL are located in the posterior intralaminar thalamic nucleus and some adjacent brain areas including the parvicellular subparafascicular nucleus, and the lateral territory of the caudal zona incerta (Cservenak et al., 2010), which we call the posterior intralaminar complex of the thalamus (PIL). Since there was another neuropeptide, calcitonin gene-related neuropeptide (CGRP) with similar localization of cell bodies as TIP39, we performed double labeling of the 2 peptides and found no double labeled cells in the PIL (Dobolyi et al., 2005). Rather, CGRP cells are located immediately lateral to the TIP39 cell group (Brenner et al., 2008).

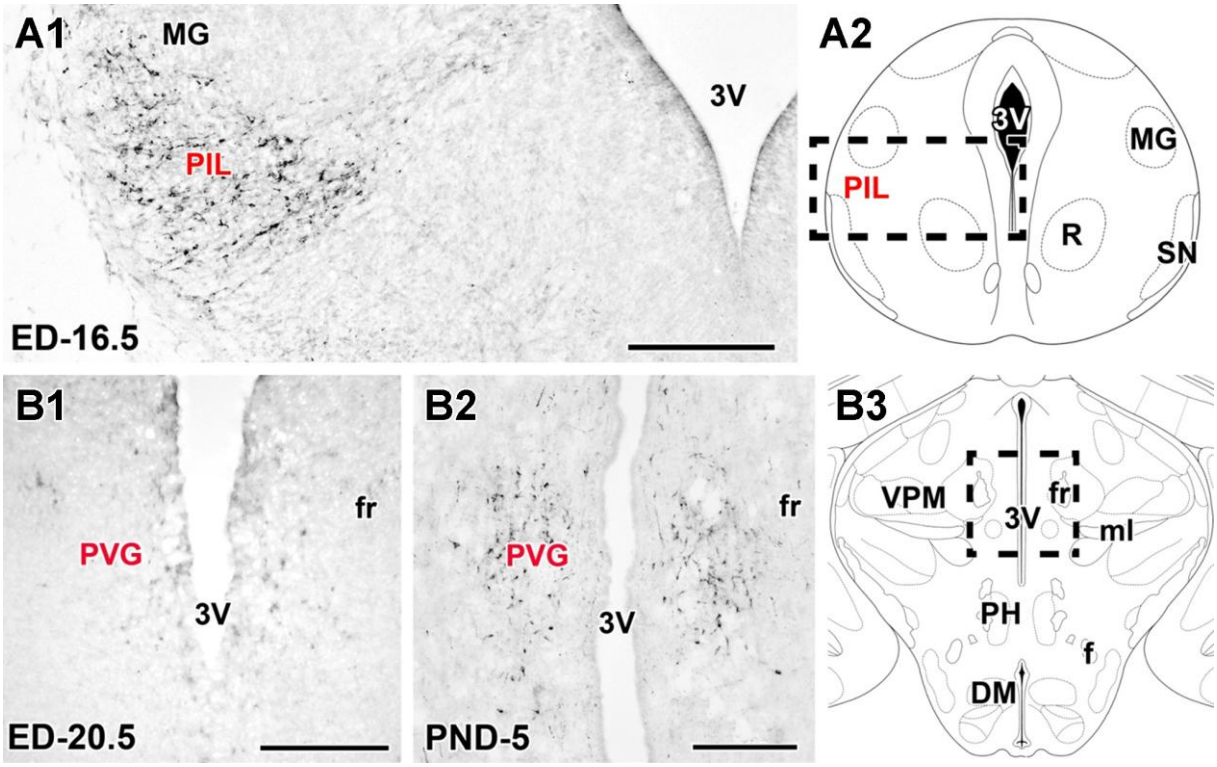

Fig. 10. TIP39 neurons in the posterior intralaminar complex of the thalamus at embryonic day (ED)-16.5. A1: TIP39-ir neurons are abundant by ED-16.5 in the posterior intralaminar complex of the thalamus. A2: A drawing of a coronal brain section at ED-16.5 (Paxinos et al., 1991). The framed area corresponds to panels A. B1: Only a few TIP39-ir neurons are faintly labeled in the periventricular gray of thalamus (PVG) between the third ventricle (3V) and the fasciculus retroflexus (fr) at ED-20.5. B2: TIP39-ir neurons are distinctly labeled in the PVG at PND-5. B3: A drawing of a coronal brain section (Paxinos et al., 1991) indicates the position of the PVG at PND-1. The framed area corresponds to panels B1 and B2. Scale bars = 200 μm for A1, 250 μm for B1, and 300 μm for B2. The panels are selected from different figures of our previous publication (Brenner et al., 2008).

6.2.4.1. Chemoarchitecture of the PIL

In seeking to improve demarcation of the posterior intralaminar complex, we investigated the distribution of calcium-binding proteins in and around the PIL area in mother rats (in order to be able to detect TIP39 neurons). Parvalbumin-immunoreactive (PV-ir) neurons were present in the substantia nigra, at the PIL's ventral border, and in the anterior pretectal area along its dorsomedial border. While the abundance of PV-ir fibers in the medial geniculate body and medial lemniscus make the PIL's dorsolateral and medial borders easy to delineate, their low density throughout the PIL, peripeduncular area, and the triangular

subdivision of the posterior thalamic nucleus make it less useful for distinguishing the PIL's lateral and dorsal borders (Fig. 11).

The distribution of calbindin (CB) immunoreactivity contrasted sharply with that of PV-ir. While the density of CB-ir cell bodies was low in most brain regions adjacent to the PIL, it was high in both the PIL and in the PIL's immediate dorsal neighbor, the triangular subdivision of the posterior thalamic nucleus. TIP- and CB-ir cell bodies were evenly distributed within the PIL. While almost all TIP39-ir neurons contained CB immunoreactivity the PIL also contained neurons negative for TIP39 that were positive for CB. Since the distributions of TIP39 neurons and calcium-binding proteins in the posterior intralaminar thalamic nucleus, the parvicellular subdivision of the subparafascicular nucleus, and the lateral subdivision of the zona incerta appear to be indistinguishable, we concluded that the PIL comprises all three areas.

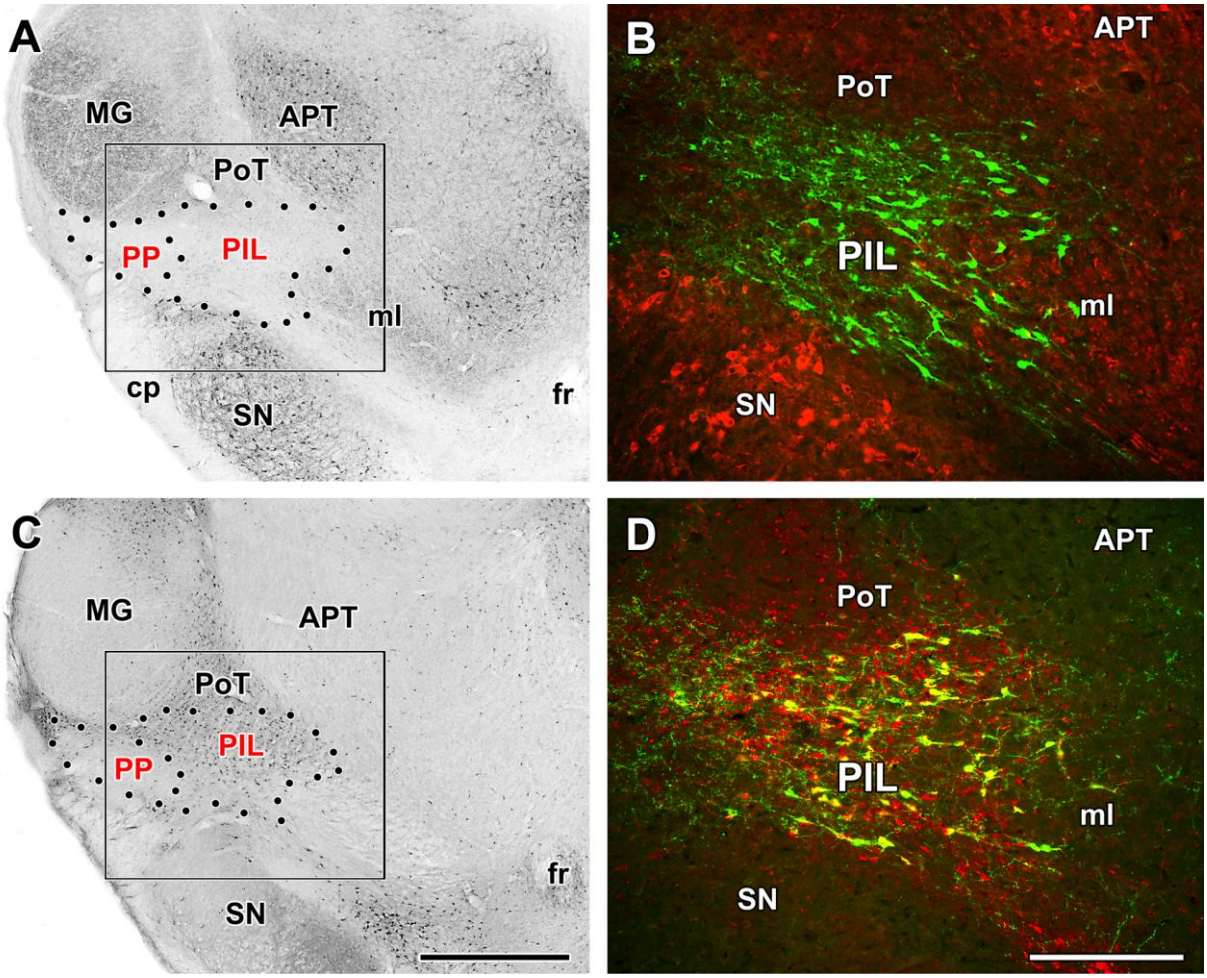

Fig. 11. Chemical topography of the posterior intralaminar complex of the thalamus (PIL). A: Localization of parvalbumin-ir neurons. Parvalbumin-ir neurons are abundant in the anterior pretectal area (APT) and in the substantia nigra (SN). In addition, a high density of

parvalbumin-ir fiber terminals is present in the medial geniculate body (MG), while only a few labeled terminals are found in the PIL, the peripeduncular area (PP), and the triangular subdivision of the posterior thalamic nucleus (PoT). B: The fluorescent image of a section double labeled with parvalbumin (red) and TIP39 (green) corresponding to the framed area in A indicates that the distribution of TIP39 neurons does not overlap with that of parvalbumin-ir neurons as TIP39 neurons are confined to the PIL. C: Localization of calbindin-ir neurons in and around the PIL. Calbindin-ir neurons are present in the PIL and PoT but are absent in the MG, APT, SN, and PP. D: The fluorescent image of a section double labeled with calbindin (red) and TIP39 (green) corresponding to the framed area in C indicates that the distribution of TIP39 neurons overlap with that of calbindin-ir neurons in the PIL but not in the PoT. It is also visible that the majority of TIP39 neurons express calbindin (double labeling appears yellow). Scale bar = 1 mm for C and 400 μm for D.

6.3. TIP39- and PTH2 receptor-containing neuronal networks and fibers

6.3.1. TIP39- and PTH2 receptor-containing neuronal networks and fibers in rodents

TIP39 fibers are abundant in a variety of limbic, endocrine, nociceptive and auditory brain regions including the medial prefrontal cortex, the nucleus accumbens, the lateral septum, the paraventricular thalamic nucleus, the fundus striati, a variety of hypothalamic and amygdaloid areas (Fig. 12), the periaqueductal gray, the superior and inferior colliculi, the lateral parabrachial nucleus, the locus coeruleus and subcoeruleus areas, the paraolivary nuclei, and the nucleus of the solitary tract (Dobolyi et al., 2003b). The distribution pattern of TIP39 fibers was found to be very similar to that of the PTH2 receptor (Fig. 13).

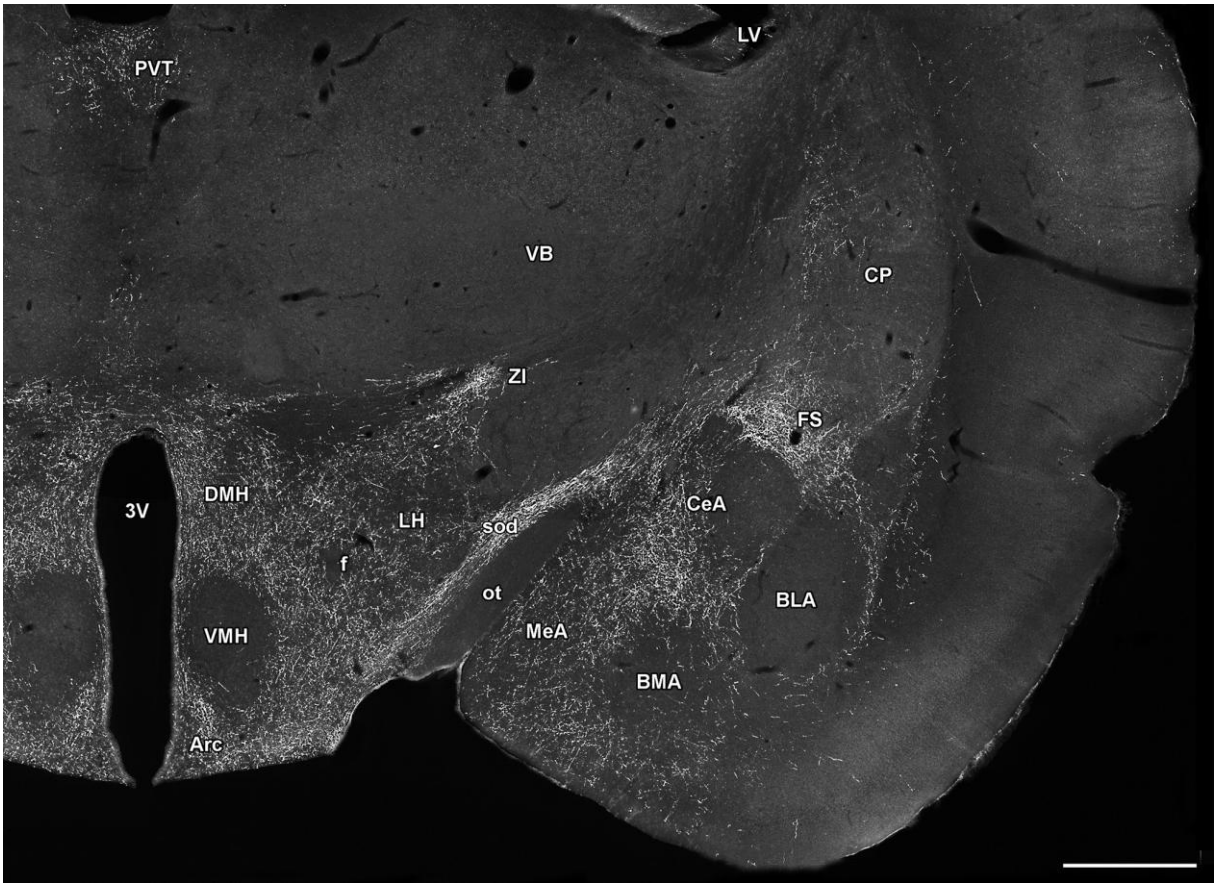

Fig. 12. The localization of TIP39-ir fibers in the diencephalon, and the amygdala. The photomicrograph demonstrates the topographically organized distribution of TIP39-ir fibers in a coronal section of the rat brain at the level of the tuberal region of the hypothalamus. While some nuclei such as the paraventricular thalamic nucleus (PVT), the dorsomedial nucleus (DMH), the arcuate nucleus (Arc), and the fundus striati (FS) contain dense fiber networks, and a medium density of TIP39 fibers are present in the lateral hypothalamic area (LH), the central and medial amygdaloid nuclei (CeA and MeA), TIP39 fibers are absent in most thalamic regions, the ventromedial hypothalamic nucleus (VMH), or the basolateral amygdaloid nucleus (BLA). Scale bar = 1 mm. The figure is a modification of a panel from our previous publication (Dobolyi et al., 2006a).

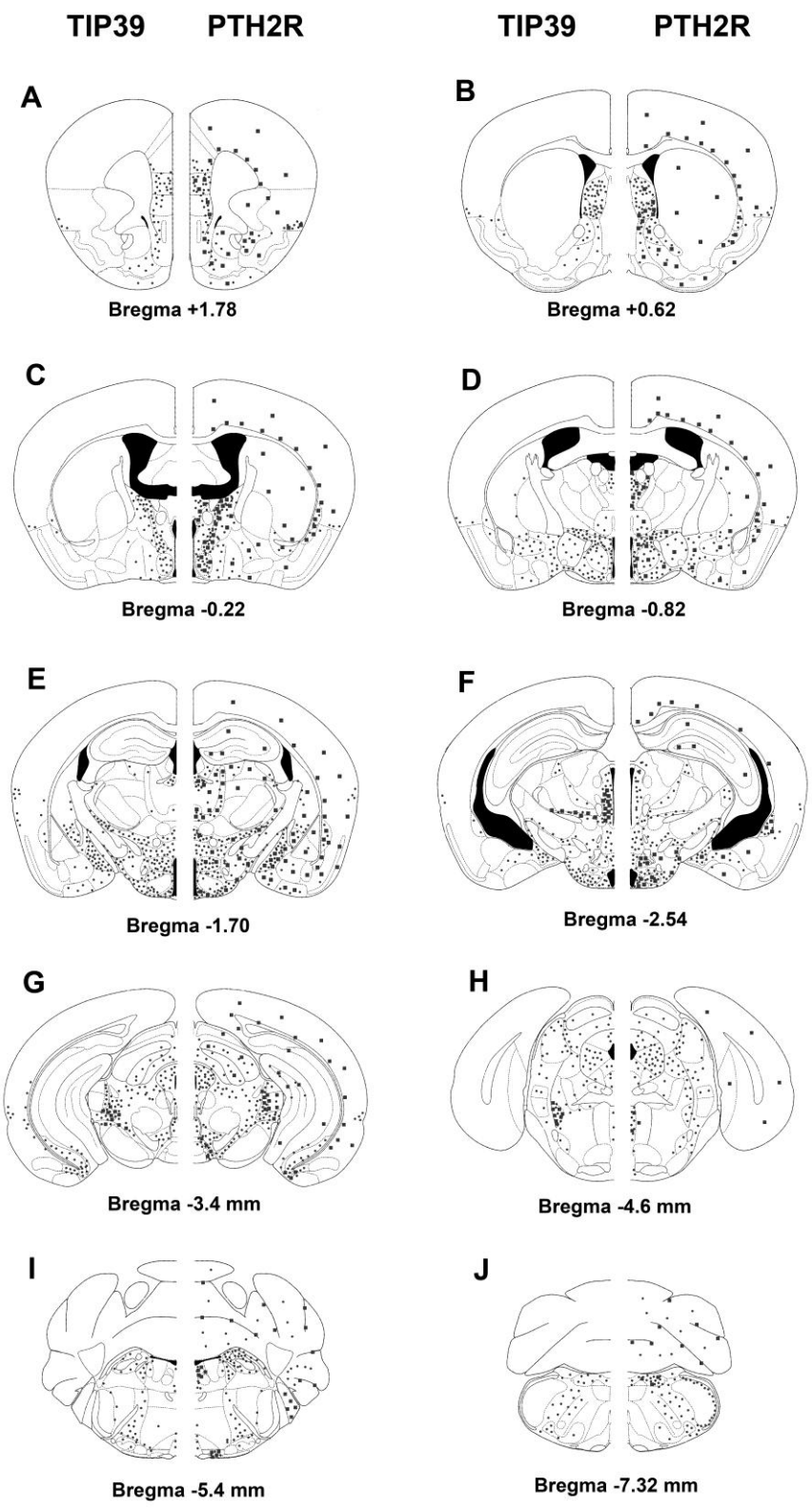

Fig. 13. Schematic diagrams demonstrate the distribution of TIP39 (left side) and the PTH2R (right side) in the brain of mice. The diagrams are modifications from a mouse stereotaxic atlas (Franklin and Paxinos, 1997). Dots represent fibers and fiber terminals, while squares represent cell bodies. The figure is taken from our previous publication (Dobolyi et al., 2010).

The distribution of TIP39-ir and PTH2 receptor-ir fibers also shows remarkable similarities within particular brain regions (Dobolyi et al., 2006a; Faber et al., 2007) In the preoptic region, for example, a high density of TIP39- and PTH2 receptor-ir fibers is present in the medial preoptic nucleus whereas a low density of TIP39- and PTH2 receptor-ir fibers is seen in other parts of the medial preoptic area and the lateral preoptic area (Fig. 14). In the anterior hypothalamus, a high density of TIP39- and PTH2 receptor-ir fibers is present in the parvicellular subdivisions of the paraventricular nucleus and in the periparaventricular zone. The latter is particularly conspicuous on the side of the magnocellular subdivisions of the paraventricular nucleus, which lack of TIP39- and PTH2 receptor-ir fibers. A moderate density of TIP39- and PTH2 receptor-ir fibers is present in the periventricular nucleus and the anterior hypothalamic nucleus whereas only a few immunoreactive fibers can be seen in the lateral hypothalamic area and the supraoptic nucleus, and no immunoreactive fibers are present in the suprachiasmatic nucleus. In the middle part of the hypothalamus, a high density of TIP39- and PTH2 receptor-ir fibers was found in the ventrolateral subdivision of the ventromedial nucleus, and in the dorsomedial and arcuate nuclei (Dobolyi et al., 2006a; Dobolyi et al., 2003b; Faber et al., 2007).

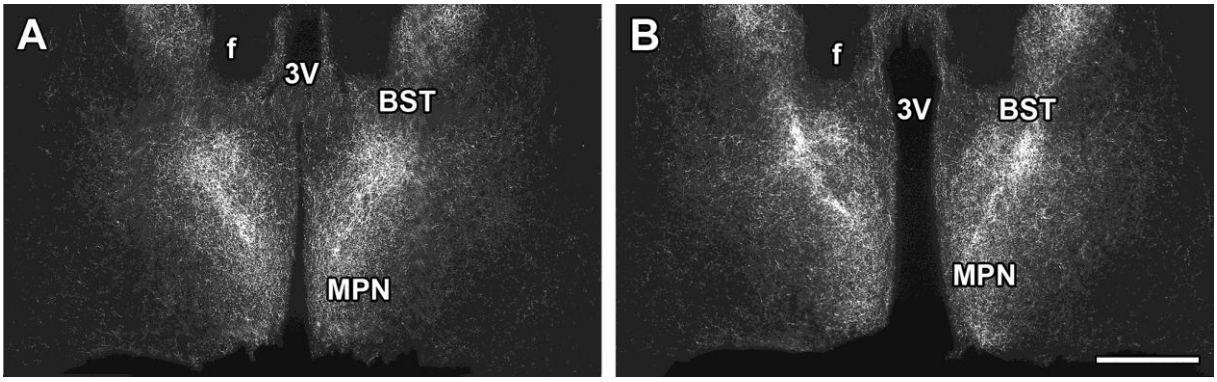

Fig. 14. Comparison of TIP39 and PTH2 receptor immunolabeling in the preoptic region of female mice. Sections were labeled using fluorescent amplification immunocytochemistry. The distribution of PTH2 receptor-immunoreactive fibers (A) looks strikingly similar as the distribution of TIP39-immunoreactive fibers (B). Both immunoreactivities are intense in the bed nucleus of the stria terminalis (BST), particularly in its ventral subdivision, parts of the medial preoptic area, and in the medial preoptic nucleus. Scale bar = 500 μm. The panels are taken from a figure of our previous publication (Faber et al., 2007).

6.3.2. Distribution of PTH2 receptor-expressing cell bodies

Since PTH2 receptor-containing cell bodies were not or only faintly immunolabeled, we used X-gal histochemistry in mice expressing the beta-galactosidase enzyme driven be the PTH2 receptor promoter to describe the distribution of PTH2 receptor expressing neurons (Faber et al., 2007). This distribution was essentially identical to the distribution of PTH2 receptor mRNA expressing neurons detected by in situ hybridization histochemistry (Table 2) described in rodents (Dobolyi et al., 2006a; Faber et al., 2007) and also in macaque (Bagó et al., 2009).

Most brain regions that contain PTH2 receptor-ir fibers also contained PTH2 receptor-expressing neurons with a very similar distribution (Dobolyi et al., 2006a; Faber et al., 2007). For example, PTH2 receptor-expressing neurons are abundant in many regions of the hypothalamus. In the preoptic region, a high density of PTH2 receptor-expressing neurons is present in the medial preoptic nucleus whereas a low density of PTH2 receptor-expressing neurons is seen in other parts of the medial preoptic area (Fig. 15A,B). In the anterior hypothalamic region, a moderate density of PTH2 receptor-expressing neurons is present in the paraventricular and periventricular nuclei whereas the anterior hypothalamic nucleus contains a low density of PTH2 receptor-expressing neurons (Fig. 15C). In the middle portion of the hypothalamus, a high density of PTH2 receptor-expressing neurons is present in the arcuate nucleus whereas a moderate density was observed in the dorsomedial and perifornical hypothalamic nuclei, and some parts of the lateral hypothalamic area including the so-called far-lateral hypothalamus (Forel´s field) immediately next to the internal capsule (Fig. 15D). In the posterior hypothalamus, a high density of PTH2 receptor-expressing neurons was present in the medial subdivision of the superior mamillary nucleus (Fig. 15A,C) while its lateral subdivision (Fig. 15A,C), and the ventral premamillary, and the tuberomamillary nuclei contained a moderate density of PTH2 receptor-expressing neurons. In contrast, the medial and lateral nuclei of the mamillary body did not contain PTH2 receptor-expressing neurons (Dobolyi et al., 2006a; Faber et al., 2007).

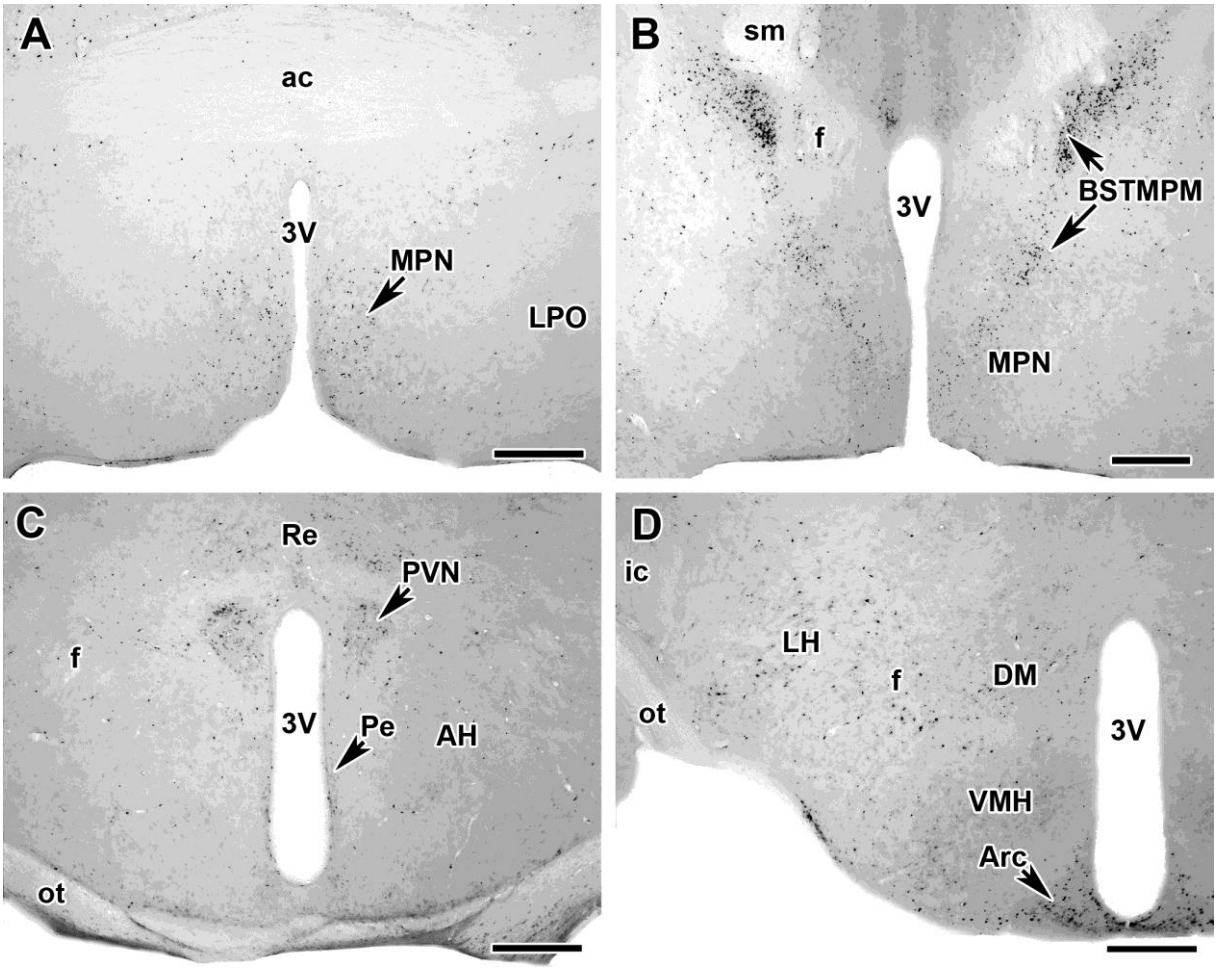

Fig. 15. PTH2 receptor-expressing neurons in preoptic and hypothalamic regions of the mouse brain. A: PTH2 receptor-expressing neurons are demonstrated by X-gal histochemistry in the medial preoptic nucleus of a knock-in transgenic mouse expressing β-galactosidase driven by the PTH2 receptor promoter. B: X-gal histochemistry in the bed nucleus of the stria terminalis (BST) of a knock-in transgenic mouse expressing β-galactosidase driven by the PTH2 receptor promoter. PTH2 receptor-expressing neurons are particularly abundant in the postero-medial part of the medial subdivision of the BST (arrows). C: PTH2 receptor-expressing neurons are demonstrated by X-gal histochemistry in the paraventricular and periventricular hypothalamic nuclei of a knock-in transgenic mouse expressing β-galactosidase driven by the PTH2 receptor promoter. PTH2 receptor-expressing neurons are also present in the reuniens thalamic nucleus. D: PTH2 receptor-expressing neurons are demonstrated by X-gal histochemistry in the middle part of the hypothalamus of a knock-in transgenic mouse expressing β-galactosidase driven by the PTH2 receptor promoter. The density of PTH2 receptor-expressing neurons is very high in the arcuate nucleus and high in the lateral hypothalamic area, the perifornical, and dorsomedial hypothalamic nuclei. Scale

bars = 300 μm for A, B, C, and D. The figure is taken from our previous publication (Faber et al., 2007).

6.3.3. Mapping of the expression of the PTH2 receptor in the human brain by RT-PCR

Human brain tissue samples yielded 2-10 μg total RNA. When run on denaturing formaldehyde gels, the intensity of the 28S rRNA band was at least equal to that of the 18S rRNA band in all RNA samples, suggesting acceptable RNA quality. When these RNA samples were reverse transcribed and amplified using PTH2 receptor specific primer pairs, a single band appeared, as shown in Fig. 16. The PCR product length corresponded to the expected 440 bp suggesting appropriate specific PCR products for the primer pair, which was also confirmed by sequencing (Bagó et al., 2009). A band with high intensity signal was found for samples from the septum, the caudate nucleus, the medial geniculate body, the medial hypothalamus, the pretectal area, the pontine tegmentum, and the cerebellar cortex (Fig. 16). A lower intensity band was found for the frontal cortex, hippocampus, amygdala, lateral geniculate body, subthalamic nucleus, ventral tegmental area, dorsal vagal complex, and the spinal trigeminal nucleus (Fig. 16). In contrast, no band was detected for the ventral thalamus, the mediodorsal thalamic nucleus, the pulvinar, the substantia nigra, the pontine nuclei, the ventrolateral medulla, and the inferior olive (Fig. 16). There were 9 brain regions analyzed in samples from 2 different brains. Samples from the hippocampus, the subthalamic nucleus, and the pontine reticular formation resulted in indistinguishable PCR bands. The ventral thalamus, the mediodorsal thalamic nucleus, and the pontine nuclei did not contain detectable PTH2 receptor mRNA in either brain. The pretectal area, the pontine tegmentum, and the cerebellar cortex were also all positive for PTH2 receptor but the intensity of the band was lower in the samples from the second brain (Bagó et al., 2009). Using primers specific for the housekeeping gene GAPDH resulted in bands of the expected length of 423 bp with about the same intensity for all the samples except for the no RNA negative control (Fig. 16).

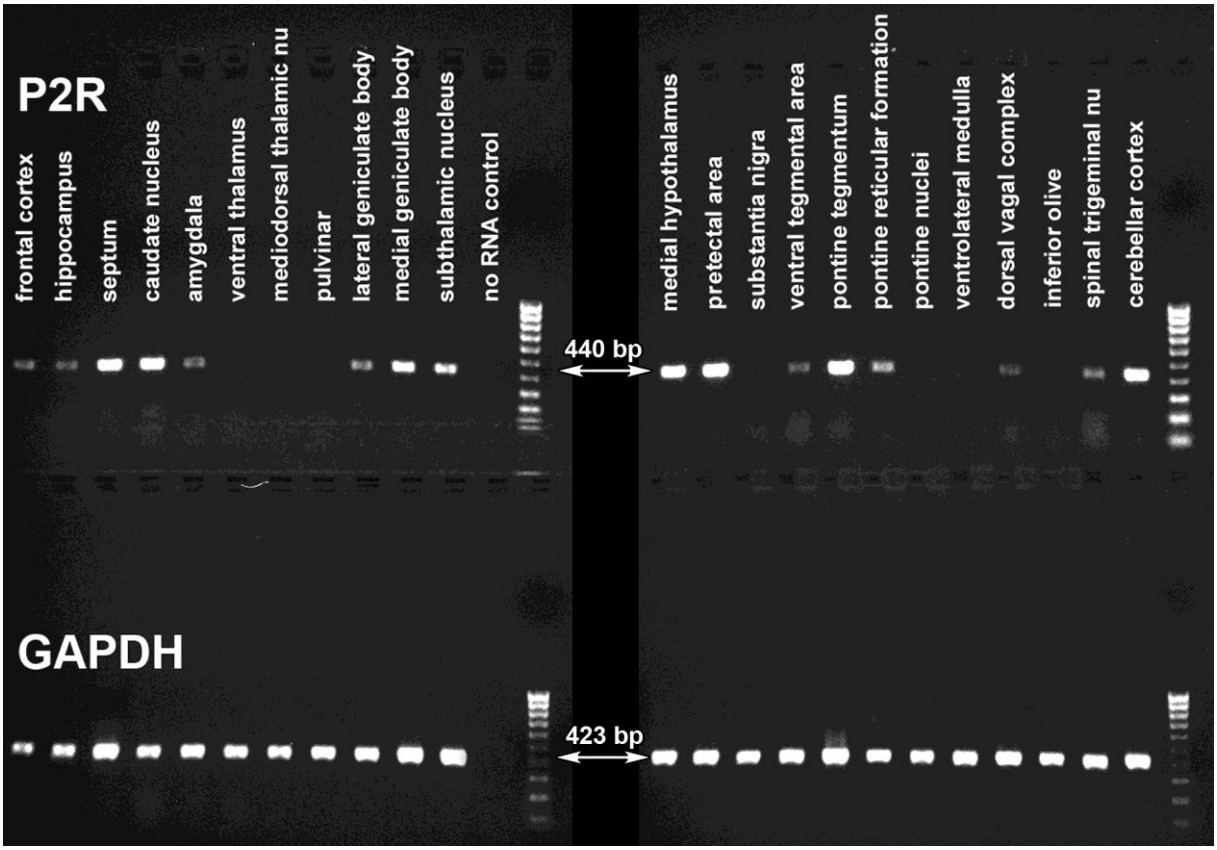

Fig. 16. Expression of the PTH2 receptor in the human brain detected by RT-PCR. Products of PCR reactions performed using cDNA templates from different human brain regions were run on gels. In the upper line, PTH2 receptor-specific 440 bp PCR products are visible. The positive bands in several brain areas suggest a widespread expression of the PTH2 receptor. In the lower line, bands of 423 bp from control PCR reactions performed using primers specific for the housekeeping gene GAPDH are present. The figure was taken from our previous publication (Bagó et al., 2009).

6.3.4. Distribution of PTH2 receptor immunoreactivity in the human brain

PTH2 receptor-ir fibers had a widespread distribution in several brain areas (Bagó et al., 2009), as shown below (Table 2). The hypothalamus contained some dense areas of PTH2 receptor-ir nerve fibers and terminals. A particularly dense network of PTH2 receptor-ir fibers was seen in the medial preoptic area (Fig. 17A,B), in contrast to the low density in the lateral preoptic area. The paraventricular (Fig. 17D) and infundibular nuclei (Fig. 17E) also contained a very dense fiber network, with PTH2 receptor-ir fibers projecting towards the median eminence where very intense PTH2 receptor immunolabeling was visible, particularly in the external layer. Immunopositive fibers were also numerous throughout the entire lateral

hypothalamic area, the supraoptic (Fig. 17B), dorsomedial, posterior hypothalamic, tuberomamillary and premamillary nuclei. A moderate to high density of PTH2 receptor-ir fibers were present in the anterior hypothalamic, ventromedial, perifornical, and subthalamic nuclei, as well as in the nuclei of the mamillary body, whereas only a few scattered PTH2 receptor-ir fibers were detected in the suprachiasmatic nucleus (Fig. 17B).

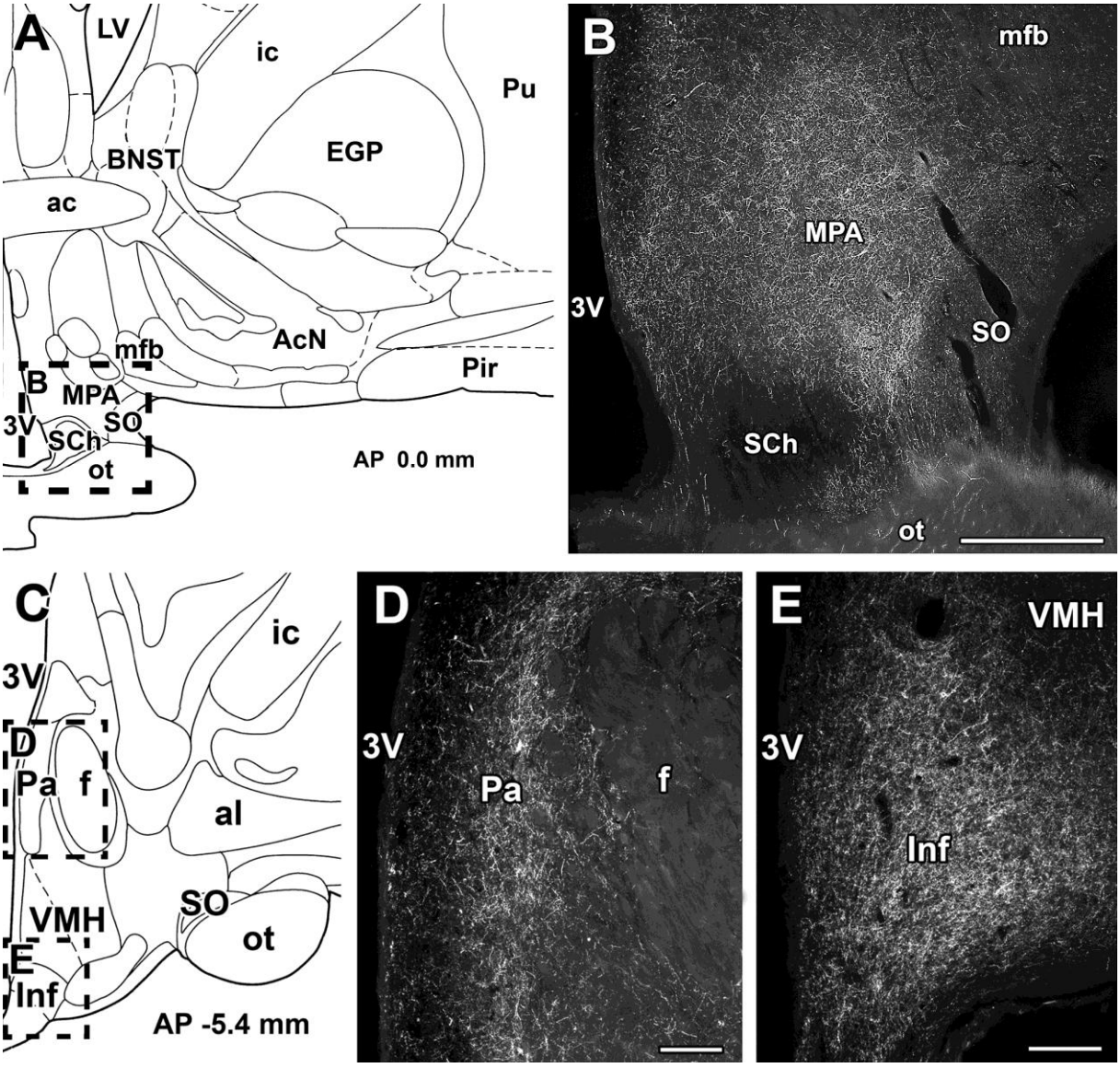

Fig. 17. Immunolabeling of the PTH2 receptor in the human diencephalon. Photomicrographs demonstrate PTH2 receptor immunoreactivity visualized by FITC-tyramide fluorescent amplification immunocytochemistry. The presence of PTH2 receptor-ir fibers is demonstrated in coronal sections of the human diencephalon. A - A schematic drawing shows a part of the human brain at the level of the preoptic area in the coronal plane. The framed area indicates the field in B. B - A dense network of PTH2 receptor-ir fibers is present in the medial preoptic area. In contrast, the density of PTH2 receptor-ir fibers is very low in the supraoptic nucleus,

and PTH2 receptor-ir fibers are absent in the suprachiasmatic nucleus. C - A schematic drawing shows a part of the human brain at the level of the paraventricular nucleus in the coronal plane. The framed areas correspond to fields in D, and E, respectively. D - A high density of PTH2 receptor-ir fibers is present in the hypothalamic paraventricular nucleus. E - The infundibular nucleus contains a high density of PTH2 receptor-ir fibers. Schematic drawings (A, and C) are modifications from an atlas of the human brain (Mai et al., 1997). In agreement with the scaling of this atlas, antero-posterior coordinates (AP) are indicated from the level of the anterior commissure set as zero. Scale bars: 1 mm for B, and 500 μm for D, E, and F. The figure was taken from our previous publication (Bagó et al., 2009).

Table 2. Summary of the location of PTH2 receptor mRNA and PTH2 receptor-ir fibers in human and macaque, and their comparisons to mouse data. The table was taken from our previous publication (Bagó et al., 2009).

Area	**mRNA by RT-PCR in human**	**mRNA by ISHH in macaque**	**Cell bodies in mice**	**PTH2 receptor-ir fibers in human**	**PTH2 receptor-ir fibers in mice**
Forebrain					
Cerebral cortex					
Frontal cortex	+		+		0
Insular cortex			++	+	+
Hippocampus	+	+	+		0
Septum	+++				
Medial septal nucleus			0		0
Lateral septal nucleus			+++		++
Amygdala	+				
Central nucleus		+++	++		++
Basal nuclei		+	+		0
Lateral nucleus		+	+		0
Medial nucleus		++	++		++
Cortical nucleus		+	+		+
Basal ganglia					
Caudate nucleus	+++	+	++		0
Putamen		0			
Globus pallidus		0	+		0
Claustrum			++		+

Nucleus accumbens			+		++
Substantia innominata		+	+		+
Diencephalon					
Thalamus					
Anterior thalamic nuclei		0	0	+	0
Midline thalamic nuclei		+	++	++	++
Lateral thalamic nuclei		0	0	+	+
Ventral thalamic nuclei	0	0	0	0	0
Reticular nucleus		0	0	0	0
Mediodorsal thalamic nucleus	0	0	0	0	0
Habenular nuclei		+	+	+	+
Posterior thalamic nuclei		0	0	+	+
Peripeduncular area		+	+	+	+
Suprageniculate thalamic nucleus		+	+	+	+
Medial geniculate body	+++				
dorsal nucleus		0	0	0	0
ventral nucleus		++	++	+	+
medial nucleus		+++	+++	++	++
Lateral geniculate body	+	+	+	+	+
Pulvinar	0	0			
Hypothalamus	+++				
Medial preoptic area		+++	+++	+++	+++
Lateral preoptic area		+	+	+	+
Supraoptic nucleus		+	+	++	++
Supraoptic decussations				++	++
Suprachiasmatic nucleus		0	0	0	0
Anterior hypothalamic nucleus		+	+	+	+
Paraventricular nucleus		+++	++	+++	+++
Periventricular nucleus		++	++	++	++
Arcuate (infundibular) nucleus		+	++	+++	+++
Median eminence				+++	+++
Ventromedial nucleus		+	+	+	+
Dorsomedial nucleus		+	+	++	++
Lateral hypothalamic area		++	+	++	++
Perifornical nucleus		+	+	+	+
Posterior hypothalamic nucleus		+	+	++	++
Tuberomamillary nucleus		+	+	++	++
Premamillary nuclei		+	+	++	++
Mamillary body					
Superior mamillary nucleus		+	++	+	++

Medial mamillary nucleus		0	0	0	0
Lateral mamillary nucleus		0	0	+	++
Subthalamic nucleus	++	+	+	+	+
Brainstem					
Midbrain					
Zona incerta		+	++	++	+++
Substantia nigra	0	0	0	0	0
Red nucleus		0	0	0	0
Subbrachial nucleus		+	+	++	++
Praetectal area	+++	+	+	++	++
Superior colliculus		+++	++	++	++
Inferior colliculus		+	+	++	++
Parabigeminal nucleus		+++			
Periaqueductal gray		++	++	+++	+++
Dorsal raphe nucleus		+++	++	++	+++
Ventral tegmental area	+	+	++	++	+++
Oculomotor nuclei		*0*	*0*	*0*	*0*
Pons					
Lateral lemniscal nuclei		0	0	0	0
Medial paralemniscal nucleus		0	0	+	+
Pontine tegmentum.	+++	++	++	++	++
Parabrachial nuclei		+	+		
medial				+	+
lateral				+++	+++
Pontine nuclei	0	0	0	0	0
Superior olive		0	0	+	+
Pontine reticular formation	+	+	0	+	+
Principal trigeminal nu.		+	+	++	++
Motor trigeminal nucleus		0	0	0	0
Pontine raphe nucleus		0	0	+	++
Vestibular nuclei		0	0	+	+
Medulla Oblongata					
Cochlear nuclei				0	0
Spinal trigeminal nucleus	+		+	+++	+++
Prepositus hypoglossal nucleus			0	0	0
Medullary reticular formation	0		0	+	+
Inferior olive	0		0	0	0
Dorsal vagal complex	+				
Nucleus of the solitary tract			++	++	++
Dorsal motor vagal nucleus			0	0	0

Area postrema		0	0	0
Motor hypoglossal nucleus		0	0	0
Nucleus ambiguus		0	0	0
Medullary raphe nuclei		0	0	0
Cerebellum				
Cortex	+++	++		+
Nuclei		0		0

The average number of labeled cells per section in the nucleus is none (0), 1-10 (+), 11-20 (++), or over 20 (+++). Similarly, the density of PTH2 receptor-ir fibers and fiber terminals is represented as none to low (0), moderate (+), high (++), and very high (+++). The density of PTH2 receptor immunolabeling in the hypothalamus and medulla oblongata is determined as the average of 2 brains. The data are based on our previous studies (Bagó et al., 2009; Faber et al., 2007).

6.4. Neuronal connections of TIP39 neurons

6.4.1. Mapping of the disappearance of TIP39 fibers following selective lesion of TIP39 cell groups

Bilateral lesions of TIP39 cell groups resulted in a disappearance of TIP39 fibers from their target areas (Dobolyi et al., 2003a). Unilateral lesions also caused a reduced density of TIP39 fibers ipsilateral to the lesion. We found no obvious reduction contralateral to the lesion in any brain region as compared to intact animals suggesting predominantly ipsilateral projections. The residual density was typically somewhat higher for unilateral than bilateral lesions suggesting some contribution of contralateral projection to TIP39 fibers in some brain regions (Cservenak et al., 2010; Dobolyi et al., 2003a). Still, the results of unilateral lesions are shown for demonstration because of the apparently striking difference between the two sides of the brain in the same section.

6.4.1.1. The effects of lesioning TIP39 cells in the PVG on TIP39 fibers

In the medial prefrontal cortex including the prelimbic, the infralimbic and the dorsal peduncular cortices, the TIP39-containing fibers disappeared after the lesions (Dobolyi et al., 2003a). This was best observed in the infralimbic cortex (Fig. 18A) as the normal density of TIP39 fibers is the highest in this part of the medial prefrontal cortex. In the nucleus accumbens, where TIP39-containing fibers are normally present in the shell and cone (anterior medio-dorsal part or rostral pole) portions but not in the core portion, almost all the

fibers disappeared following PVG lesions. The high density of TIP39-containing fibers that is normally present in the lateral septum also disappeared completely in PVG lesioned rats (Fig. 18B). In the bed nucleus of the stria terminalis, the highest density of TIP39-containing fibers is in the medial division, with a particularly dense network in the anterior part, which disappeared following PVG lesions (Fig. 18C). The TIP39-containing fibers did not disappear from the hypothalamus following PVG lesions but a sharp reduction was observed in some areas including the paraventricular (Fig. 18D) and the dorsomedial nucleus. In the intact rat, the thalamus and the hippocampus contain very few TIP39-containing fibers. The greatest density is in the paraventricular thalamic nucleus and the subiculum. The density of TIP39-containing fibers showed a marked reduction in both regions following PVG lesions. There are many areas in the midbrain, and lower brainstem that normally contain TIP39-containing fibers (Dobolyi et al., 2003b), however, PVG lesions did not affect the density of TIP39-containing fibers in these regions, except the periaqueductal gray, where a moderate reduction was seen (Dobolyi et al., 2003a).

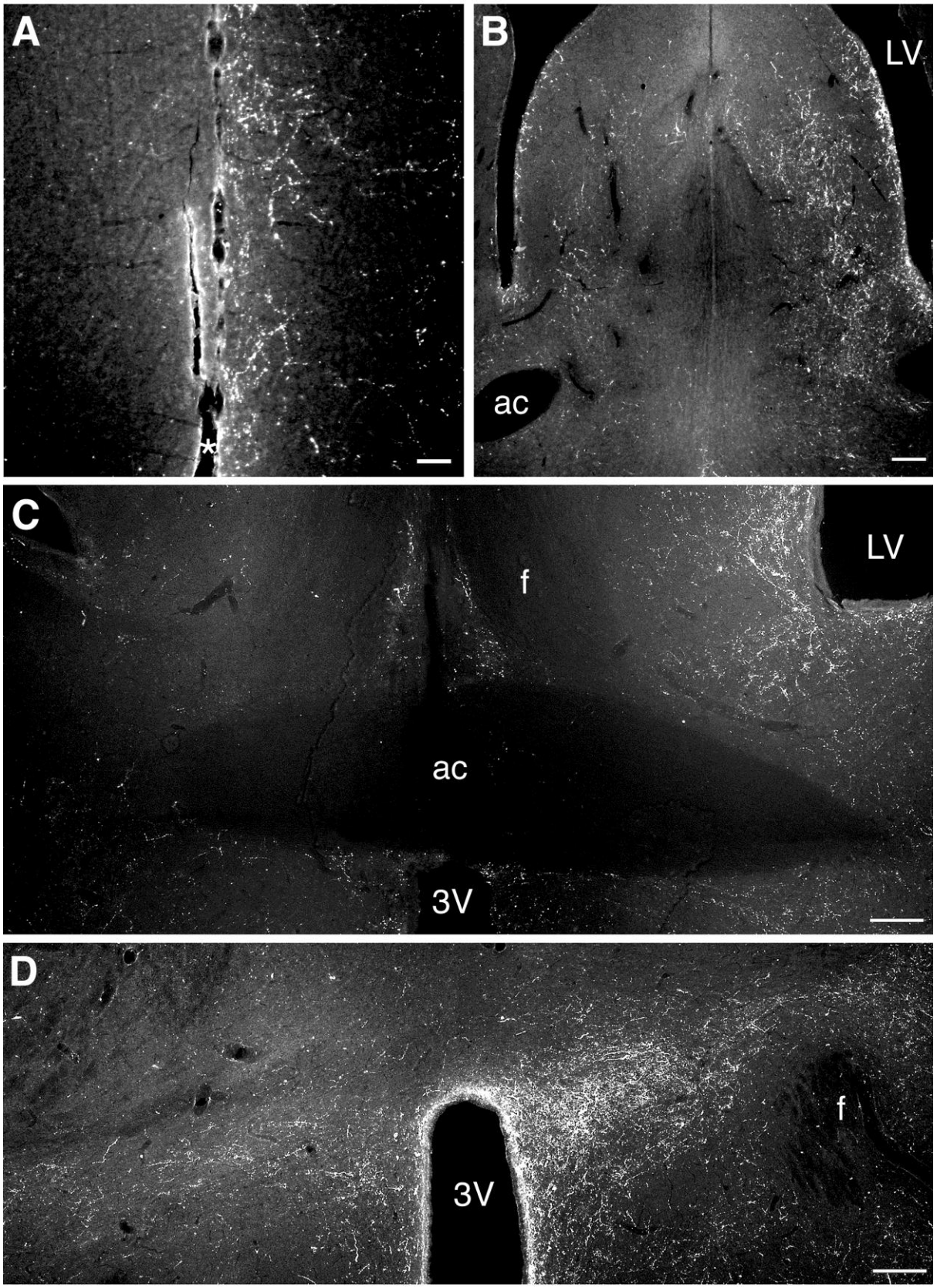

Fig. 18. The effect of unilateral (left side) lesions of the PVG on TIP39 fibers. Disappearance of TIP39 immunoreactive fibers ipsilateral to the lesion in the dorsal peduncular and infralimbic cortices (A), lateral septum (B), bed nucleus of the stria terminalis (C), and strong

ipsilateral reduction in the hypothalamic paraventricular nucleus (D). Scale bars = 200 μm. The figure is from our previous publication (Dobolyi et al., 2003a).

6.4.1.2. The effects of lesioning TIP39 cells in the MPL on TIP39 fibers

Lesions in the medial paralemniscal nucleus resulted in complete, or almost complete disappearance of the TIP39-containing cells in the midbrain, lower brainstem and the spinal cord, while forebrain structures were not affected (Dobolyi et al., 2003a). Following unilateral medial paralemniscal lesions, there was an almost complete disappearance of TIP39-containing fibers ipsilaterally from the superior colliculus, the external cortex of the inferior colliculus (Fig. 19A) and the cuneiform nucleus while a moderate density of TIP39-containing fibers remained in the periaqueductal gray. In the intact pons and medulla, the ventral nucleus of the lateral lemniscus (Fig. 19B,C), the lateral parabrachial nucleus, the locus coeruleus, the subcoeruleus area, the medial nucleus of the trapezoid body (Fig. 19D), and the periolivary nuclei contain a considerable density of TIP39-containing fibers. Following unilateral medial paralemniscal lesions, TIP39-containing fibers completely or almost completely disappeared from these pons and medulla regions ipsilateral to the lesion without any apparent change in the density of TIP39-containing fibers contralateral to the side of the lesions (Dobolyi et al., 2003a).

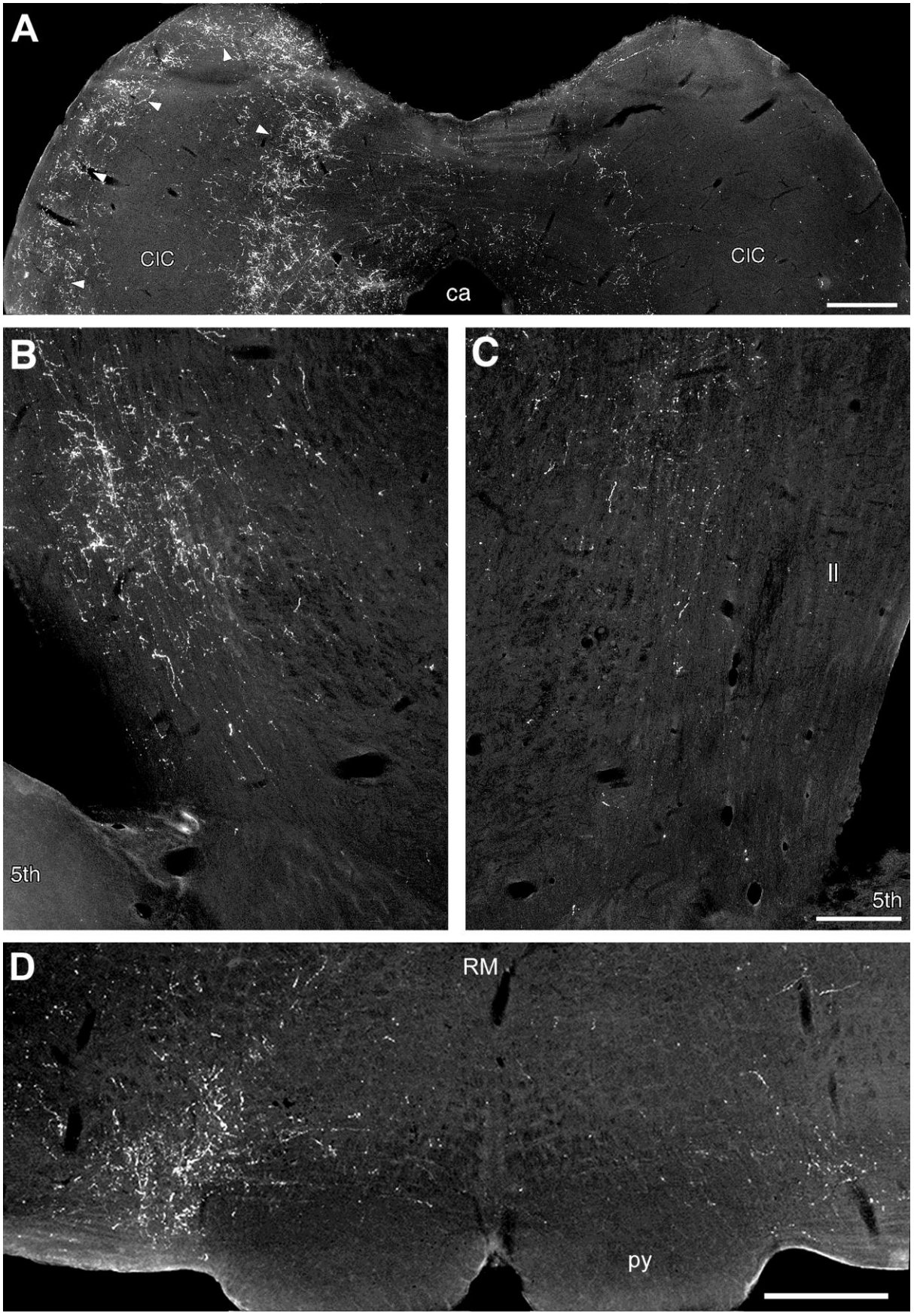

Fig. 19. The effect of unilateral (right side) medial paralemniscal lesion on TIP39 fibers in brainstem auditory areas. An almost complete disappearance of TIP39 immunoreactive fibers

ipsilateral to the lesion in the external cortex of the inferior colliculus (arrowheads) (A), in the nuclei of the lateral lemniscus (B – contralateral to the lesion, C – ipsilateral to the lesion), and in the medial nucleus of the trapezoid body (D). Scale bars = 500 μm for A, D and 250 μm for B, C. The figure is from our previous publication (Dobolyi et al., 2003a).

6.4.1.3. *The effects of lesioning TIP39 cells in the PIL on TIP39 fibers*

Following lesions of the PIL, TIP39 fibers almost completely disappeared from the ipsilateral amygdala, and most parts of the ipsilateral hypothalamus (Dobolyi et al., 2003a). In addition, smaller, but visible reductions in the density of TIP39 fibers were observed ipsilateral to the lesion in many other forebrain regions including the infralimbic cortex, the nucleus accumbens, the ventral subdivision of the lateral septum and the bed nucleus of the stria terminalis (Dobolyi et al., 2003a).

Since TIP39 fibers could be followed from the PIL towards the supraoptic decussations (Palkovits et al., 2010) to project in a ventromedial direction (Fig. 20A), the effect of transaction of this pathway was studied in mother rats. Transections reaching the optic tract ventrally at bregma level AP = -2.64, L = 3.0 resulted in the accumulation of TIP39 immunoreactivity immediately caudal to the transection within the fibers of the supraoptic decussations (Fig. 20B, C). In these animals, a marked reduction was found in the density of TIP39-containing fibers and terminals in the arcuate (Fig. 20D), paraventricular, and periventricular nuclei, and the preoptic area ipsilateral to the transection (Cservenak et al., 2010).

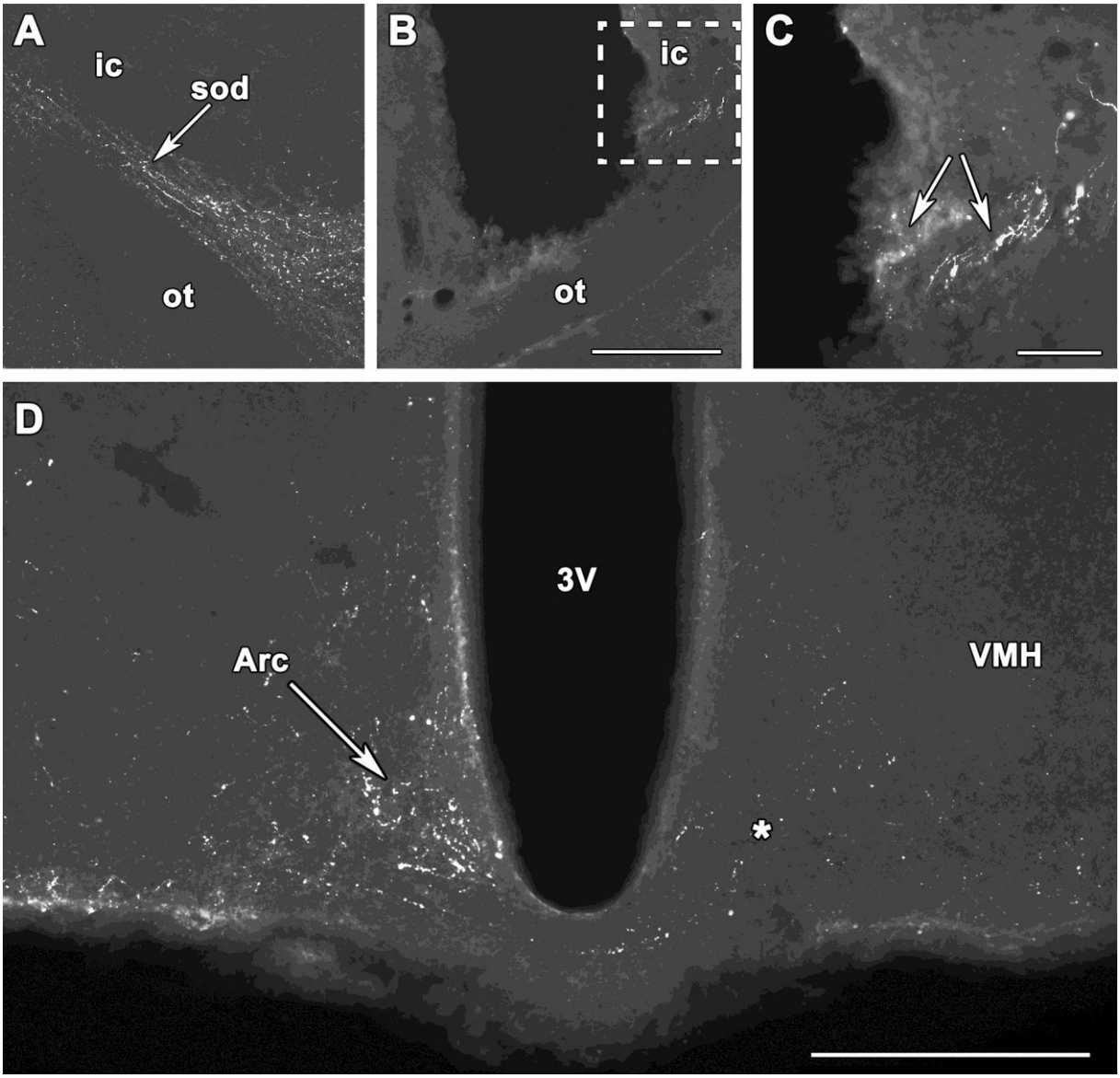

Fig. 20. Projection of TIP39 neurons is demonstrated to the arcuate nucleus in rat dams. A: TIP39 fibers project towards the hypothalamus in the supraoptic decussations. B: A transection perpendicular to the supraoptic decussations is shown in a coronal section. The disappearance of TIP39 fibers is observed medial to the transaction. C: A high-magnification photomicrograph showing the framed area in panel B demonstrates the accumulation of TIP39 immunoreactivity (arrows) in the supraoptic decussations immediately lateral to the transection. D: TIP39 fibers are abundant in the arcuate nucleus of rat dams (white arrow) contralaterally but disappeared from the arcuate nucleus on the side of transaction indicated by a star (*). Scale bar = 400 μm for B, 100 μm for C, and 500 μm for D. The panels are from our previous publication (Cservenak et al., 2010).

6.4.2. Retrograde labeling of TIP39 neurons following injections into the arcuate nucleus and the medial preoptic area

The retrograde tracer CTB was injected unilaterally into two major target areas of PIL neurons: the medial preoptic and the arcuate nuclei. The tracer deposition overlapped with TIP39 terminal fields and separate injections into both sites resulted in the predominantly ipsilateral labeling of cells that were distributed uniformly throughout the PIL. Cells in brain regions adjacent to the PIL did not contain label. Following the medial preoptic nucleus injection (Fig. 21A), the majority of TIP39 neurons in the PIL were labeled with the retrograde tracer (Fig. 21B) and a relatively large number of CTB-labeled but TIP39-negative cells were also visible. Following injections into the arcuate nucleus (Fig. 21C), there were also some CTB-labeled TIP39 neurons in the PIL (Fig. 21D). Cells in brain regions adjacent to the PIL did not contain label following either CTB injection. TIP39 neurons located in the periventricular gray of the thalamus and the medial paralemniscal nucleus were also not labeled with CTB. Altogether, these data suggest that PIL TIP39 neurons project both to the medial preoptic area and the arcuate nucleus (Fig. 21E).

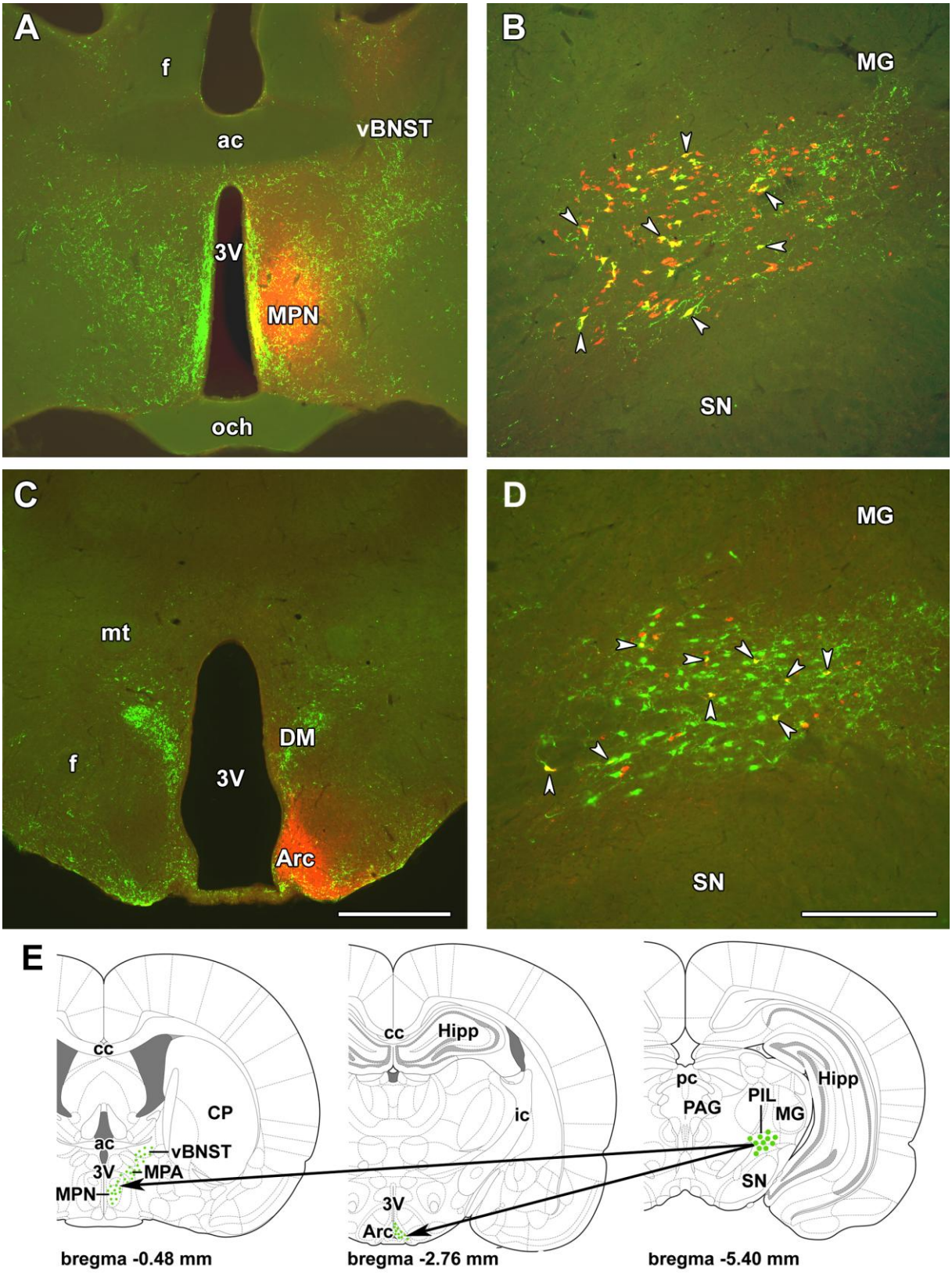

Fig. 21. Projections of the PIL into the medial preoptic and arcuate nuclei, demonstrated using the retrograde tracer cholera toxin beta subunit (CTB). CTB is shown in red and TIP39 in green. A: A site of CTB injection into the medial preoptic nucleus (MPN) is shown in relation

to TIP39 fibers. B: In the PIL, the majority of TIP39 neurons are labeled with CTB following medial preoptic CTB injection (yellow; white arrowheads). In addition, a number of TIP-negative CTB-labeled neurons are also present. C. A site of CTB injection into the arcuate nucleus (Arc) is shown. D: A portion of the PIL TIP39 neurons are labeled with CTB (shown by white arrowheads) following its injection into the arcuate nucleus. E: A drawing prepared by modifications of panels from a rat brain atlas (Paxinos and Watson, 2007) shows the schematics of the PIL-hypothalamic projections. Large green dots in the PIL represent TIP39 cell bodies while small green dots in the preoptic area and the arcuate nucleus represent TIP39 fiber terminals. The arrows show the projections from the PIL to the medial preoptic area and the arcuate nucleus, respectively. Scale bar = 1 mm for C, and 500 μm for D.

6.4.3. Afferent neuronal connections of the PIL

We injected the retrograde tracer CTB into the PIL to identify neurons that project there, and also injected CTB into adjacent regions for comparison. Injections that did not overlap the PIL (including into varying parts and amounts of the substantia nigra, triangular subdivision of the posterior thalamic nucleus, medial lemniscus, and peripeduncular nucleus) resulted in labeling patterns that differed markedly from those following injections into the PIL, and the two sets of labeled areas rarely overlapped. Most projections to the PIL were from the ipsilateral side, with the exception of the gracile and cuneate nuclei and the spinal cord, where there was contralateral dominance (Fig. 22).

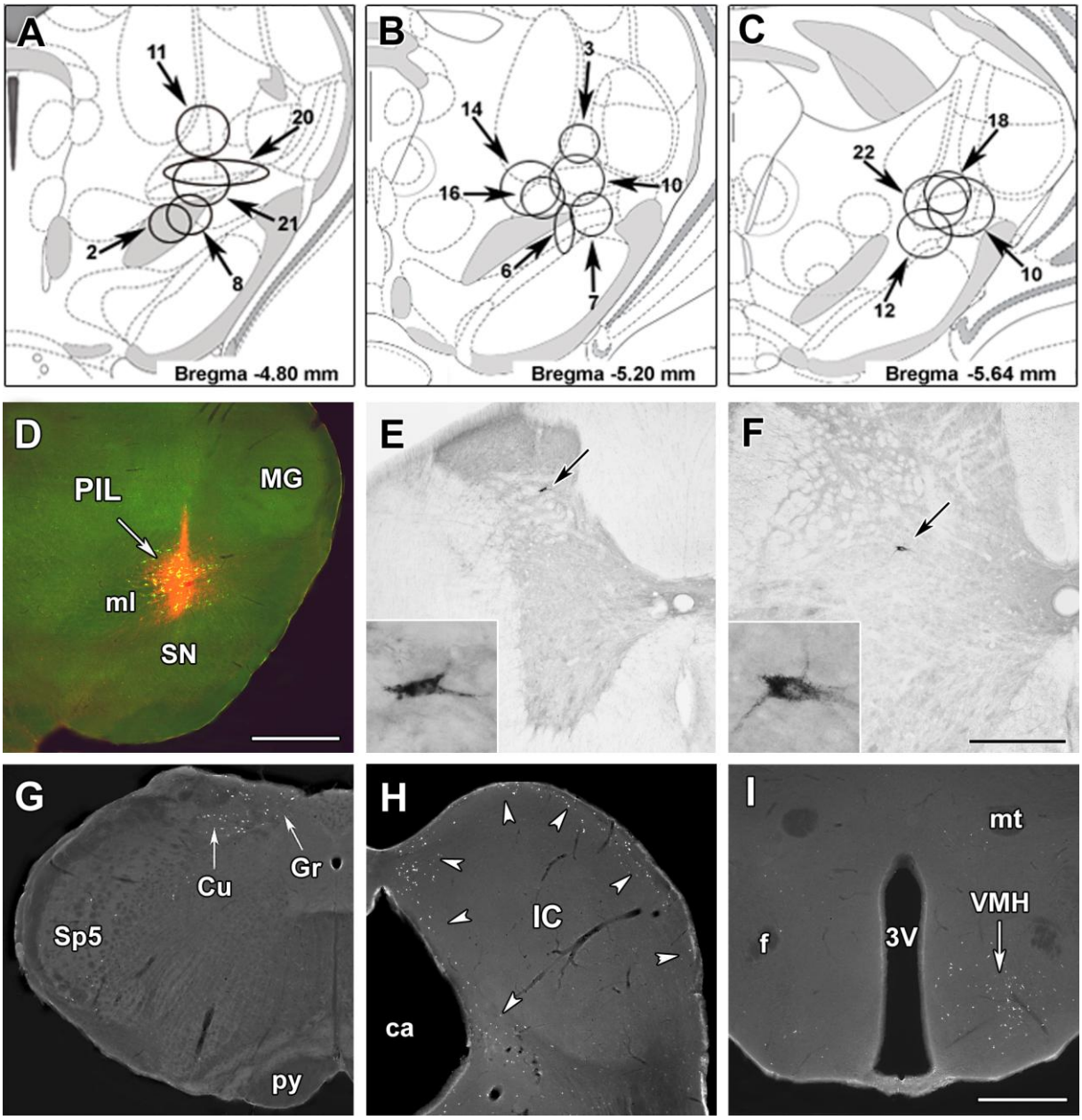

Fig. 22. Afferent neuronal connections of the posterior intralaminar complex of the thalamus (PIL). A-C: The sites where the retrograde tracer cholera toxin beta subunit (CTB) spread in the coronal plane following injections in particular animals are circled. Drawings were prepared by aligning the pictures adapted from a rat brain atlas (Paxinos and Watson, 2007). The 3 drawings represent coronal sections at bregma levels -4.8 mm, -5.2 mm, and -5.64 mm. The injection sites are shown at the level closest to the center of the injection. D: The injection site belonging to animal #10 is shown double labeled with TIP39 to show that CTB injection site (red) overlaps with the location of TIP39 neurons (green; yellow in combination with red) in the PIL. E-I: CTB-labeled cell bodies are shown in the spinal cord at the level of thoracic segment 2 (E) and lumbar segment 5 (F) as well as in several brain regions including the gracile (Gr) and cuneate nuclei (Cu) in the medulla oblongata (G), the external cortex of

the inferior colliculus (H), and the ventromedial hypothalamic nucleus (VMH), especially its ventrolateral subdivision (I). Scale bars = 400 μm for F, and 1 mm for D and I.

6.4.3.1. Inputs from caudal brain regions and the spinal cord

We analyzed the thoracic and lumbar spinal cord segments. CTB-labeled neurons were predominantly contralateral to the injection site, in Rexed laminae IV-VII. Most of the labeled thoracic cells were located in laminae IV-V and the labeled lumbar cells in laminae VI-VII. There was rarely more than one labeled cell in a coronal section. On average every 4th 50 mcoronal section contained a labeled cell, usually characterized by oval perikarya with multiple dendrites. In the medulla oblongata, the highest density of CTB-labeled cells was in the gracile nucleus, the cuneate nucleus, and the spinal trigeminal nucleus (particularly in the deep layers of its ventral portion). CTB-labeled neurons in these nuclei were located contralateral to the injection site. Only a few upper brainstem regions contained CTB-positive neurons. The greatest number was in the external cortex of the inferior colliculus. CTB-labeled neurons were far less numerous in the lateral parabrachial nucleus, periaqueductal gray, and deep layers of the superior colliculus.

6.4.3.2. Inputs from higher brain regions

The infralimbic cortex contained the highest density of labeled cell within the cerebral cortex. There were also a considerable number of retrogradely labeled neurons in auditory areas. In contrast, there were few CTB-positive neurons in the insular and medial prefrontal cortex. CTB signal was altogether absent from other cortical areas. Retrograde labeling was also largely absent from most other forebrain structures. There were a significant number of labeled neurons only in the central amygdaloid nucleus, the substantia innominata, and the anterior portion of the lateral septal nucleus. Within the diencephalon, the largest number of labeled cells was in the ventromedial hypothalamic nucleus, particularly in its ventrolateral subdivision. There were also a considerable number of CTB containing neurons in the lateral preoptic area and *zona incerta*.

6.4.4. Afferent neuronal connections of the MPL

Following CTB injections into the MPL there was a relatively widespread distribution of CTB labeled cells in the brain (Varga et al., 2008). The topographical distribution of CTB labeled cells following injections into the MPL, identified regularly by double labeling with

TIP39 (Fig. 23A) was distinct from those observed following injections into adjacent brain regions including receipt of major inputs, e.g. from the auditory cortex and some hypothalamic structures. The majority of labeled cells were always ipsilateral to the injection side with only a low density of labeled cells present contralaterally (Varga et al., 2008).

6.4.4.1. Inputs from auditory brain regions

In the cerebral cortex, CTB-containing cells were restricted to particular regions (Varga et al., 2008). The most abundant labeling was in pyramidal cells of layer V in the ventral part of the secondary auditory cortex (Fig. 28B) in an area corresponding to cortical temporal area 3 (Te3), as defined previously (Roger and Arnault, 1989; Webster, 1977; Zilles and Wree, 1985). An almost equally high density of labeled pyramidal cells continued dorsally in the primary auditory cortex (Te1) while a lower number of retrogradely labeled cells were found caudally in cortical temporal area 2 (Te2), ventrally in the ectorhinal and perirhinal cortices. In addition, a few CTB-labeled cells were visible in layer VI of the ventral part of the auditory cortex, immediately adjacent to the external capsule. In the thalamus, the medial subdivision of the medial geniculate body contained a considerable density of retrogradely labeled cells following MPL injections. In the inferior colliculus, CTB-labeled cells were restricted to the external and dorsal cortices whereas the central nucleus contained no retrogradely labeled cells (Figs. 23E). In the pons, a high density of CTB-labeled cells following MPL injections was present in the contralateral MPL. Interestingly, the vast majority of these retrogradely labeled cells did not contain TIP39 immunoreactivity. Apart from the MPL, a moderate to high number of labeled cells was also present in the nucleus of the central acoustic tract, the superior paraolivary nucleus, and the periolivary area including the dorsal periolivary nucleus (Figs. 23F).

6.4.4.2. Major non-auditory inputs to the MPL

The density of CTB-labeled cells was high in several regions of the hypothalamus (Varga et al., 2008). A high density of retrogradely labeled neurons was present in the lateral preoptic area while the medial preoptic area contained only a few labeled cells (Fig. 23C). The ventromedial nucleus contained the greatest density of CTB-containing cells particularly in its ventrolateral subdivision (Fig. 23D). Different parts of the lateral hypothalamic area also contained a high density of retrogradely labeled cells. A cell group in the dorsolateral hypothalamic area, the area around the A13 catecholaminergic neurons, the lateral hypothalamic area next to the internal capsule, and the perifornical nucleus had a high density

of CTB-labeled cells. In addition, a high density of retrogradely labeled cells was also present in the zona incerta (Fig. 23D).

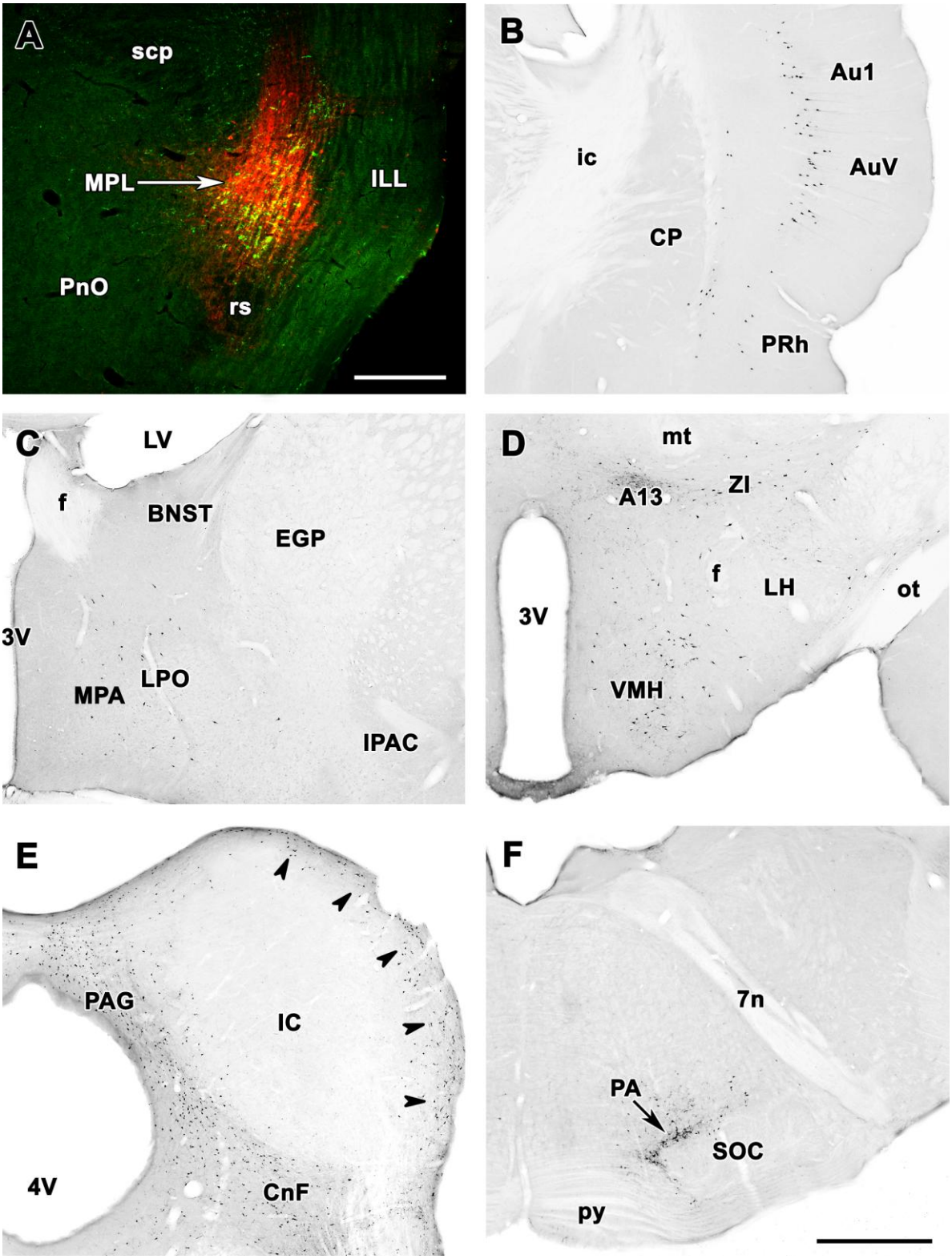

Fig. 23. Topographical distribution of retrogradely labeled neurons after CTB injection into the MPL. A: The CTB injection site (red) is shown in relation to TIP39-immunoreactive neurons (green) in a double fluorescent labeled coronal section. The injection site covers most of the MPL. B–F: Photomicrographs of coronal sections single labeled with DAB immunocytochemistry demonstrate retrogradely labeled neurons in the same brain. B: A high density of retrogradely labeled neurons is shown in layer V of the primary auditory cortex and the ventral secondary auditory cortex. Labeled cells in a lower density are present in layers Vi and V of the perirhinal cortex and layer VI of the ventral secondary auditory cortex. C: Retrogradely labeled neurons are distributed in the preoptic region. D: A high density of retrogradely labeled neurons in the ventrolateral subdivision of the hypothalamic ventromedial nucleus, the dorsolateral hypothalamic area, the area of the A13 dopamine cell group, and the zona incerta. Scattered cells are also present in the lateral hypothalamus. E: CTB labeled neurons are abundant in the external cortex of the inferior colliculus. F: Retrogradely labeled neurons are concentrated in the periolivary area immediately dorsal to the superior olive. Scale bar = 500 μm in A and 1 mm in F (applies to B–F). The figure is from our previous publication (Varga et al., 2008).

6.5. Assessment of c-Fos activation in TIP39 neurons of lactating dams

6.5.1. Fos activation in the brain in response to suckling

When pups were returned to their mothers after a 20h separation, the dams all began care for them immediately, and suckling started within 5 min. Following pup return, c-Fos-expressing (c-Fos-ir) neurons appeared in a number of regions in the dams' brains including the PIL, MPL, lateral septal nucleus, anteroventral periventricular nucleus, medial preoptic nucleus, medial preoptic area, the ventral subdivision of the bed nucleus of the stria terminalis, some parts of the periaqueductal gray but not the periventricular gray of the thalamus (Cservenak et al., 2010; Varga et al., 2012).

6.5.2. Suckling-induced Fos expression in TIP39 neurons of the PIL

While c-Fos-ir neurons were evenly distributed within the PIL, none appeared in adjacent regions, except in the peripeduncular area lateral to the PIL (Fig. 24A). In the PIL section with the largest number of labeled cells, the number of Fos-ir neurons changed significantly with pup exposure ($F=82.95$). In suckling dams, it was 161±10, which was significantly greater ($p<0.001$) than the 27±8 labeled cells following pup exposure without

any physical contact (Fig. 24B). This number was somewhat greater ($p<0.05$) than the number of Fos-ir neurons (8±6) in the control group, dams whose pups were removed and not returned.

While the number of TIP39 labeled cells in the PIL did not differ between the three groups and was an average of 42±5 per side in the densest section, the number of Fos-expressing TIP39 neurons was changed significantly by pup exposure ($F=34.17$). The number of double labeled cells was greater in suckling rat dams than in those exposed to pups without physical contact (35±6 vs. 6±2; $p<0.001$), while the number of double-labeled cells did not significantly differ between dams without physical pup contact and dams whose pups were not returned (Fig. 24C,D).

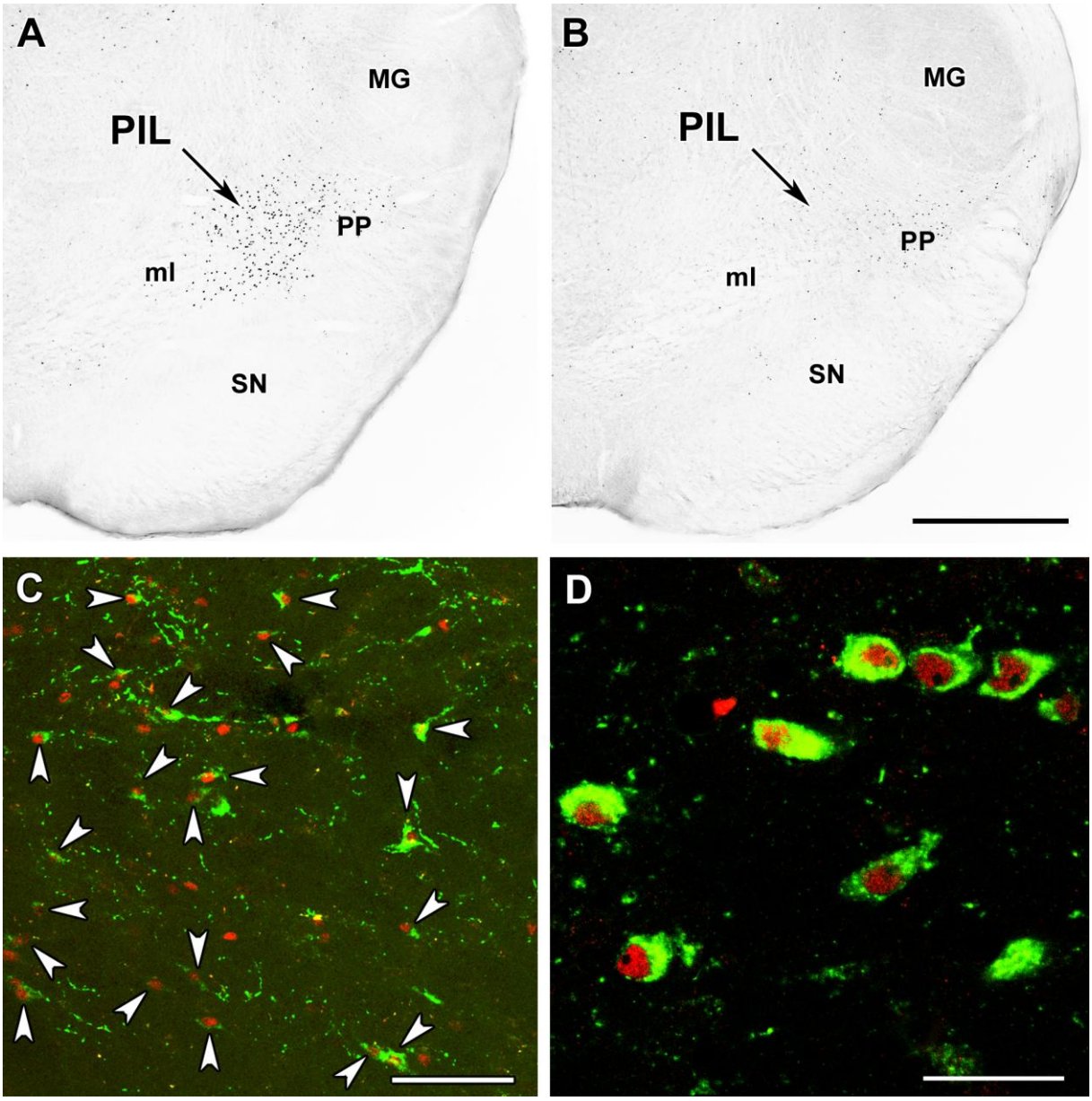

Fig. 24. Fos activation in the posterior intralaminar complex of the thalamus (PIL) in mother rats in response to suckling. A: A high density of Fos immunoreactive cell nuclei (black dots) can be seen in the PIL of mother rats that were deprived of their pups for 22h, and then reunited with them for 2h. B: The PIL contained only a very small number of Fos-ir neurons in mothers who were deprived of their pups for 22h and then reunited for 2h in such a way that the dams could see, smell and hear their pups but suckling was prevented. It is interesting to note that some Fos-ir cells appear in the peripeduncular area (PP) lateral to the PIL, in both groups. C: The majority of TIP39 neurons (green) contain Fos (red) in the PIL (white arrowheads), in response to suckling. D: A high-magnification confocal image demonstrates Fos labeling of TIP39 neurons. Scale bar = 1 mm for C, and 100 μm for D.

6.5.3. Suckling-induced Fos expression in TIP39 neurons of the MPL

In the MPL, also a very few Fos-ir neurons (less than 3 per section) were detected in rat dams 22 h after separating them from their pups (Varga et al., 2012). However, when the dams were exposed to their pups for 2 h following 20 h of separation, Fos-ir nuclei (over 30 per section) appeared in the MPL (Fig. 25). We observed that Fos-ir nuclei were evenly distributed within the MPL while other parts of the paralemniscal area remained devoid of Fos-positive cells, except for a few cells dorsal to the MPL. The number of TIP39-ir neurons with an identifiable nucleus in the MPL was 31±3 (mean±SE) in randomly selected sections (1 section from each side of 4 lactating mother) containing the MPL. Double labeling revealed that 91% of TIP39-ir neurons in the MPL were Fos-positive. The few TIP39-ir neurons whose cell bodies lacked Fos immunoreactivity did not seem to form a separate cell group but rather were present in all parts of the MPL (Fig. 30). The co-localization between TIP39- and Fos-positive neurons was very high as 95% of neurons expressing Fos in response to pup exposure contained TIP39 in pup-exposed mothers (Varga et al., 2012).

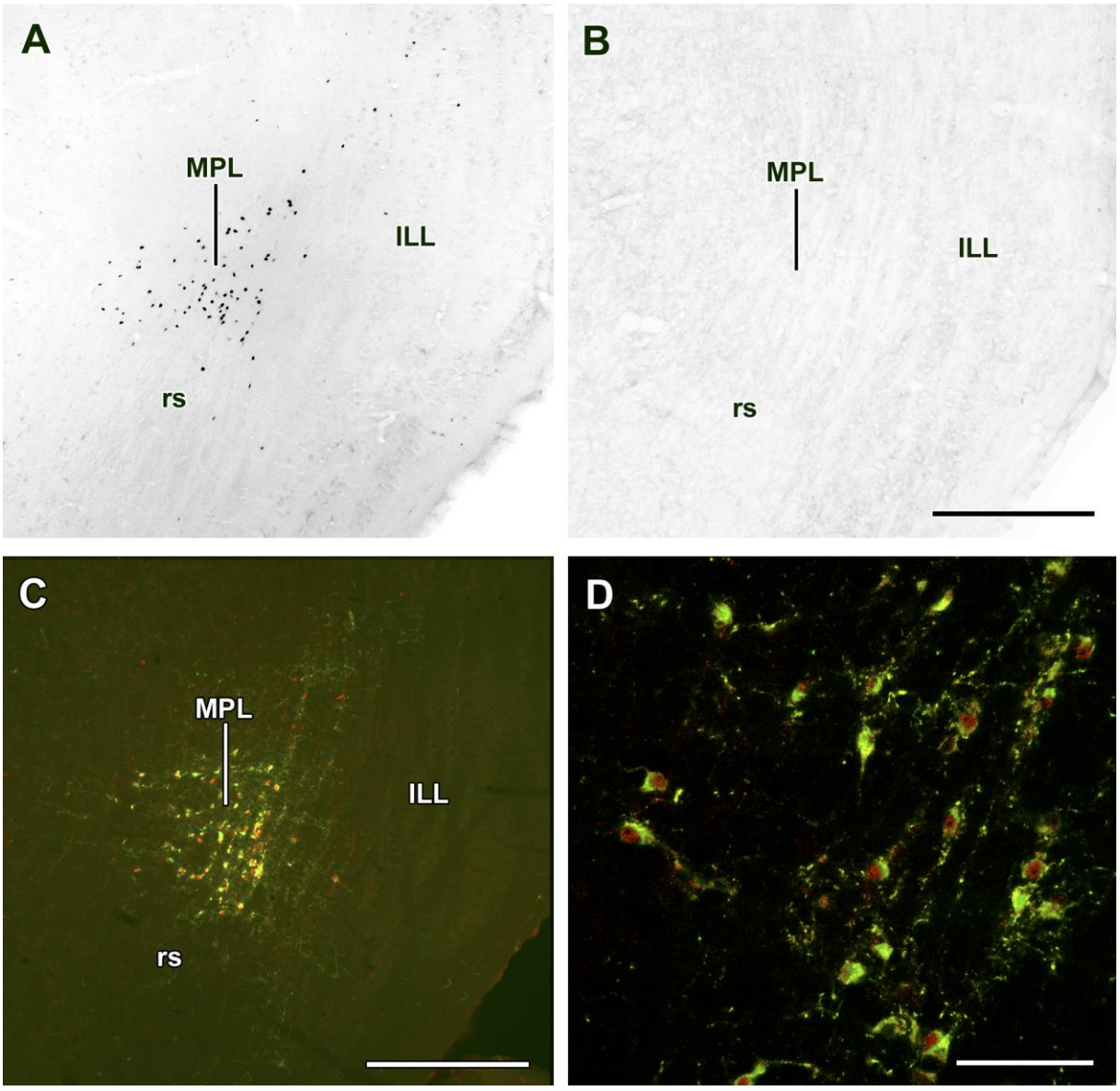

Fig. 25. Fos expression is demonstrated in response to pup exposure in the medial paralemniscal nucleus (MPL) of mother rats. A: Fos-ir neuronal cell bodies are present in the MPL of mother rats 2h after returning their pups following their removal for 20h. B: Fos-immunopositive neurons are absent in the MPL of mother rats deprived of pups for 22h. C, D: Double fluorescent immunolabeled sections of mother rats demonstrate that most Fos-expressing cells contain TIP39 in the MPL. C: The low magnification photomicrograph shows that the distribution of green TIP39-ir cell bodies and red Fos-ir nuclei overlaps. D: The confocal image shows that the vast majority of TIP39-labeled cells contain red labeled Fos protein in their nuclei. Scale bars = 500 μm for A-C, and 100 μm for D. The figure is taken from our previous publication (Varga et al., 2012).

6.6. The effect of the PTH2 receptor block on the plasma prolactin level

6.6.1. Effect of intracerebroventricular injection of a PTH2 receptor antagonist on suckling-induced prolactin secretion

The plasma prolactin concentration was at a basal level by the end of the separation period (44±10 ng/ml) and remained low immediately after the injection (0 min) of saline, or the lower (0.075 mg) or higher (0.375 mg) concentration of HYWY-TIP39 (Fig. 26). During the initial 3 time points (-240, -5 and 0 min), plasma prolactin levels in the 3 groups of animals did not differ significantly as determined by one-way ANOVA at each time point (F=0.16, 2.58, and 2.51, respectively). At 0 min, the pups were returned to the mothers, which led to pup attachment and suckling. The plasma prolactin levels rose following suckling in the control group until 423±118 ng/ml 30 min after reunion whereas the antagonist injection significantly ($p<0.001$) reduced the elevation in plasma prolactin level as determined by using two-way repeated measures ANOVA (Cservenak et al., 2010). The plasma prolactin levels rose following suckling in the control group whereas the antagonist injection significantly ($p<0.001$) reduced the elevation in plasma prolactin level as demonstrated by using two-way repeated measures ANOVA (F=11.68). Plasma prolactin concentrations at 5, 15, 30, and 60 min after returning the pups were as follows (expressed in ng/ml): 145±26, 280±79, 423±118, and 185±31 after saline injection, 37±13, 53±36, 94±76, and 75±28 after the injection of 0.075 mg HYWY-TIP39, and 27±8, 25±7, 38±8, and 28±10 after the injection of 0.375 mg HYWY-TIP39, respectively**.** The suckling-induced prolactin release was significantly ($p<0.01$) reduced by the injection of the antagonist at 5, 15, 30, and 60 min after returning the pups determined at each time point independently by one-way ANOVA (F=12.36, 8.75, 5.55, and 11.01, respectively). Bonferroni Post-Tests following ANOVA for posthoc comparisons revealed that both 0.075 mg ($p<0.05$) and 0.375 mg HYWY-TIP39 ($p<0.01$) significantly reduced plasma prolactin levels at 5, 15, 30, and 60 min after returning the pups (for 0.075 mg HYWY-TIP39, t=3.54, 3.05, 2.31, 2.78; for 0.375 mg HYWY-TIP39, t=4.51, 3.98, 3.11, 4.56, respectively). Injection of 0.075 mg PTH2 receptor antagonist into the lateral ventricle significantly ($p<0.05$) reduced the suckling-induced elevation of the plasma prolactin level 5, 15, 30, and 60 min after giving back the pups as determined by using one-way ANOVA followed by Bonferroni Post-Tests for posthoc comparisons. Injection of 0.375 mg PTH2 receptor antagonist completely prevented the prolactin release (Cservenak et al., 2010).

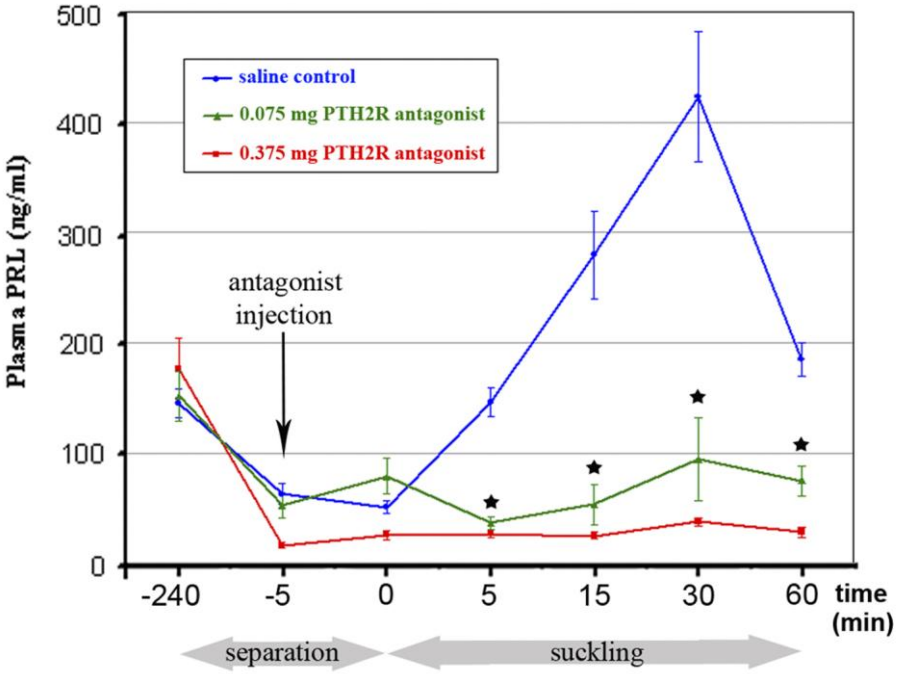

Fig. 26. Effect of the PTH2 receptor antagonist HYWY-TIP39 on the suckling induced prolactin release. Plasma prolactin concentrations are shown in groups of mothers by saline (blue curve), 0.075 mg HYWY-TIP39 (green curve), or 0.375 mg HYWY-TIP39 (red curve) dissolved in saline. Plasma prolactin levels are expressed in ng/ml. Each data point represents 6-8 animals. The X axis shows time (min) in a non-linear fashion. Below the X axis, the periods of pup separation and suckling are indicated in gray background. The time points of significant changes are indicated by *. The figure is taken from our previous publication (Cservenak et al., 2010).

6.6.2. Effect of local viral production of a PTH2 receptor antagonist on suckling-induced prolactin secretion

To evaluate a potential causal relationship between TIP39 signaling in the arcuate nucleus and prolactin level we infected cells in the mediobasal hypothalamus near the arcuate nucleus with a virus encoding a secreted PTH2-receptor antagonist (HYWH-TIP39) and enhanced GFP (Fig. 27A). At least 10 infected cells per the injection site were seen in the most densely infected section of the animals as illustrated in Fig. 27B. Basal plasma prolactin levels in the mother rats expressing HYWH-TIP39 were significantly lower than that in the control dams (82.8±20.8 vs. 153.8±11.1 ng/ml; $p<0.05$). After 4h of separation from their pups, levels of plasma prolactin in the two groups of mothers had fallen to similar levels

(HYWH-TIP39, 18.1±7.9, control virus 18.5±7.3 ng/ml). When pups were returned after the 4h separation period, attachment and suckling began within less than 5 min for all animals. The control virus and the PTH2 receptor antagonist-expressing virus injected animals had a significantly different prolactin response as determined using two-way repeated-measures ANOVA (F=9.962). Plasma prolactin levels in the control dams reached 215±48 ng/ml at 15 min, and 267±36 ng/ml at 30 min after reunion with their pups. In the antagonist expressing dams, the increase in plasma prolactin was significantly less, reaching only 46±21 ng/ml at 15 min and 74±28 ng/ml at 30 min after reunion ($p<0.001$ for both time points; Fig. 27C). In contrast, virus injected into the preoptic area did not significantly change either the basal plasma prolactin level (190±61 ng/ml in control vs. 146±31 ng/ml in the antagonist expressing rats) or the suckling-induced release of prolactin. At 15 and 30 min after returning the pups to the mothers, the concentrations (ng/ml) of prolactin were 186±62 and 287±77 in controls, and 245±75 and 357±83 in antagonist-expressing dams (Fig. 27D).

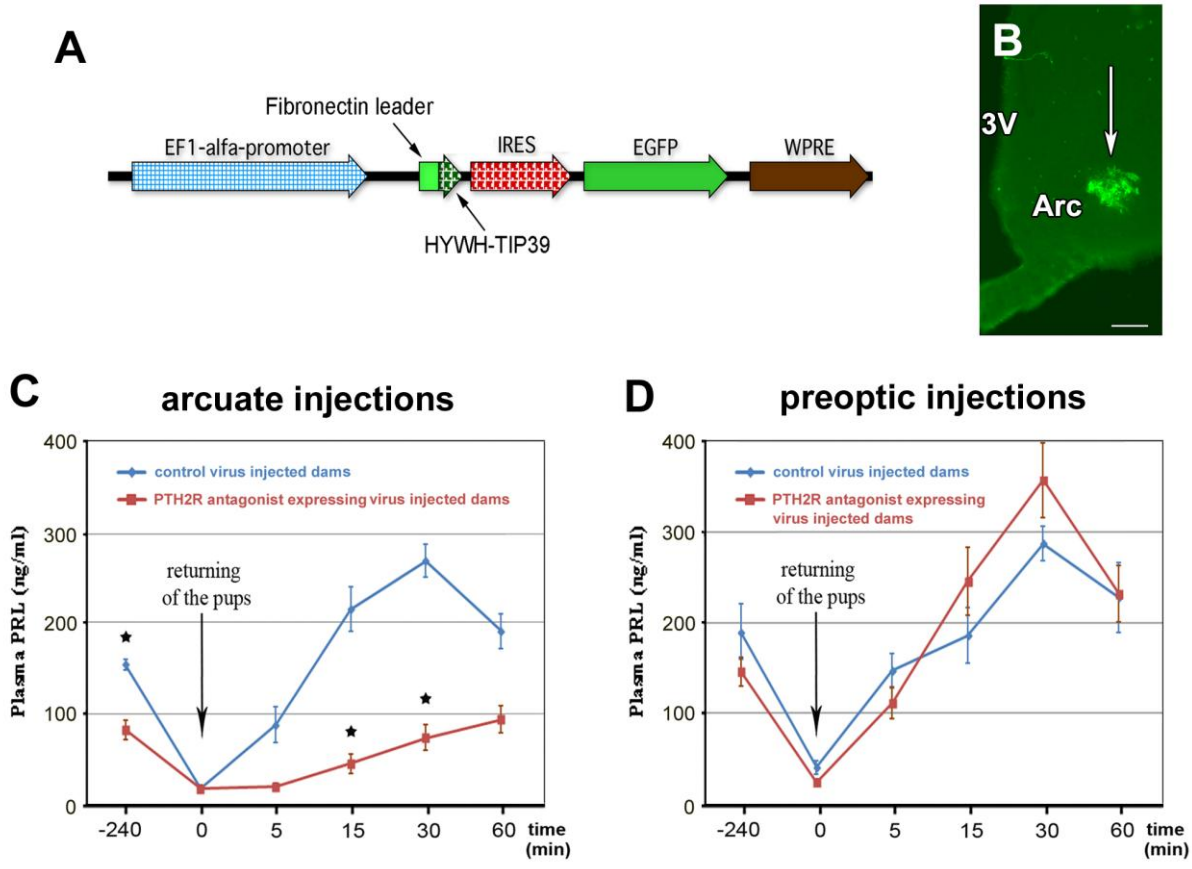

Fig. 27. Effect of virus encoding a peptide PTH2 receptor antagonist on prolactin release. A: Structure of the viral construct expressing HYWH-TIP39, an antagonist of the PTH2 receptor. A strong mammalian promoter (EF-1α) drives expression of a fusion protein between the

fibronectin leader sequence with signal peptide cleavage site and the HYWH-TIP39 sequence. This is followed by an internal ribosome reentry site (IRES) and then enhanced green fluorescent protein (EGFP) sequence and a woodchuck hepatitis post-transcriptional regulatory element (WPRE). B: Hypothalamic virus injection site. The white arrow indicates cells infected by the injected virus visualized with EGFP. The injection site is located just lateral to the arcuate nucleus. C: Basal plasma prolactin levels in mother rats injected with the PTH2 receptor antagonist expressing virus were significantly lower than in mothers injected with the control virus, with injections targeted to the arcuate nucleus. After returning their pups, the elevation of serum prolactin level was also blocked in the PTH2 receptor antagonist expressing virus injected mothers (*: $p<0.01$). D: Prolactin levels did not differ between PTH2 receptor antagonist expressing virus injected and control virus injected mothers with injections targeted to the medial preoptic area. Abbreviations: Arc – arcuate nucleus, 3V – third ventricle. Scale bar = 100 μm for B.

6.7. Preoptic actions of TIP39

6.7.1. Evaluation of maternal motivation after preoptic antagonism of the PTH2 receptor

Preoptic area virus injections resulted in a number of infected cells similar to the mediobasal hypothalamic injections. The behavior of mother rats that received virus injections into the preoptic area was analyzed using a place preference test. Defining a preferred cage as one that animals spend at least 20% more time in than the non-preferred cage, 10 out of 11 control dams preferred the pup associated cage. Dams injected in the preoptic area with the PTH2 receptor antagonist expressing virus had a significantly different cage preference ($X^2=8.023$, $p<0.05$) as only 5 out of 13 rats preferred the pup-associated cage evaluated in this way, while 4 rats showed preference for the control cage (Fig. 28A). The amount of time spent in the different compartments was also analyzed. The control virus injected mothers did not spend an equal amount of time in the different compartments ($F=3.84$). Rather, they spent significantly more time in the pup-associated cage than in the control cage (25.9±1.9 *vs.* 15.7±2.1 min; $p<0.05$). In contrast, the time spent in the different compartments did not differ for the rats infected with the antagonist producing virus ($F=0.783$). When the time spent in the different cages were compared between the control animals and the animals expressing the PTH2 receptor antagonist expressing virus we found a significant difference ($F=9.83$). The mothers expressing the PTH2 receptor antagonist spent less time in the pup-associated cage than control mothers (19.1±1.7 *vs.* 25.9±1.9 min;

p<0.05). This data is illustrated in Fig. 28B as a preference index (100 * (time spent in the pup associated cage – time spent in the control cage) / (time spent in the pup associated cage + time spent in the control cage)). The preference index for control virus injected dams was significantly greater than for the antagonist injected dams (25.7±7.6 *vs*. 3.4±5.5; p<0.05). The latter group did not show preference as the index value was not significantly different from 0. The nulliparous females did not show significant cage preference either: the index values for the groups injected with the control, and the antagonist-expressing virus were 0.9±11.6 and -7.3±4.6, respectively. In fact, the antagonist injected nulliparous females exhibited a tendency to prefer the white cage (the control cage for mothers) indicated by the negative preference index value.

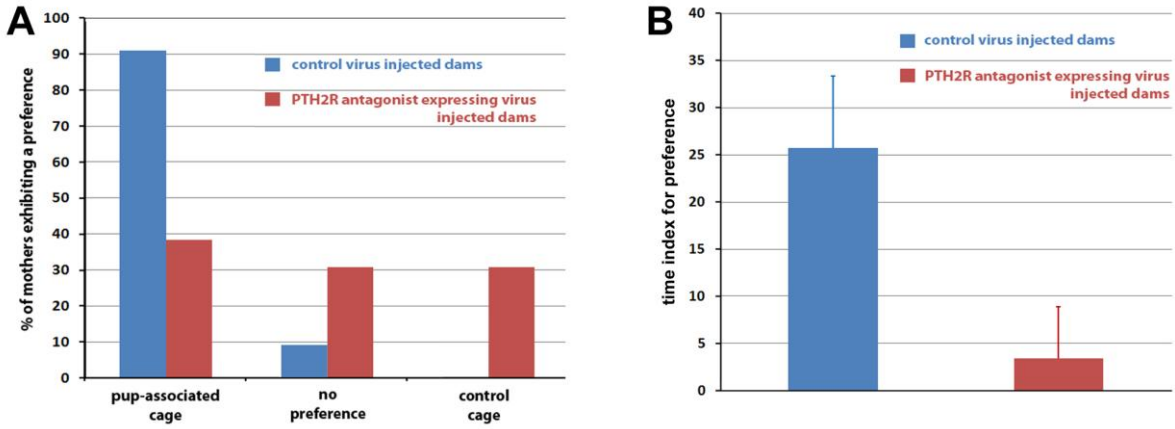

Fig. 28. A: Mother rats with medial preoptic area control virus injection deprived of their pups for 2h demonstrate significant preference (X^2=8.023, p<0.05) for a cage visually similar to one in which they were housed with their litter defined as >20% more time in that cage than in the control cage. In contrast, rats injected with a virus continuously expressing the PTH2 receptor antagonist do not show preference for the pup associated cage. B: The time animals spent in the pup-associated and control cage is expressed as a time index for preference: 100 * (time spent in the pup associated cage – time spent in the control cage) / (time spent in the pup associated cage + time spent in the control cage). The control virus injected mother rats spend significantly more time in the preferred pup-associated cage than PTH2 receptor antagonist expressing animals. The latter group does not have preference for the pup-associated cage.

6.7.2. Association of PIL TIP39 neurons with suckling-activated preoptic neurons

At the preoptic level, the anteroventral periventricular nucleus, the medial preoptic nucleus, the medial preoptic area, and the ventral subdivision of the bed nucleus of the stria terminalis all contained a high density of Fos-expressing neurons following suckling. The distribution pattern of Fos-expressing neurons was very similar to the distribution patterns of TIP39 labeled fibers and terminals observed in the area (Fig. 29A). Using immunreactivity for the potassium channel Kv2.1 to help define the plasma membrane, TIP39 containing fibers appeared to closely appose Fos-expressing neurons (Fig. 29B) in all regions of the preoptic area that contain Fos-expressing neurons following suckling. Fos-expressing neurons closely apposed by TIP39 fibers were abundant in both the medial preoptic nucleus (Fig. 29C), and the ventral subdivision of the bed nucleus of the stria terminalis (Fig. 29D). The percentage of Fos-expressing neurons that were closely apposed by TIP39 fibers was 78% in the former and 85% in the latter brain region.

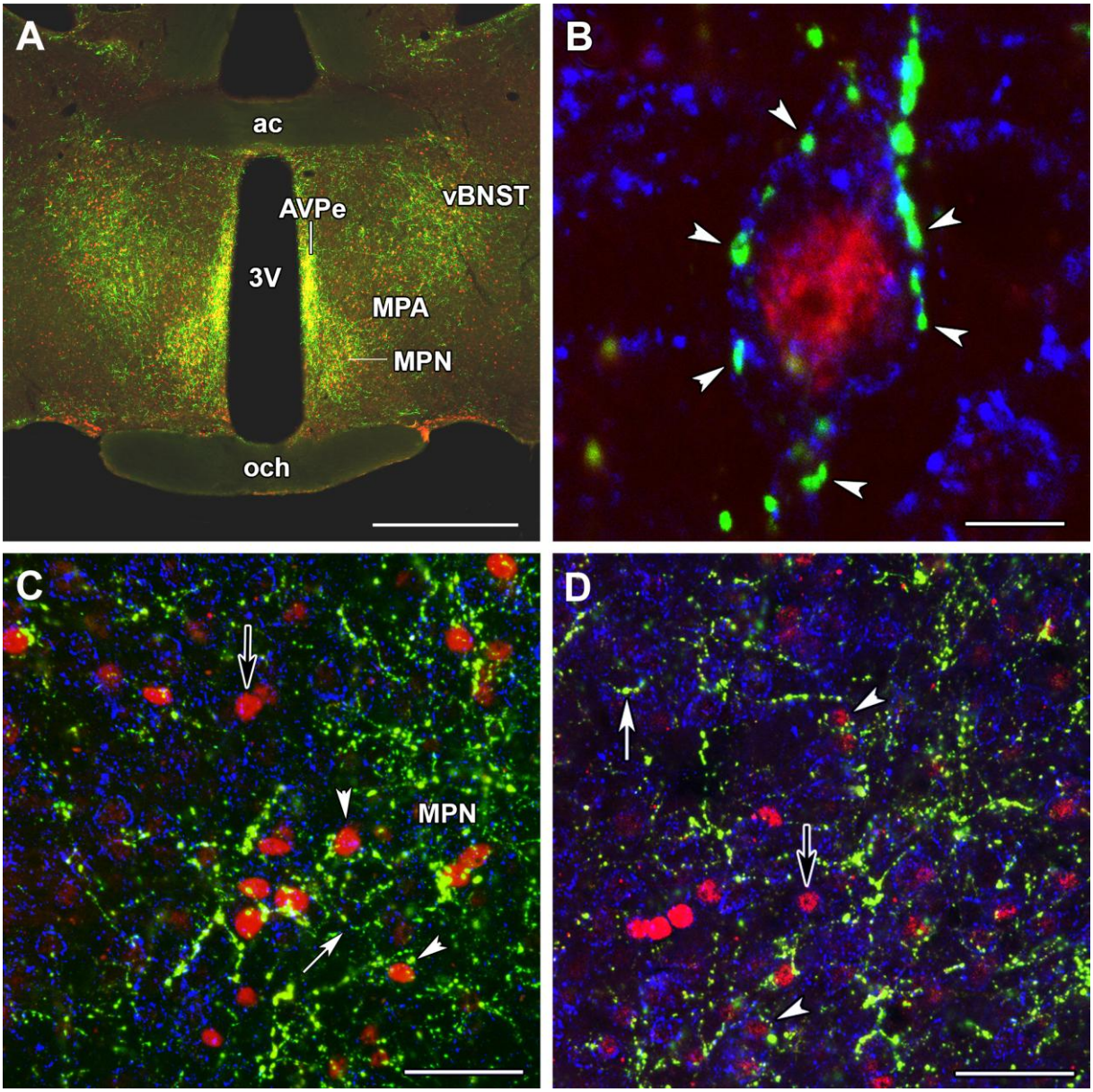

Fig. 29. The distribution of TIP39 fibers around activated neurons in the maternal preoptic area. A: A low magnification photomicrograph demonstrates the similarity of the distribution of TIP39 fibers (green) and Fos-ir neurons (red) in pup exposed mother rats in the anteroventral periventricular nucleus, the medial preoptic nucleus (MPN), medial preoptic area (MPA), and in the ventral subdivision of the bed nucleus of the stria terminalis (vBNST). B: A high magnification confocal image of a section triple labeled with TIP39 (green), Fos (red), and Kv2.1 potassium channel (blue) demonstrates that TIP39 terminals closely appose Fos-expressing neurons, as they appear to contact the cell surface as indicated by Kv2.1 immunoreactivity. C, D: Low magnification confocal images of the preoptic area that includes part of the MPN (C) and the vBNST (D), respectively. A number of Fos-activated cells that are closely apposed by TIP39 fibers are demonstrated (white arrowheads). There are also a

few Fos-positive neurons that may not be innervated by TIP39 (black arrows). In addition, some Fos-negative neurons seem to be surrounded by TIP39 fibers, too (white arrows). Some examples are shown with white arrowheads. Scale bars = 1 mm for A, 10 μm for B, and 50 μm for C and D.

6.8. Induction of TIP39 in mother rats

6.8.1. Alterations of TIP39 mRNA expression in mother rats

In the forebrain of lactating mother rats, TIP39 neurons were found in the ventral part of the posterior thalamus concentrated in the periventricular gray of the thalamus (PVG) medial to the fasciculus retroflexus (Fig. 30A-C) and the posterior intralaminar complex of the thalamus, an area ventromedial to the medial geniculate body (Fig. 30D-F). TIP39 mRNA-containing neurons in the PIL were situated in the posterior intralaminar thalamic nucleus, the parvicellular (lateral) subparafascicular nucleus, and the caudal portion of the zona incerta (Cservenak et al., 2010). Apart from these posterior thalamic locations, we detected no signal for TIP39 mRNA in the examined parts of the brain in lactating mothers. The intensity of the autoradiography signal was high in the PIL of mother rats (Fig. 30E). Neurons with high intensity signal were evenly distributed (Fig. 30E). In contrast, the vast majority of TIP39 neurons in the PVG showed a low intensity signal in mothers (Fig. 30B).

TIP39 mRNA induction in the MPL was apparent using in situ hybridization histochemistry, too (Varga et al., 2012). TIP39 mRNA-containing neurons were evenly distributed within the MPL of mother rats (Fig. 31A-C). This location of TIP39 mRNA expressing neurons was the same as that described earlier in young adult male and female rats (Dobolyi et al., 2003b). However, the intensity of the autoradiography signal was markedly higher in the MPL of mother rats as compared to nulliparous females and pup-deprived mothers (Fig. 31A-C).

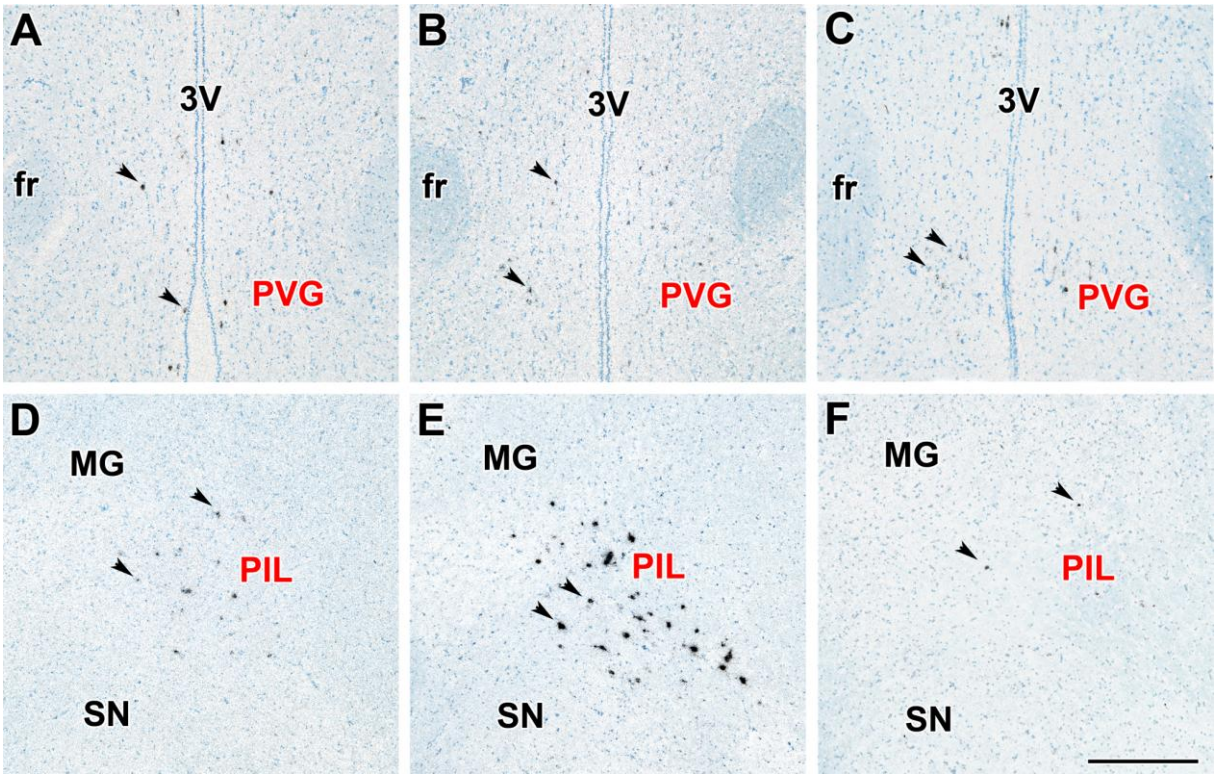

Fig. 30. Bright-field photomicrographs of *in situ* hybridization histochemical sections demonstrate the expression of TIP39 mRNA in the periventricular gray of the thalamus (PVG, A-C) and the posterior intralaminar complex of the thalamus (PIL, D-F). Arrowheads indicate some examples of the autoradiography signal above TIP39-expressing neurons. In the PVG, most TIP39 neurons have a weak autoradiography signal in control female (A), lactating mother (B), as well as in a pup deprived mother (C). In contrast, the low level of TIP39 mRNA in the control female (D) is increased in all parts of the PIL in lactating mother (E) while removing the pups reduced the level of TIP39 mRNA as indicated by the low density of TIP39-expressing cells and their weak labeling (F) similar to the image in D. Scale bar = 500 µm. The figure is taken from our previous publication (Cservenak et al., 2010).

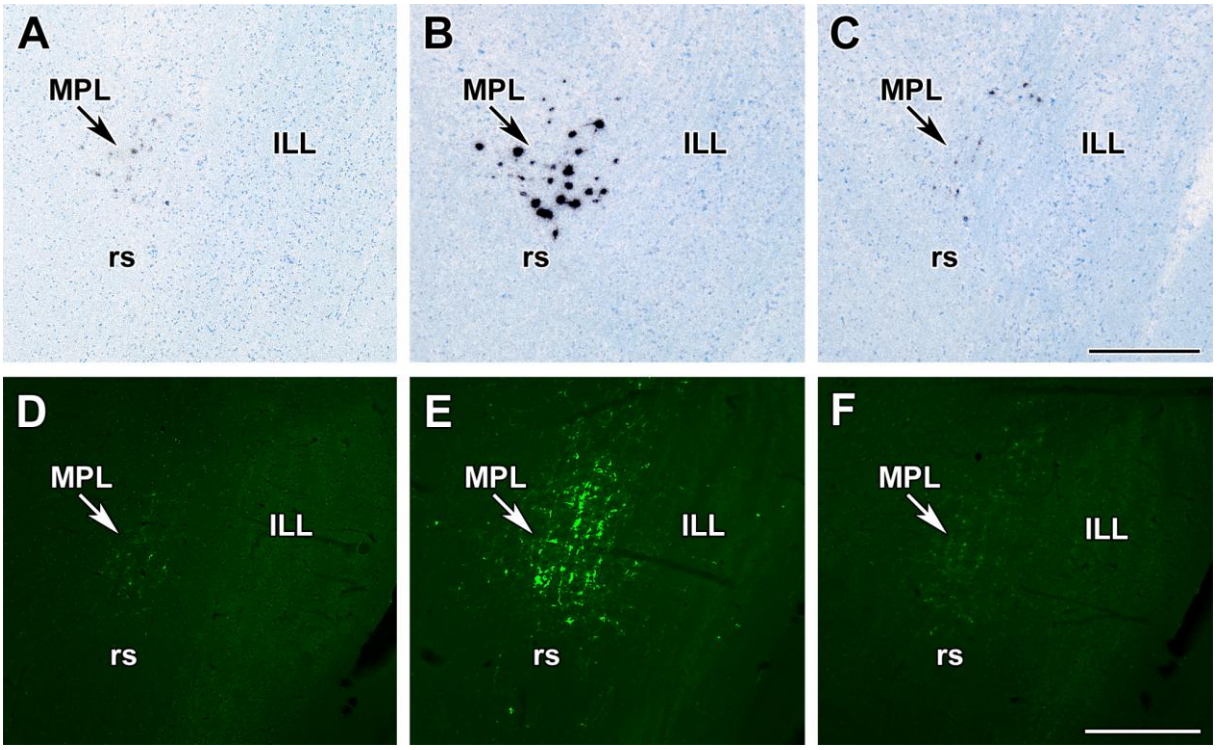

Fig. 31. The induction and distribution of TIP39 within the medial paralemniscal nucleus (MPL). An increased level of TIP39 mRNA expression is shown in the MPL of mother rats in bright-field photomicrographs of *in situ* hybridization histochemical sections (A-C) and in sections fluorescent immunolabeled for TIP39 (D-F). A: TIP39 mRNA signal is barely detectable in the MPL of a 4 months old control nulliparous female rat. B: Intense autoradiography signal is shown for TIP39 in all parts of the MPL in lactating mother rats. C: In mother rats whose pups had been removed immediately after delivery, TIP39 mRNA signal is as low as in the nulliparous control female. TIP39 immunoreactivity in the MPL changes in parallel with mRNA levels. D: The MPL contains only a low density of weakly immunolabeled neuronal cell bodies the control female rats. E: Intensely immunolabeled TIP39 cell bodies are distributed in all parts of the MPL in lactating mother. F: After removal of the pups, the intensity of the immunolabeling was reduced to the level of the control female shown in panel D. Scale bars = 400 μm for each panel. The figure is taken from our previous publication (Varga et al., 2012).

6.8.2. Increased TIP39-immunoreactivity in the brain of rat dams

TIP39-ir cell bodies were present in the PVG (Fig. 32A-C) as well as in the PIL (Fig. 32D-F). In the PVG, we observed similarly weak TIP39 immunolabeling in control female rats (Fig. 32A), lactating mothers (Fig. 32B), and mothers separated from their pups

immediately after delivery (Fig. 32C). In contrast, in the PIL, the intensity of immunolabeling was increased in lactating mother rats (Fig. 32E). Thus, a large number (more than 40 per section) of TIP39-ir cell bodies were observed in the PIL of rat dams (Fig. 32E) while only a few (less than 10 per section) TIP39-ir cell bodies were detected in the PIL of control female rats (Fig. 32D) and mothers separated from their pups immediately after delivery (Fig. 32F). In rat dams, these immunolabeled neuronal perikarya were located in the posterior intralaminar thalamic nucleus, the parvicellular (lateral) subparafascicular nucleus, and the caudal zona incerta (Fig. 32E). Thus, the distribution of TIP39-immunoreactive neurons in the PIL of lactating mother rats was the same as that of TIP39 mRNA-expressing neurons (Cservenak et al., 2010).

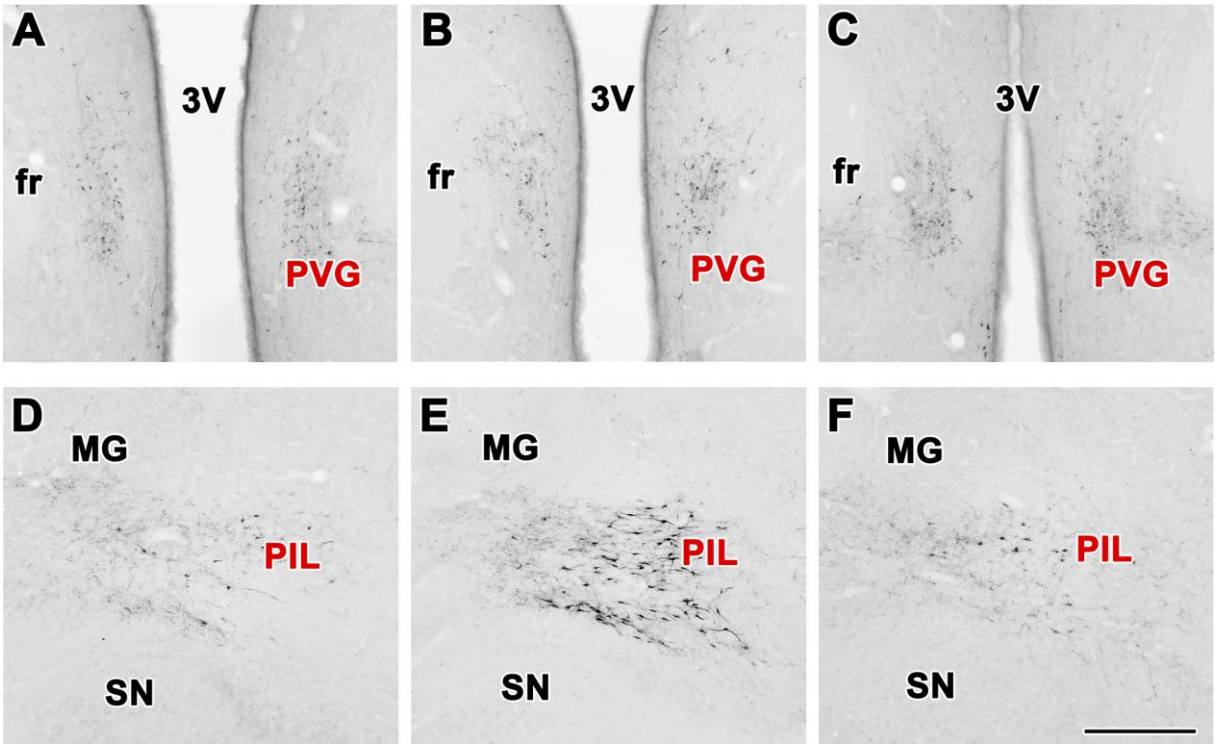

Fig. 32. TIP39-immunoreactive neurons in the periventricular gray of the thalamus (PVG) and the posterior intralaminar complex of the thalamus (PIL). In the PVG, immunocytochemistry reveals TIP39-positive neuronal cell bodies in control females (A), lactating mothers (B), as well as in pup deprived mothers (C). The distribution of the relatively weakly stained cell bodies is similar in the three groups and also to that of TIP39 mRNA-containing neurons. In contrast, the PIL contains only a low density of weakly immunolabeled neuronal cell bodies the control female rats (D), however, intensely immunolabeled TIP39 cell bodies are distributed in all parts of the PIL in lactating mother (E). After removal of the pups, the intensity of the immunolabeling was reduced (F) to the

level of the control female shown in panel D. Scale bar = 500 µm. The figure is taken from our previous publication (Cservenak et al., 2010).

The distribution of TIP39-immunoreactive neurons (Fig. 31D-F) within the paralemniscal area was similar to that of TIP39 mRNA-containing (Fig. 31A-C) neurons (Varga et al., 2012). The intensity of immunolabeling was increased in lactating mother rats as compared to control females and pup-deprived mothers (Fig. 31E). Thus, a large number (more than 30 per section) of TIP39-ir cell bodies were observed in the MPL of rat dams (Fig. 31E) while only a few (less than 10 per section) TIP39-ir cell bodies were detected in control female rats (Fig. 31D) and mothers separated from their pups immediately after delivery (Fig. 31F).

6.8.3. Measurement of TIP39 mRNA level in mother rats with real-time RT-PCR

In the PIL, lactating mother rats had a 6.9 times higher level of TIP39 mRNA than age-matched nulliparous control female rats, while the TIP39 mRNA level decreased to the level of control females when the pups were taken away from mothers (Fig. 33A). The mRNA level of TIP39 (expressed as 100000*mRNA level of TIP39 / mRNA level of GAPDH) was 30±7 in control female rats, 210±47 in lactating mother rats and 25±9 for mothers deprived of pups (Cservenak et al., 2010). These values represent a significant increase in the lactating rats with pups, based on one-way ANOVA. The change is in TIP39 mRNA as there was no difference in the level of GAPDH mRNA in the PIL between the 3 groups (4944±1871 fg/µl in control females, 6018±1726 fg/µl in rat dams, and 7894±2064 fg/µl in mother rats deprived of pups). In contrast to changes in the PIL, there was no significant difference in the TIP39 mRNA level in the PVG (Fig. 33B) between the 3 groups as determined by one-way ANOVA. The measured values were the following (expressed as 100000*mRNA level of TIP39 / mRNA level of GAPDH): 34±13 in control female rats, 18±11 in lactating mother rats and 46±19 for mothers deprived of pups (Cservenak et al., 2010). There was also no significant difference in the level of GAPDH mRNA between the 3 groups in the PVG (6277±2323 fg/µl in control females, 3310±919 fg/µl in rat dams, and 4712±1099 fg/µl in mother rats deprived of pups). In the MPL, lactating mother rats had a 4.0 times higher level of TIP39 mRNA than age-matched nulliparous control female rats (Varga et al., 2012). In contrast, TIP39 mRNA level was as low as that in control females when the pups were taken away from mothers immediately after delivery (Fig. 33). The mRNA level of TIP39

(expressed as 100000*mRNA level of TIP39 / mRNA level of GAPDH) was 65±23 (mean±SE) in control female rats, 259±46 in lactating mother rats and 62±11 for mothers deprived of pups representing a significant increase in the mother rats with pups. The change was in TIP39 mRNA levels as there was no difference in the level of GAPDH mRNA between the 3 investigated groups (Varga et al., 2012).

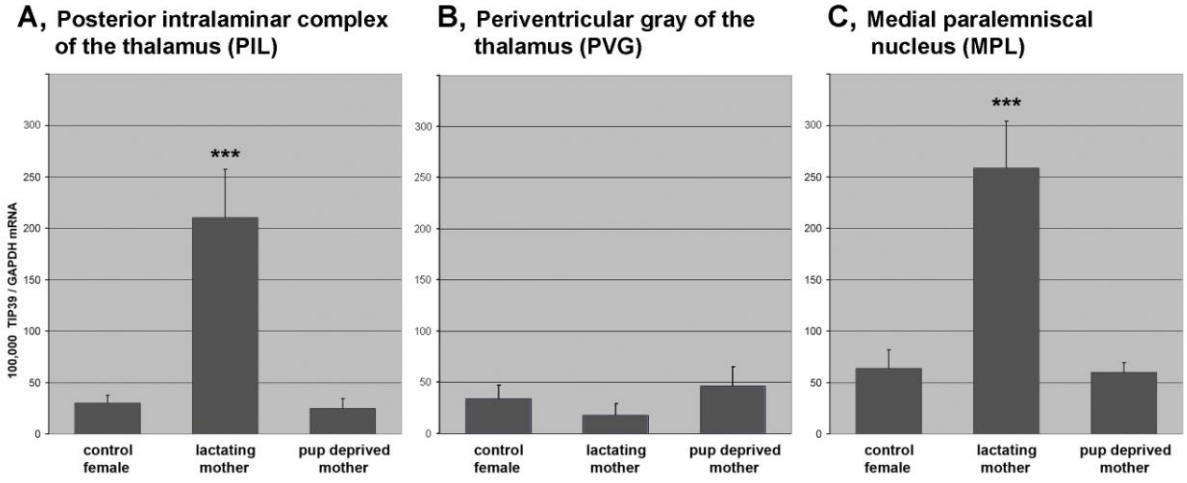

Fig. 33. TIP39 is selectively induced in the PIL of rat dams as demonstrated by quantitative real-time RT-PCR. A: In the PIL, the level of TIP39 mRNA is significantly higher (***: $p<0.001$) in lactating mothers than in age-matched nulliparous control female rats and mother rats deprived of pups immediately after delivery (n=8 in each group) as revealed by using one-way ANOVA (F=15.03). Bonferroni Post-Tests for posthoc comparisons further demonstrated that TIP39 mRNA level in the lactating mother was significantly ($p<0.001$) higher than that in control female rats (t=4.43) and mothers deprived of their pups (t=5.03) while the TIP39 mRNA levels did not differ in the latter two groups (t=0.08). B: In the PVG, there was a tendency for a reduced level of TIP39 mRNA in lactating mothers. However, there were no significant differences between rat dams and controls in the level of TIP39 mRNA in the PVG as determined by one-way ANOVA (F=0.82). C: In the MPL, the level of TIP39 mRNA is significantly higher (***: $p<0.001$) in lactating mothers than in age-matched nulliparous control female rats and mother rats deprived of pups immediately after delivery (n=8 in each group) as revealed by using one-way ANOVA (F=15.81). Bonferroni Post-Tests for posthoc comparisons further demonstrated that TIP39 mRNA level in the lactating mother was significantly ($p<0.001$) higher than that in control female rats (t=5.21) and mothers deprived of their pups (t=5.04) while the TIP39 mRNA levels did not differ in the latter two

groups (t=0.09). Data are expressed in the ratio of TIP39 to GAPDH mRNA. The panels are from our previous publications (Cservenak et al., 2010; Varga et al., 2012).

6.8.4. Levels of TIP39 mRNA in the PIL of pregnant females and postpartum rat dams

The level of TIP39 mRNA was highly significantly increased in mothers in the postpartum period ($F=24.46$; $p<0.0001$; Fig. 34). On day 21 of pregnancy, PIL neurons contained a very little TIP39 mRNA. The few mRNA-expressing cells observed contained only a small number of autoradiographic grains, and the intensity of the TIP39 mRNA signal was similar to that reported in virgin female rats (Cservenak et al., 2010). After parturition, however, both the number of TIP39 mRNA-expressing neurons and the number of autoradiographic grains per neuron increased dramatically ($p<0.0001$). At one day after delivery, a large number of TIP39-expressing neurons appeared in the PIL, and their autoradiographic signal was intense. At 9 and 23 days after parturition, TIP39 expression was increased over pre-partum dams similarly to at day one postpartum. These findings indicate that TIP39 mRNA levels remain elevated throughout the lactation period. Neurons demonstrating increased TIP39 mRNA levels were relatively evenly dispersed in the PIL (Fig. 34). On the 7th day after pups were weaned, the dams' expression of TIP39 was markedly reduced as compared to the lactating mothers ($p<0.0001$) and had returned to the basal level.

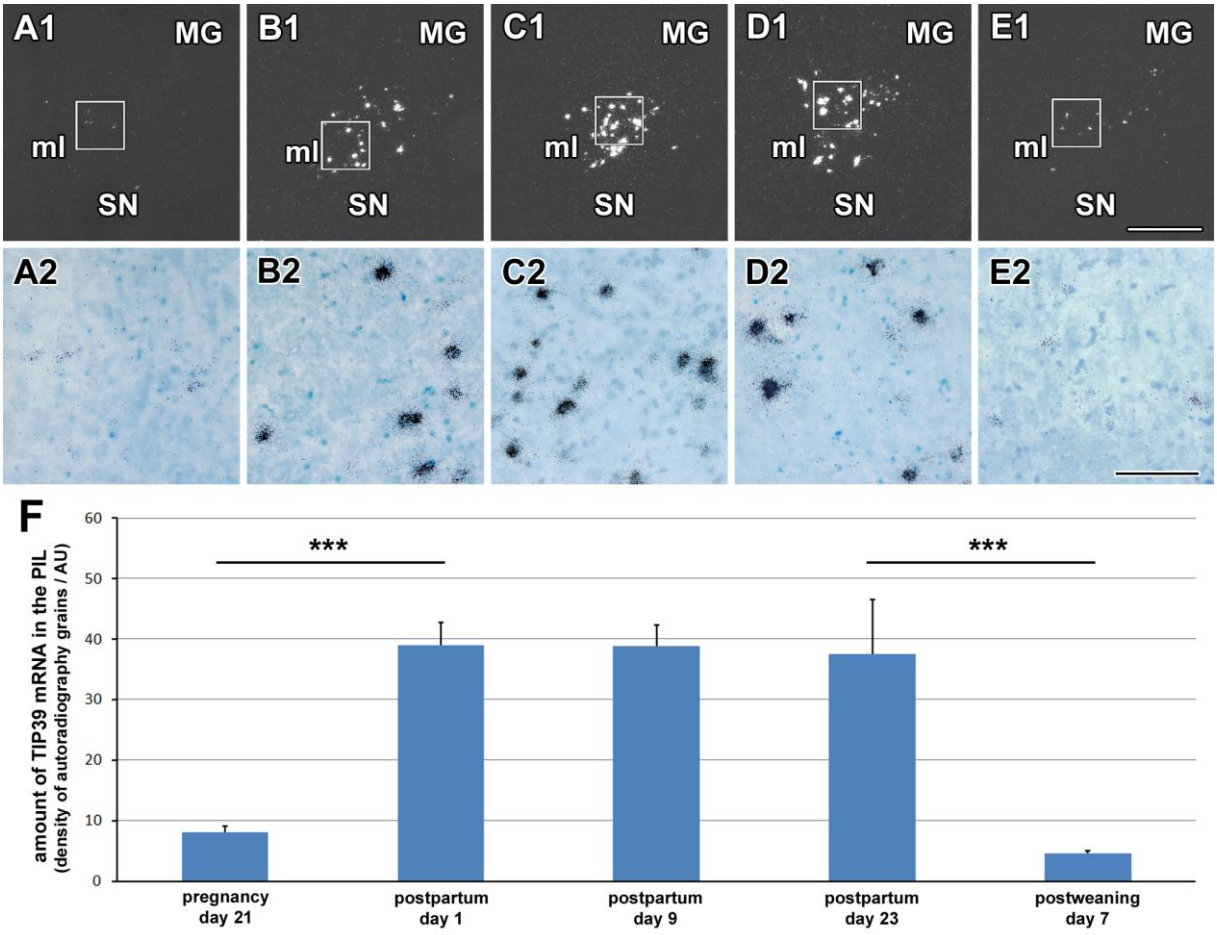

Fig. 34. Variation in TIP39 mRNA level during the reproductive cycle. A1-E1: Dark-field images of coronal brain sections of mother rats show TIP39 mRNA in the PIL detected by *in situ* hybridization histochemistry at different time points during the reproductive cycle. A2-E2: Higher magnification bright-field images of the framed area in the corresponding image in A1-E1, in which black grain clusters mark cells that express TIP39 mRNA. Sections are shown from the 21st day of pregnancy, which is 1 day before the expected day of delivery (A1,2), 1 day after parturition (B1,2), from the 9th (C1,2), and 23rd postpartum day (D1,2), and from the 7th day after weaning of the pups (E1,2) to demonstrate that elevated TIP39 expression is confined to the lactation period. F: Quantitative measurement of the amount of TIP39 mRNA by the density of autoradiography grains indicates a significant increase (***: $p<0.0001$) around parturition and a significant decrease after weaning (***: $p<0.0001$). *Abbreviations*: MG – medial geniculate body, ml – medial lemniscus, SN – substantia nigra. Scale bar = 500 µm for E1, and 100 µm for E2.

6.9. Amylin as the gene with the most salient expressional change in the preoptic area

Since we were successful in describing the maternal functions of a neuropeptide, which is markedly elevated during motherhood, we also addressed the genes with induced gene expression in the preoptic area, the established central element of brain maternal circuitry. In addition, as posterior thalamic TIP39 neurons project here, we also wanted to identify the targets of TIP39 projections in the preoptic area by determining the genes that also increase their expression level in mother rats.

6.9.1. Genes with altered mRNA expression in the preoptic area of rat dams

The microarray experiments on the 4 lactating mother – pup deprived mother pairs identified genes with altered gene expression in the preoptic area between the 2 groups (Dobolyi, 2009). There were 20 genes, which demonstrated highly significant ($p<0.001$) increase in their preoptic mRNA levels in lactating mothers (Table 3). The mRNA level of these genes increased to 2-2.5 times except for amylin whose mRNA level elevated to a marked 25.73 times. There were other genes whose mRNA levels were higher in mothers deprived of their pups. The number of genes, which demonstrated highly significant ($p<0.001$) decrease in their mRNA levels in lactating mothers was 14 (Table 3). The levels of these genes in lactating mothers were 36-49% of those in mothers deprived of their pups (Dobolyi, 2009).

Table 1. Microarray data in lactating dams

Fold change	Unigene code	Name of gene product
25.73	Rn.11394	amylin (islet amyloid polypeptide)
2.48	Rn.113868	ubiquitin-conjugating enzyme E2D 2
2.48	Rn.163633	transcribed locus
2.36	Rn.7700	brain protein I3
2.34	Rn.18772	similar to hypothetical protein FLJ10579
2.31	Rn.144660	eukaryotic translation elongation factor 1 alpha 1
2.30	Rn.25154	transcribed locus
2.29	Rn.16878	transcribed locus
2.26	Rn.2579	similar to RIKEN cDNA 0610008C08
2.10	Rn.89460	similar to Nucleoporin 62
2.09	Rn.63881	transcribed locus
2.07	Rn.1318	NADH dehydrogenase (ubiquinone) 1
2.06	Rn.154404	farnesyl diphosphate farnesyl transferase 1
2.06	Rn.99891	similar to hypothetical protein
2.06	Rn.18313	chondrolectin
2.05	Rn.8350	similar to hypothetical protein
2.03	Rn.187184	heat shock 70kD protein 1-like
2.03	Rn.53170	transcribed locus
2.02	Rn.25212	leucine zipper transcription factor-like 1
2.02	Rn.135283	similar to Homeobox protein Hox-C11
0.49	Rn.139226	similar to RIKEN cDNA 1110017I16 (predicted)
0.47	Rn.195358	tumor necrosis factor alpha induced protein 6
0.47	Rn.504	S100 calcium-binding protein A4
0.47	Rn.18057	RNA binding motif protein 3
0.46	Rn.16371	similar to aldo-keto reductase family 1, C19
0.44	Rn.2455	microtubule-associated protein tau
0.44	Rn.3247	procollagen, type III, alpha 1
0.42	Rn.32702	aldo-keto reductase family 1, member B7
0.42	Rn.25033	transcribed locus
0.41	Rn.76819	macrophage scavenger receptor 2 (predicted)
0.39	Rn.8484	ectonucleotide phosphodiesterase 6
0.37	Rn.44300	asialoglycoprotein receptor 1
0.37	Rn.9974	S100 calcium binding protein G
0.36	Rn.66008	KiSS-1 metastasis-suppressor

Table 3. List of genes demonstrating highly significant ($p<0.001$) changes in the level of their mRNA in the preoptic area of lactating mother rats as compared to mothers deprived of their pups immediately after delivery. The induction of amylin (islet amyloid polypeptide) is salient with a 25.7 fold increase. The table is from our previous publication (Dobolyi, 2009).

6.9.2. RT-PCR validation of the induction of amylin in the preoptic area of rat dams

RT-PCR validation of the change in amylin mRNA detected by microarray was performed using preoptic samples from 13 lactating mothers and 12 mothers deprived of their pups immediately after parturition and 10 nulliparous control females (Dobolyi, 2009). A 24 times higher mRNA level of amylin ($p<0.005$) was measured in the preoptic area of lactating dams as compared to mothers deprived of their pups and nulliparous control females while amylin levels in the latter 2 groups did not differ (Fig. 35). The mRNA level of amylin

(expressed as 100000*mRNA level / mRNA level of GAPDH) was 16±5 for nulliparous control female rats, 393±88 for lactating mother rats and 16±6 for mothers deprived of their pups (Fig. 35) while there was no difference in the level of GAPDH mRNA between the 3 groups (595±167 fg/µl in control females, 592±184 fg/µl in rat dams vs. 513±72 fg/µl in mother rats deprived of their pups).

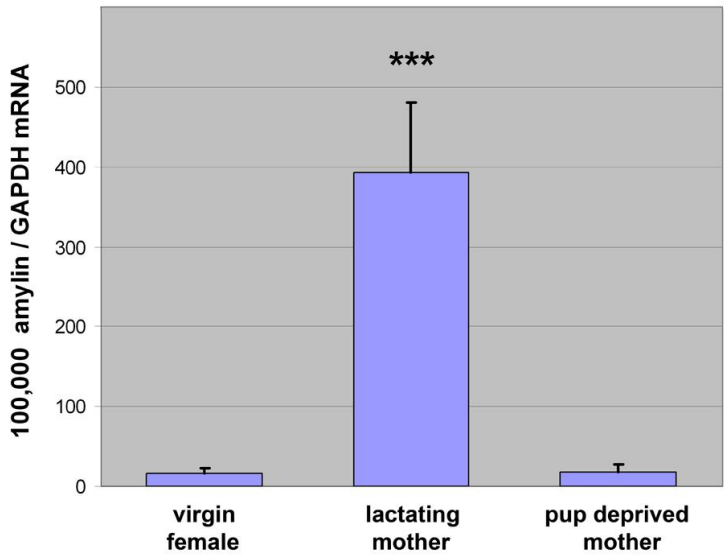

Fig. 35. Verification of an elevated amylin mRNA level in the preoptic area of lactating mother rats. A highly significantly increased amylin mRNA level was found by quantitative real-time RT-PCR in lactating mother rats as compared to control virgin female rats and mother rats deprived of their pups immediately after parturition (***: $p<0.005$). Data are expressed in the ratio of GAPDH mRNA. The figure is from our previous publication (Dobolyi, 2009).

6.10. Amylin neurons in the preoptic area

6.10.1. The distribution of amylin mRNA in the female rat brain

Using 2 different in situ hybridization probes specific for amylin provided identical distribution patterns and expression levels. A low intensity signal of amylin mRNA was detected in the medial preoptic nucleus and surrounding preoptic area of nulliparous control female rats while other regions of the forebrain demonstrated no signal for amylin mRNA (Dobolyi, 2009). The intensity of the signal in the preoptic area was markedly elevated in lactating mother rats, which allowed the description of the distribution of amylin-expressing neurons in the preoptic area (Fig. 36). A large number of neurons expressing mRNA of

amylin were located in the rostral part of the medial preoptic nucleus lateral to the third ventricle and to the preoptic periventricular nucleus. Labeled neurons were also located in the medial preoptic area dorsolateral to the medial preoptic nucleus. Further dorsolaterally, labeled neurons were distributed in the ventralmost part of the bed nucleus of the stria terminalis. Apart from these locations, we detected no signal for amylin mRNA in the examined part of the brain from bregma level +3.5 mm to -6 mm even in lactating mothers.

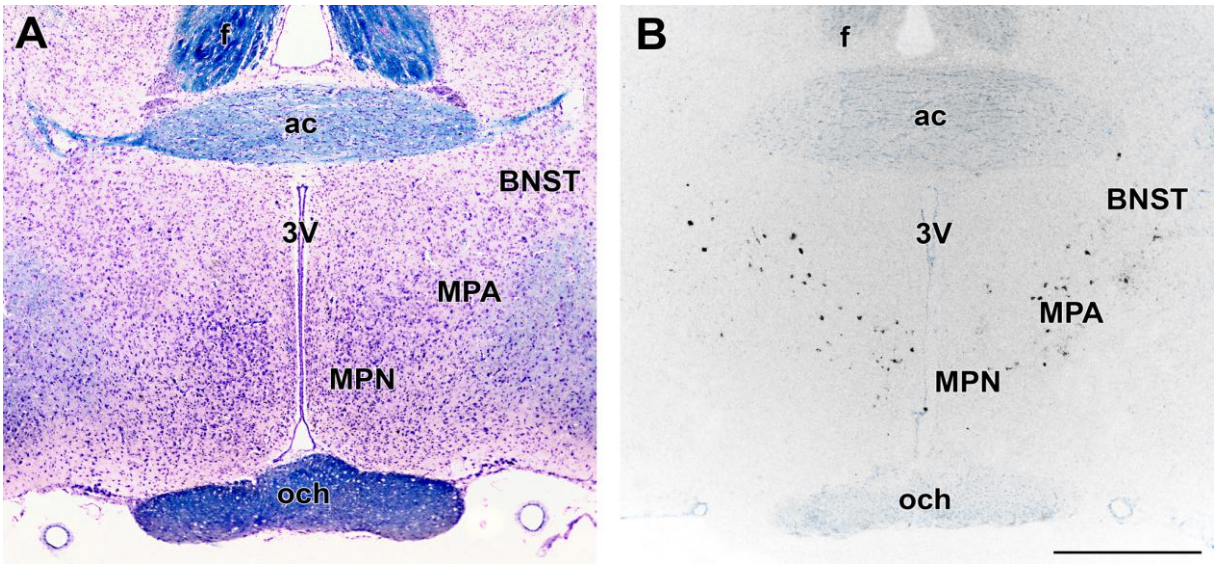

Fig. 36. Distribution of amylin-expressing neurons in the preoptic area. A: Cyto- and myeloarchitecture of the preoptic area at bregma level -0.36 mm. Blue color of luxol fast blue shows myelinated fiber bundles while cells are labeled with cresyl-violet. A high density of cells is visible in the medial preoptic nucleus (MPN). Dorsolateral to the MPN, cells in the medial preoptic area (MPA) are visible without the presence of surrounding myelinated fibers. Further dorsolateral to this cell group of the MPA, the ventral part of the bed nucleus of the stria terminalis (BNST) is located. B: A bright-field in situ hybridization histochemistry photomicrographs shows amylin mRNA-expressing neurons (black) evenly distributed in the MPN, the MPA, and the ventral part of the BNST of a lactating mother rat. Additional abbreviations: ac – anterior commissure, f – fornix, och – optic chiasm, 3V – third ventricle. Scale bar = 1 mm. The figure is from our previous publication (Dobolyi, 2009).

6.10.2. Time course and distribution of amylin mRNA expression in the peri- and postpartum periods in preoptic amylin neurons

A very low level of amylin mRNA was detected on the 21st day of pregnancy (Fig. 37A). We found a combined 5.3±1.0 amylin mRNA-expressing cells in one side of the brains (Szabo et al., 2012). The number of autoradiography grains per cell was 30.8±5.2. After parturition, a significant increase was detected in both the number of amylin mRNA expressing neurons (F=60.86), and the number of autoradiography grains per neuron (F=44.82). One day after delivery, a large number of amylin-expressing neurons (81.3±8.7 amylin mRNA-expressing cells in one side of the brains) appeared in the preoptic area (Fig. 37B). The autoradiography signal was intense in these labeled neurons (66.5±5.3 autoradiography grains per cell). 9 and 23 days after parturition, amylin established an even higher level of expression in the same preoptic brain regions than in the first postpartum day (Fig. 37C,D). The combined number of amylin mRNA-expressing cells in one side of 3 consecutive sections was 120±9.5, and 108±3.3, respectively. The number of autoradiography grains per cell was 105.6±5.3, and 102.1±7.3, respectively (Fig. 37E,F). Amylin-expressing neurons were situated in the MPN, parts of the MPA, and BNSTv at the level of the anterior commissure. Within these regions, amylin mRNA-expressing neurons did not form a compact cluster of cells but were relatively evenly dispersed among other types of neurons. In addition to these preoptic locations, we detected no signal for amylin mRNA in the examined parts (between bregma levels +3 mm and -3 mm) of the brain in pregnant rats and lactating mothers (Szabo et al., 2012).

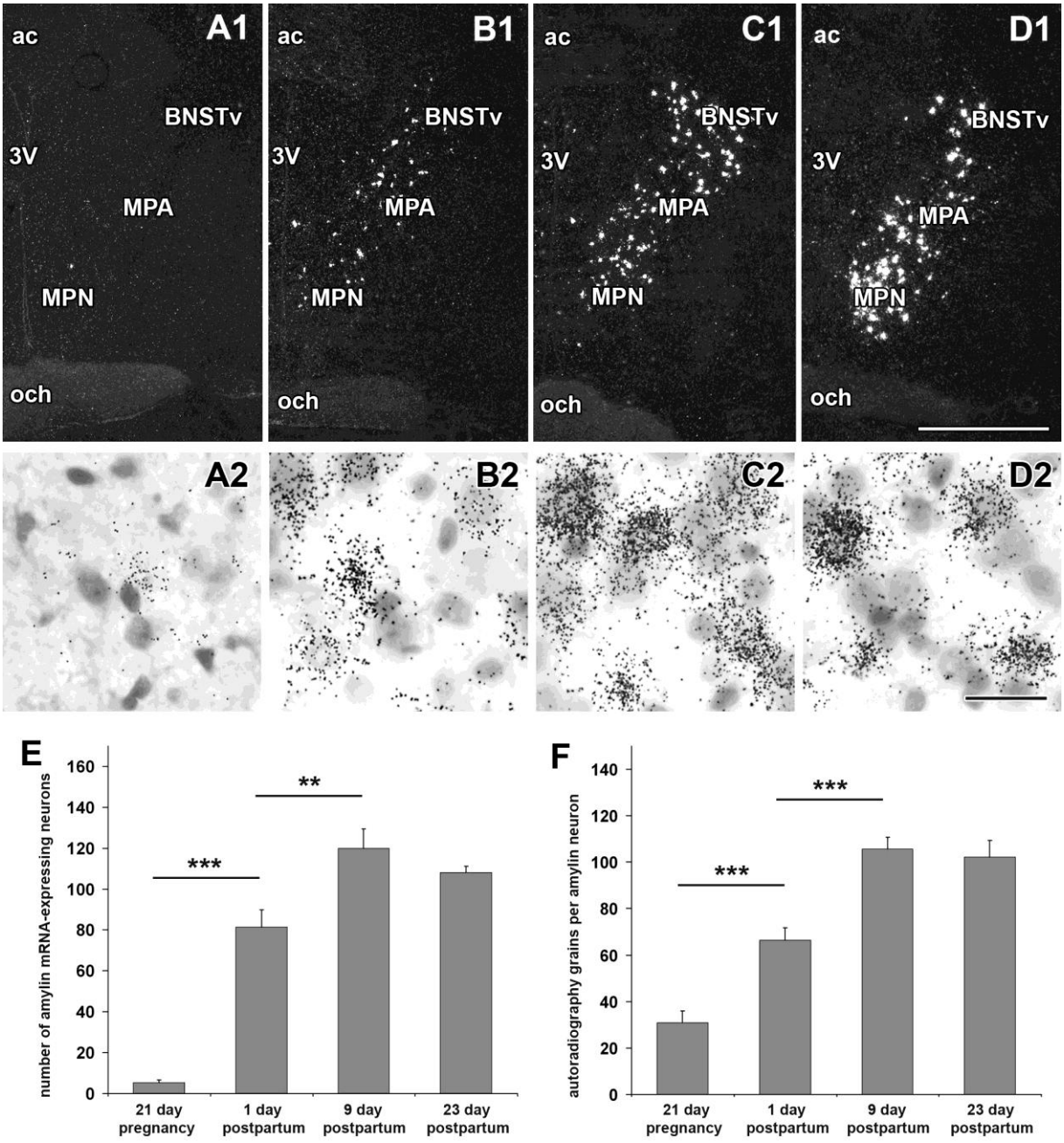

Fig. 37. Radioactive *in situ* hybridization histochemistry demonstrates amylin mRNA expressing neurons in the preoptic area at bregma level -0.24 mm. **A1-D1**: The distribution of amylin mRNA is shown in dark-field photomicrographs, in which white signal represents amylin mRNA. Amylin mRNA is distributed in the medial preoptic nucleus (MPN), dorsolateral to the MPN in parts of the medial preoptic area (MPA) and further dorsolateral to this cell group in the ventral part of the bed nucleus of the stria terminalis (BNSTv). **A2-D2**: High magnification bright-field photomicrographs demonstrate individual autoradiography grains (black dots) above amylin mRNA-expressing preoptic neurons. Amylin mRNA expression is very low on the 21st day of pregnancy (**A**) but increases by the 1st postpartum day (**B**) and becomes even higher by the 9th (**C**) and 23rd (**D**) postpartum days. **E**: The total

number of amylin mRNA-expressing neurons counted in the same side of 3 consecutive coronal sections positioned at 216 μm distances from each other is shown (n=6 at each time point). A significant increase was found between the 21st day of pregnancy and the 1st postpartum day (***: p<0.001). Further significant increase takes place in the number of amylin mRNA-expressing neurons between the 1st and 9th postpartum day (**: p<0.01). **F**: The number of autoradiography grains in randomly selected amylin mRNA-expressing neurons (10 neurons per one side of the brain) is shown. A significant increase was found between the 21st day of pregnancy and the 1st postpartum day and also between the 1st and 9th postpartum day (n=6 at each time point; ***: p<0.001). Scale bar = 1 mm for A1-D1 and 30 μm for A2-D2. The figure is taken from our recent publication (Szabo et al., 2012).

6.10.3. Amylin-immunoreactivity in the preoptic area of the female rat brain

Amylin-immunoreactive neurons were found in the preoptic area of rat dams but not in mothers separated from their pups immediately after delivery (Fig. 38). In rat dams, the immunolabeled neuronal perikarya were located in the rostral part of the medial preoptic nucleus, the medial preoptic area dorsolateral to the medial preoptic nucleus while labeled neurons were also found in the ventralmost part of the bed nucleus of the stria terminalis (Fig. 38). The distribution of amylin-immunoreactive neurons in the preoptic area was the same as that of amylin mRNA-expressing neurons (Dobolyi, 2009).

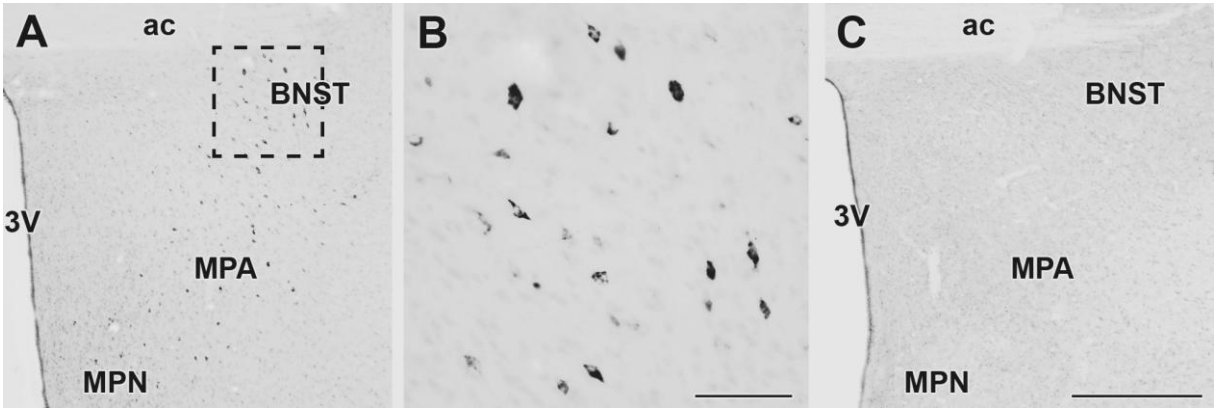

Fig. 38. Amylin immunoreactivity in the preoptic area of female rats. A: In the preoptic area of lactating rat dams, immunolabeled neurons can be observed in the medial preoptic nucleus (MPN), parts of the medial preoptic area (MPA), and the ventral part of the bed nucleus of the stria terminalis (BNST). B: Magnified image of the framed area in A demonstrates amylin-immunolabeled cell bodies. C: In pup-deprived mother rats, immunolabeled cells are not

visible in the preoptic area. Additional abbreviations include: ac – anterior commissure, 3V – third ventricle. Scale bar = 500 μm for A and C, and 100 μm for B. The figure is from our previous publication (Dobolyi, 2009).

6.11. Pup exposure-induced activation of amylin-neurons in the preoptic area of rat dams

Upon returning the pups, the dams all took care of them immediately, and suckling started within 10 min. Fos-ir neurons appeared in response to pup exposure in a number of brain regions, including parts of the preoptic area (Szabo et al., 2012).

6.11.1. Fos-labeled amylin mRNA-expressing neurons in the preoptic area in response to suckling

The co-expression of amylin and *c-fos* genes in the preoptic area of pup exposed mother rats was also evident based on the double labeling of amylin mRNA and Fos immunoreactivity (Fig. 39). The number of amylin mRNA-containing neurons was 113±15 in a side of the sections that contained amylin mRNA expressing neurons. Fos immunoreactivity was present in 93.2% of these amylin-expressing neurons (Szabo et al., 2012).

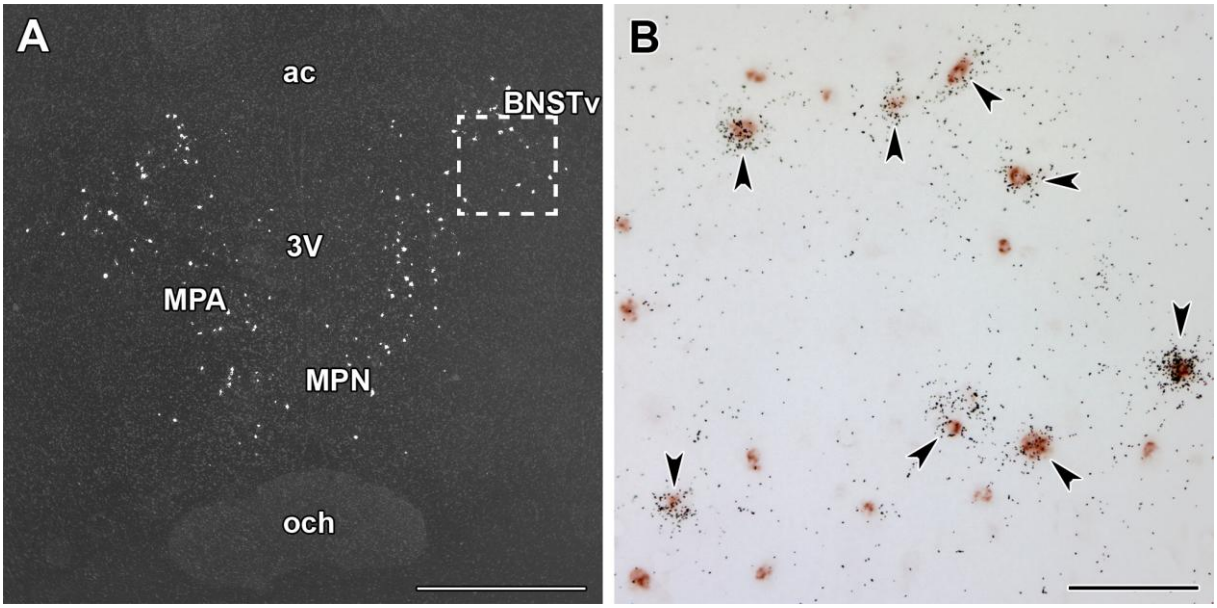

Fig. 39. Fos activation of amylin mRNA expressing neurons in response to pup exposure. A: A high density of amylin mRNA expressing neurons (white labeling) can be seen in a dark-field photomicrograph of the preoptic area in mother rat at bregma level -0.4 mm. B: The

framed area in A is shown in bright-field picture at a high magnification. Most amylin mRNA-expressing neurons (situated below the black autoradiography dots) contained Fos-immunoreactivity (brown nuclei) in the preoptic area 2h after pup exposure following 22h separation. A considerable number of Fos-ir but amylin-negative neurons are also visible. Fos-ir neurons were present in the MPN, MPA, and BNSTv with a distribution similar to that of amylin-expressing neurons. Scale bar = 1 mm for A and 100 μm for B. The figure is taken from our previous publication (Szabo et al., 2012).

6.11.2. Fos-labeled amylin-immunoreactive neurons in the preoptic area in response to suckling

Within the preoptic area, Fos-immunoreactive (Fos-ir) neurons appeared (a combined 584±72 in 3 consecutive preoptic sections) in the MPN, MPA, and BNSTv when the dams were exposed to their pups for 2 h following 20 h of separation (Fig. 40A). Thus, the distribution of neurons activated by pup exposure was very similar to the distribution of amylin-expressing neurons. In turn, only a low number of Fos-ir neurons (a combined 71±21 in 3 consecutive sections) were detected in the preoptic area of rat dams 22 h after separating them from their pups (Fig. 40B). Fos-ir nuclei were evenly distributed within the region of the preoptic area that contained Fos-ir neurons whereas adjacent brain areas, including other parts of the preoptic area and the bed nucleus of the stria terminalis, remained almost completely devoid of Fos-ir cells (Szabo et al., 2012).

The number of amylin-ir neurons with an identifiable nucleus in the preoptic area was a combined 174.2±61.0 in 3 consecutive preoptic sections (n=5 brains). The number of amylin neurons was about equally high in the MPN and MPA and lower in the BNSTv (Fig. 40E). Double immunolabeling revealed that 85.6% of amylin-ir neurons in the preoptic area were Fos-positive (Fig. 40C,D). The percentage of Fos-positive amylin neurons did not differ between the MPN, MPA, and BNSTv (Fig. 40E). The few amylin-ir neurons whose cell bodies lacked Fos immunoreactivity and the Fos-positive but amylin-negative neurons did not have a distinct distribution from that of Fos-positive amylin neurons (Szabo et al., 2012).

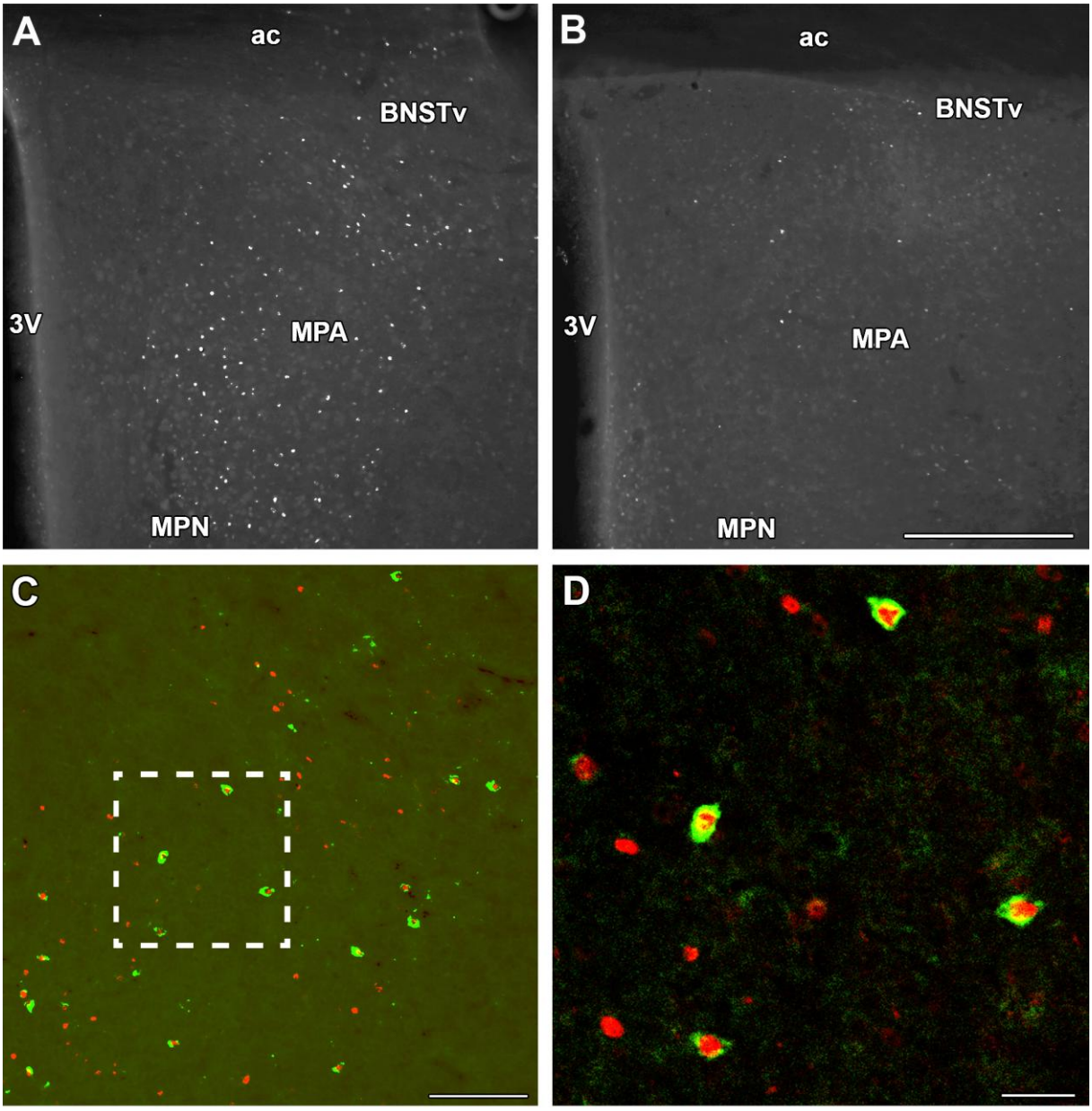

E

Medial preoptic nucleus (MPN)		Medial preoptic area (MPA)		Bed nu. of stria terminalis (BNSTv)	
Number of amylin neurons with nucleus	Percentage of Fos-ir amylin neurons	Number of amylin neurons with nucleus	Percentage of Fos-ir amylin neurons	Number of amylin neurons with nucleus	Percentage of Fos-ir amylin neurons
65.0±30.7	85.9±2.1	70.0±29.9	82.9±3.7	39.2±23.7	90.4±5.2

Fig. 40. Fos activation of amylin-ir neurons in response to pup exposure at bregma level -0.40 mm. A: A high density of Fos-ir neurons (white dot-like nuclei) was present in the preoptic area of mother rats 2 h after pup exposure following 22 h separation. Fos-ir neurons were present in the MPN, MPA, and BNSTv with a distribution similar to that of amylin-

expressing neurons. B: The number of Fos-ir neurons was very low in the preoptic area of mother rats whose pups were not given back to them. C: Most amylin-ir neurons (green cell bodies) contain Fos (red stained nuclei) in the preoptic area following pup exposure, as demonstrated by double fluorescent immunolabeling. A considerable number of Fos-ir but amylin-negative neurons distributed evenly among double-labeled cells are also visible. D: A confocal photomicrograph shows neurons labeled for amylin and Fos in high magnification. E: The number of amylin-ir neurons with identifiable cell nucleus and the percentage of Fos-ir amylin neurons are shown in the MPN, MPA, and BNSTv. Amylin neurons were present in 3 coronal sections cut at 200 µm distances. All amylin-ir neurons were counted in all 3 sections of 5 rats exposed to pups. The numbers in the panel represent the average (n=5 brains) sum of labeled cells in the 3 sections that contained amylin-ir neurons. Scale bar = 500 µm for B, 200 µm for C and 50 µm for D. The figure is taken from our previous publication (Szabo et al., 2012).

6.12. The connection between TIP39 and amylin neurons

6.12.1. Innervation of amylin-immunoreactive neurons by TIP39 fibers

The distribution of amylin neurons was very similar to the distribution of TIP39-ir fibers in the preoptic area. Therefore, we performed double labeling and found that the vast majority of amylin neurons are closely apposed by TIP39 terminals (Fig. 41).

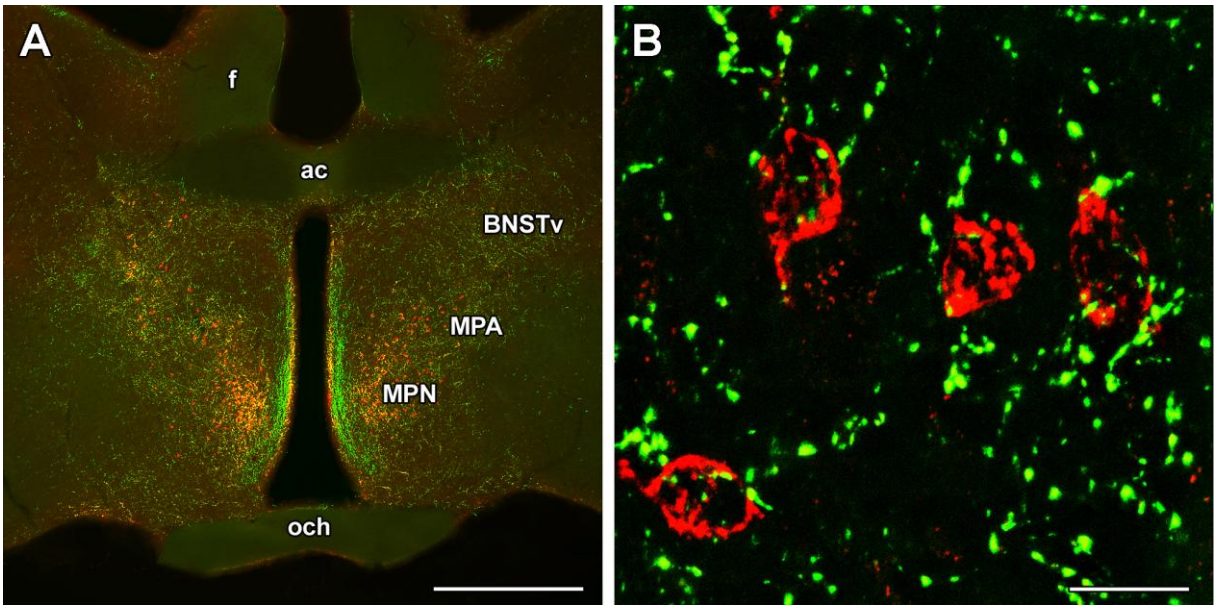

Fig. 41. TIP39 and amylin immunoreactivities in the preoptic area of rats. A: The localization of amylin neurons (red) and TIP39 fibers (green) is overlapping in the medial preoptic nucleus (MPN), and some parts of the medial preoptic area (MPA) and the ventral subdivision of the bed nucleus of the stria terminalis (BNSTv). B: A high magnification confocal image demonstrates that amylin neurons are closely apposed by TIP39 terminals. Scale bar = 1 mm for A, and 20 μm for B.

6.12.2. The maternal induction of amylin in mice lacking the PTH2 receptor

We showed that amylin is induced in the preoptic area of mice mothers with the same distribution as in rats. Furthermore, the induction of amylin was reduced in mice lacking the PTH2 receptor in all parts of the preoptic area (Fig. 42). A semi-quantitative analysis of in situ hybridization histochemistry demonstrated a 59.6% decrease in the amount of amylin mRNA present in the preoptic area of mice lacking PTH2 receptor (Fig. 42).

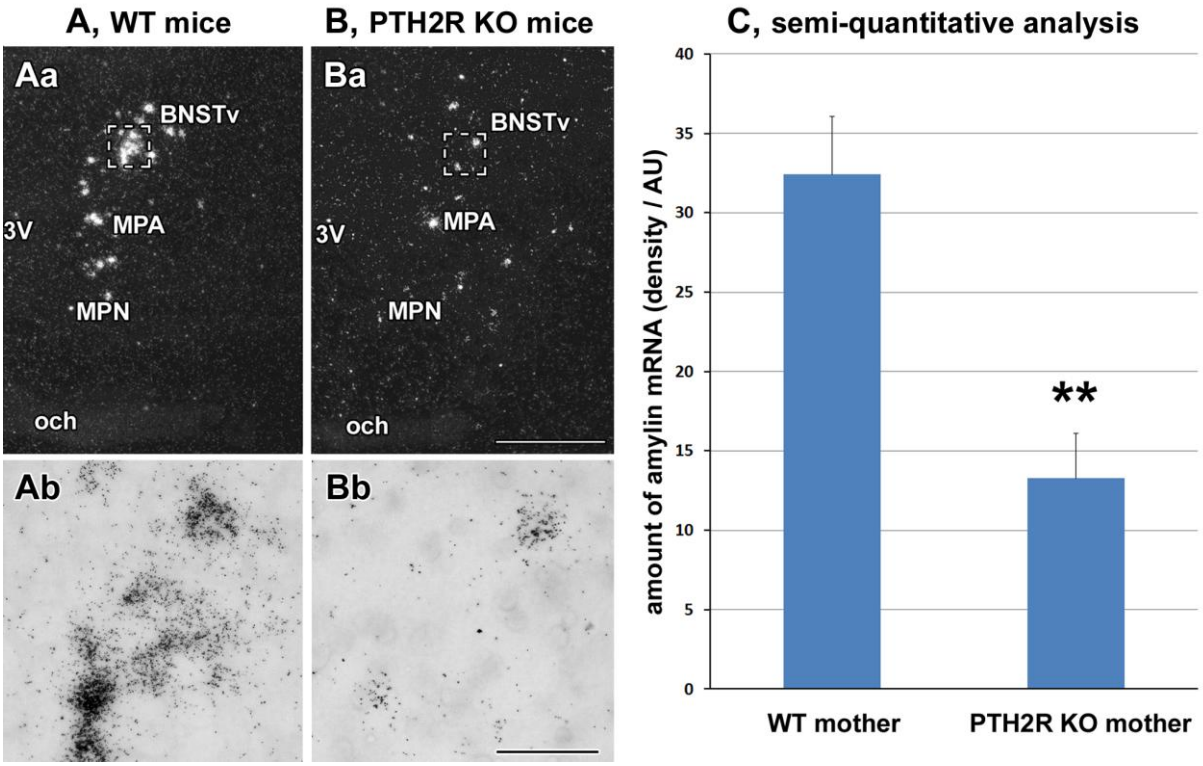

Fig. 42. The effect of the lack of the PTH2 receptor on the induction of amylin mRNA in mother mice. A: Amylin mRNA distributed in the preoptic area of wild-type mice (WT mice). B: Amylin mRNA distributed in the preoptic area of PTH2 receptor knock-out mice (PTH2R KO mice). Aa and Ba are dark-field photomicrographs taken from in situ hybridization

histochemistry sections of mother mice on postpartum day 9. Ab and Bb are bright-field photomicrographs of the framed areas in Aa and Ba. C: Semi-quantitative densitometric analysis revealed a significant ($p<0.01$) decrease in the level of amylin mRNA in mice lacking the PTH2 receptor. Scale bars = 400 μm for Ba and 50 μm for Bb.

7. DISCUSSION

We first describe the different cell groups expressing TIP39 in the central nervous system. Then, the TIP39-PTH2 receptor neuromodulator system is characterized. The maternal functions of different cell groups expressing TIP39 are separately discussed. Finally, amylin neurons, their maternal functions, and their relationship with the TIP39-PTH2 receptor neuromodulator system are described.

7.1. TIP39 in the central nervous system

TIP39 is encoded by a single gene, from which no other known neuropeptides is synthesized (Dobolyi et al., 2002). There are three different cell groups expressing TIP39 in the central nervous system, the PVG and the PIL in the posterior thalamus, and the MPL in the lateral pons. This distribution pattern is unique among neuropeptides, and some of these brain regions have not been well defined previously (Dobolyi et al., 2010). Therefore, discussion of these brain regions in relation to the exact location of TIP39 neurons and available literature data is important, especially as TIP39 neurons do not necessarily follow accepted anatomical borders of established brain nuclei.

7.1.1. TIP39 neurons in the PIL

The PIL, defined by the area containing TIP39 neurons, includes the posterior intralaminar thalamic nucleus, the parvicellular subparafascicular nucleus, and some parts of the caudal subdivision of the zona incerta. Some of the projections of PIL neurons have been described in previous studies, including the medial preoptic area (Simerly and Swanson, 1986), the paraventricular hypothalamic nucleus (Campeau and Watson, 2000), the arcuate nucleus (Li et al., 1999a; Szabo et al., 2010), and the amygdaloid nuclei (LeDoux et al., 1990). Our studies revealed projections of TIP39 neurons in the PIL as lesioning the PIL resulted in the loss of TIP39 immunoreactivity in the hypothalamus and amygdala (Dobolyi et al., 2003a). TIP39 fibers were abundant in the supraoptic decussations (Dobolyi et al., 2003b) and could be followed to their origin in the PIL in the adult (Palkovits et al., 2010) as well as in the developing brain (Brenner et al., 2008). Unilateral transection of this pathway in mother rats resulted in the disappearance of TIP39 fibers from the arcuate and periventricular nuclei suggesting that their TIP39 fibers and fiber terminals originate in TIP39 neurons in the PIL (Cservenak et al., 2010). Our retrograde tracer studies also suggest that TIP39 neurons in the PIL project to the arcuate nucleus and the preoptic area in the hypothalamus and that neurons projecting to these brain regions are confined to the PIL within the posterior thalamus. The

distribution of TIP39 neurons projecting to both hypothalamic sites were evenly distributed within the PIL. These results support the idea that the PIL constitutes a topographical unit, although it does not correspond to an obvious cytoarchitectonically defined nucleus. In addition, the lack of retrograde labeling in other TIP39 cell groups suggest that TIP39 fibers in the the arcuate nucleus and the preoptic area originate exclusively from the PIL.

7.1.2. TIP39 neurons in the PVG

The shape of the area in the PVG where TIP39-containing cell bodies are localized is complex (Dobolyi et al., 2003b). The highest density of TIP39-containing cells is in the magnocellular subparafascicular nucleus medial to the fasciculus retroflexus but some TIP39 cells are located in the most rostral part of the central gray and laterally, below the fasciculus retroflexus.

Lesions of the PVG decreased the density of TIP39 fibers in ipsilateral forebrain regions suggesting projections from the PVG to those forebrain regions (Dobolyi et al., 2003a). The PVG provides ipsilateral TIP39-containing projections to the anterior midline limbic cortex (prelimbic, infralimbic and dorsal peduncular cortices), the shell and cone (rostral pole) portions of the nucleus accumbens, the lateral septum, the bed nucleus of the stria terminalis, the ‘fundus striati’, the subiculum, and the thalamic paraventricular nucleus, and some hypothalamic nuclei. No reduction was observed in the density of TIP39-containing fibers in the midbrain, pons, medulla and spinal cord following PVG lesions. Thus, at least most of the TIP39-containing fibers in the midbrain, pons, medulla and spinal cord do not originate in the subparafascicular area but rather they arise from the MPL as discussed below. The PVG contains many cells that do not contain TIP39, among these are A11 dopaminergic cells, CGRP- and substance P-containing cells that do not co-localize with TIP39 (Dobolyi et al., 2003b). On the basis of our data, we believe that the previously reported descending projections from the PVG (Yasui et al., 1992) originate in cell types that do not contain TIP39.

Projections of the PVG TIP39-containing cells suggest the involvement of TIP39 of subparafascicular origin in limbic functions. The target regions of the TIP39 neurons in the PVG are mutually interconnected (Canteras et al., 1995; Moga et al., 1995; Risold and Swanson, 1997) suggesting that they may serve related functions. One potential candidate is the regulation of stress responses (Fegley et al., 2008). Limbic pathways are sensitive to stressors that involve higher-order sensory processing (Herman and Cullinan, 1997). Indeed, lesion or stimulation of the limbic regions that receive TIP39 fibers from the PVG influences

the response of the hypothalamic-pituitary-adrenocortical (HPA) axis to stressors that involve higher-order sensory processing, possibly *via* periparaventricular and dorsomedial projections (Herman et al., 2002).

7.1.2. TIP39 neurons in the MPL

The cone-shaped structure of the MPL can be cytoarchitectonically distinguished from adjacent brain regions in the lateral pontomesencephalic tegmentum based on the columnar arrangement of its neurons suggesting that it is a distinct nucleus (Varga et al., 2008). The MPL has a characteristic cytoarchitecture resulting from dorso-ventrally oriented columnar arrangement of its cells. It is plausible that this cellular arrangement is an inherent property of MPL; alternatively it might be due to the organization of the abundant tracts and fiber bundles passing through MPL and hence might differ in different species. The rostral part of the MPL is embedded between the pedunculopontine tegmental and the retrorubral nuclei, from which the MPL is separated by a zone of lower cell density. The dorsolateral and lateral borders of the MPL are the dorsal and intermediate nuclei of the lateral lemniscus, respectively. Medially, the MPL borders the oral part of the pontine reticular formation, which contains cells of markedly different morphology to those in MPL. In turn, the caudal borders of the MPL are the Kölliker-Fuse nucleus laterally and the region of the A7 cell group medially. Ventrally, the MPL lies on the rubrospinal tract except for the medial part of its rostral half where large acetylcholinesterase-positive cells of the epirubrospinal nucleus surround the rubrospinal tract (Paxinos and Butcher, 1985). Apart from the cytoarchitectonic differences, a distinct MPL is also supported by our finding that the afferent connections of the MPL differ markedly from those of adjacent brainstem nuclei (Varga et al., 2008).

In the literature, often no distinction is made between oral reticular pontine and paralemniscal zones. Areas including cells that correspond to the MPL have been referred by a great variety of anatomical names with poor topographical characterization, such as “lateral part of the nucleus reticularis pontis oralis” (Papez, 1926), “lateralmost nucleus reticularis pontis oralis” (Leichnetz et al., 1978), “ventrolateral tegmental area” (Herbert et al., 1997), or “dorsolateral pontomesencephalic reticular formation” (Haws et al., 1989). The term ´paralemniscal´ has also been used without detailed topographical characterization when describing an area in the “paralemniscal zone” whose stimulation elicited pinna movement in cats (Henkel and Edwards, 1978), a group of neurons whose activity changed in response to noxious stimuli in the “paralemniscal reticular formation” (Hardy et al., 1983), a group of neurons expressing Fos in response to suckling in the “caudal portion of the paralemniscal

nucleus" (Li et al., 1999b), a group of audio-vocal neurons in the "paralemniscal tegmentum" (Metzner, 1993), and a group of neurons whose stimulation elicited vocalization in the "paralemniscal tegmental area" in bats (Fenzl and Schuller, 2007; Schuller and Radtke-Schuller, 1990) and the "ventral paralemniscal area" in squirrel monkey (Hage and Jurgens, 2006; Hannig and Jurgens, 2006). Furthermore, the existence of a cell group probably corresponding to the MPL was mentioned in early studies (Fuse, 1926; Wünscher et al., 1965), and also more recently as the caudal part of the paralemniscal nucleus (Andrezik and Beitz, 1985). However, the MPL is different from the paralemniscal nucleus described in a more rostral and lateral location (Olszewski and Baxter, 1982; Paxinos and Watson, 2005; Taber, 1961). The term ´medial paralemniscal nucleus´ introduced by our studies (Dobolyi et al., 2003b) has been adopted by the widely used Paxinos rat brain atlas (Paxinos and Watson, 2005). The lack of previous description of the MPL probably stems from the difficulty in defining the area functionally and even topographically without neurochemical markers, which may have contributed to the usage of different terminologies describing overlapping parts of the paralemniscal region. However, as far as we could judge, only the area where neurons express Fos protein in response to pup exposure (Li et al., 1999b) corresponds perfectly to the MPL.

Apart from descending spinal projections from the area corresponding to the medial paralemniscal nucleus (Basbaum and Fields, 1979; Carlton et al., 1985; Holstege and Kuypers, 1982), the efferent projections of the MPL have not been previously described. On the basis of our lesion studies, the MPL provides TIP39-containing projections to the medial geniculate body, the periaqueductal gray, the deep layers of the superior colliculus, the external cortex of the inferior colliculus, the nuclei of the lateral lemniscus, the lateral parabrachial nucleus, the locus coeruleus, the subcoeruleus area, the medial nucleus of the trapezoid body, the periolivary nuclei, and the spinal cord (Dobolyi et al., 2003a). However, the contribution of the MPL to forebrain TIP39 fibers cannot be excluded but it cannot be dominant in any forebrain regions, because we observed no visible decrease in the density of TIP39 fibers in any forebrain regions following medial paralemniscal lesions (Dobolyi et al., 2003a). The major targets of TIP39-containing medial paralemniscal neurons are the components of the auditory system. However, none of the auditory regions where TIP39 neurons project from the MPL are tonotopically organized (Clopton et al., 1974) suggesting that TIP39-containing neurons in the MPL might modulate auditory functions unrelated to the fine discrimination of tones.

Through its TIP39-containing projections to the spinal cord, the medial paralemniscal TIP39-containing cell group also has the potential to regulate spinal functions. The effects of intrathecal administration of TIP39 and a TIP39 antibody in tail-flick and paw-pressure assays suggest that TIP39 potentiates some aspects of nociception within the spinal cord (Dobolyi et al., 2002) and neuropathic and inflammatory pain may be mediated by TIP39 (Dimitrov et al., 2013). Since TIP39 is not synthesized within the spinal cord (Dobolyi et al., 2003b), the potentiating effects of TIP39 on nociception may be mediated physiologically *via* descending TIP39-containing fibers arising from the MPL.

7.2. The TIP39-PTH2 receptor neuromodulator system

The PTH2 receptor, a member of the family B (type II) of G protein-coupled receptors (Dobolyi et al., 2012) was discovered based on its sequence similarity to other proteins belonging to this receptor family (Usdin et al., 1995). The novel receptor was named PTH2 receptor because of its sequence similarity to the parathyroid hormone receptor and also because the human PTH2 receptor can be activated by parathyroid hormone (Usdin et al., 2002). In rat, however, nanomolar concentrations of parathyroid hormone do not cause significant activation of the PTH2 receptor (Hoare et al., 1999a). An additional difference between the parathyroid hormone 1 receptor (PTH1R) and the PTH2 receptor is that the distinct polypeptide parathyroid hormone-related peptide is a co-ligand of the PTH1 receptor but does not bind to the PTH2 receptor (Hoare et al., 1999b) (Fig. 43). TIP39 is a high affinity and fully potent agonist for both the human and rodent PTH2 receptor (Usdin et al., 1999b). Apart from elevating cAMP (presumably *via* Gs proteins), TIP39 was also shown to elevate intracellular Ca^{2+} levels (presumably *via* Gq proteins) in some cell types (Della Penna et al., 2003; Goold et al., 2001).

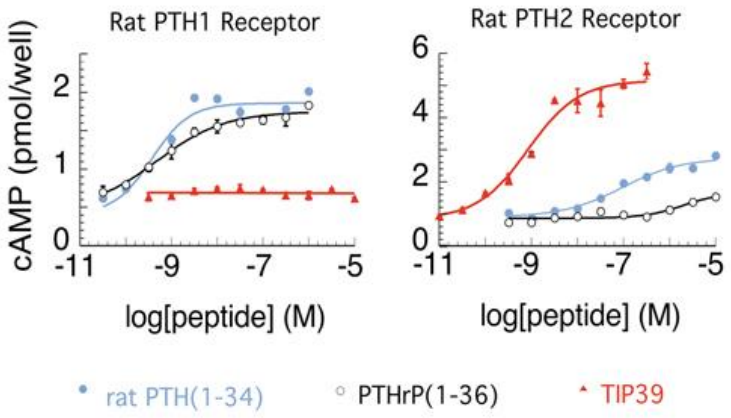

Fig. 43. Activation of rat parathyroid hormone 1 (PTH1) and PTH2 receptors. cAMP accumulation is shown in relation to increasing concentrations of PTH, PTH-related peptide, and tuberoinfundibular peptide of 39 residues (TIP39) in COS7 cells expressing the rat PTH1R (A) and the rat PTH2R (B), respectively. The figure was taken from our previous publication (Dobolyi et al., 2012).

7.2.1. Comparison of the distribution of TIP39 to that of the PTH2 receptor provides anatomical evidence for a TIP39-PTH2 receptor neuromodulator system

The localization of cell bodies that express TIP39 and those that express the PTH2 receptor are profoundly different. TIP39 expression is confined to PVG, PIL, and MPL while considerable PTH2 receptor expression is present in the infralimbic cortex, the innermost layer of other cerebral cortical areas, the basal ganglia, the lateral septum, the posteromedial part of the medial subdivision of the bed nucleus of the stria terminalis, the posterodorsal subdivision of the medial amygdaloid nuclei, the midline thalamic nuclei, the medial geniculate body, the medial preoptic, para- and periventricular, arcuate, dorsomedial, ventral premamillary, tuberomamillary and supramamillary nuclei of the hypothalamus, and some regions of the lateral hypothalamic area, the lateral subdivisions of the interpeduncular nucleus, the sphenoid nucleus, the nucleus of the trapezoid body, and the nucleus of the solitary tract. In contrast to the profoundly different localization of TIP39- and PTH2 receptor-expressing cell bodies, the distributions of TIP39-ir and PTH2 receptor-ir fibers are markedly similar. TIP39-ir and PTH2 receptor-ir fibers are present in the same nuclei and areas throughout the brain except for a few areas where PTH2 receptor- but not TIP39-ir fibers are abundant including the median eminence, the interpeduncular, and the spinal trigeminal nuclei. Furthermore, not only are TIP39-ir and PTH2 receptor-ir fibers present in the same brain regions but their subregional distributions also show remarkable similarities. In fact, the two distributions are indistinguishable in most brain nuclei and areas. This finding suggests that TIP39 is available to act on the PTH2 receptor in these brain regions and furthermore that it may act in a fairly traditional manner with its actions focused on adjacent fibers. Together with the strong *in vitro* pharmacological evidence that TIP39 is a potent and high affinity ligand for the PTH2 receptor our anatomical data suggest that TIP39 is the endogenous ligand of the PTH2 receptor. Furthermore, we propose that TIP39 and the PTH2 receptor form a neuromodulator system in many brain regions. TIP39-ir fibers are distant axons of the TIP39-expressing perikarya in the posterior thalamus and the medial

paralemniscal nuclei, which disappear following the destruction of their cell bodies (Dobolyi et al., 2003a). PTH2 receptor-ir fibers, however, are often localized in the vicinity of PTH2 receptor-expressing neurons. Therefore, they may represent either axons or dendrites on which TIP39 could act *via* the PTH2 receptor. The finding that in a few areas PTH2 receptor's but not TIP39 is present (most striking examples are the caudate nucleus and the median eminence) could be explained by the appearance of TIP39 in these areas under specific physiological conditions, although a non-functional expression of the PTH2 receptor, or the existence of another ligand for the PTH2 receptor in these areas cannot be excluded. It is possible that circulating TIP39 acts on the PTH2 receptor in the median eminence, but a source of such TIP39 has not been identified.

7.2.2. PTH2 receptor distribution in the human brain

The major purpose of the study describing the PTH2 receptor distribution in the human brain was to provide a comparison of the neuroanatomical distribution of the PTH2 receptor and TIP39 in human and non-human primates with their distributions in rodents. We evaluated this neuromodulator system in rodents and performed this comparison to help evaluate the potential extrapolation of their functions in rodents to humans. We focused on material and brain regions most likely to be informative in this regard. The major finding is that both the PTH2 receptor and TIP39 have a similar distribution in human and macaque to their distributions in rodents. Their expression is greatest in subcortical structures. The data support to the idea that they may be involved in similar functions. These topographical arrangements of PTH2 receptor-ir fibers and terminals in primates, like the distribution of receptor synthesizing cells, are very similar to that in rodents. Such similarities between distributional patterns in the brains of primates and rodents have often been reported for other neuropeptides and neuropeptide receptors suggesting similar functions in different species (de Lacalle and Saper, 2000; Kostich et al., 2004). However, judgment about the relevance of particular observations made in rodents to humans obviously requires detailed consideration of the relevant functions and structures.

7.3. TIP39 functions in the maternal brain

7.3.1. Maternal induction of TIP39

Induction of TIP39 mRNA in the PIL and the MPL of lactating mother rats was suggested on the basis of *in situ* hybridization histochemistry and confirmed by the independent technique of RT-PCR. The temporal pattern of activation of posterior

intralaminar and paralemniscal TIP39 neurons was similar (Cservenak et al., 2010). In contrast, TIP39 expression was not changed in the third group of TIP39 neurons, the PVG in mother rats (Cservenak et al., 2010). In the PIL and the MPL, the levels of TIP39 mRNA was elevated specifically in the presence of pups while TIP39 mRNA levels were at their low, basal, non-maternal level in the absence of pups. Thus, the increase in the level of TIP39 mRNA is a temporary phenomenon during lactation. The induction is likely to take place in all TIP39 neurons within the 2 cell groups as suggested by the increased autoradiography signal in the observed TIP39-expressing neurons following *in situ* hybridization histochemistry. In turn, the distribution of TIP39 neurons in the PIL and MPL of lactating mother rats was similar to that described previously in young rats (Dobolyi et al., 2003b; Dobolyi et al., 2006b) suggesting that TIP39 reappears in the same neurons, which expressed it during earlier stages of ontogenic development and no additional, TIP39-negative cells are recruited in mothers. Furthermore, the increased TIP39 immunoreactivity in rat dams suggests that the increase in TIP39 mRNA level translates into elevated peptide level, which in turn suggests a function of the induced TIP39 in mother rats. A function of the induced TIP39 is also conceivable because the expression level of the receptor of TIP39, parathyroid hormone 2 receptor does not decrease during postnatal development as TIP39 does (Dobolyi et al., 2006b). Thus, parathyroid hormone 2 receptor is available for maternally induced TIP39 to exert its actions.

7.3.2. Activation of TIP39 neurons in reponse to pup exposure

The appearance of Fos in response to pup exposure represents the activation of those neurons as Fos is the protein product of *c-fos*, a well-known immediate early gene that appears in activated neurons (Bullitt, 1990; Herdegen and Leah, 1998; Morgan and Curran, 1991). Fos appears in the nuclei of TIP39 neurons of the PIL and MPL in response to pup exposure indicating an elevated activity of TIP39 neurons in lactating rat dams in these brain areas. These findings confirmed previously reported expression of Fos in the PIL area of lactating rats (Lin et al., 1998) and the area corresponding to the MPL (Li et al., 1999b). TIP39 neurons represent about the half of neurons demonstrating Fos activation in the PIL, as a number of TIP39-negative neurons were also activated in response to suckling. In contrast, within the MPL, Fos was located almost exclusively in TIP39 neurons, which is the major neuronal cell group of this nucleus (Varga et al., 2008). Based on the very low number of Fos-positive but TIP39-immunonegative neurons, it is likely that other cell types within the MPL are generally not activated in mother rats.

Pup exposure represents a complex stimulus for the mothers. Apart from the suckling reflex, visual, auditory, or olfactory exteroceptive stimuli or hormonal changes associated with the presence of pups could induce prolactin release and maternal behaviors (Hashimoto et al., 2001; Terkel et al., 1979). Theoretically, all these inputs derived from the pups could contribute to the activation of TIP39 neurons in the PIL and MPL by increasing their neuronal activity *via* specific circuitries. However, the finding that Fos appears in TIP39 neurons of the PIL only when physical contact is allowed suggests that TIP39 is induced in the PIL of rat dams by the suckling stimulus and not by other sensory input. These experiments have not been performed in the MPL yet, thus an adequate stimulation other than suckling is conceivable for TIP39 neurons in the MPL. In fact, auditory input could play a major role in the activation of TIP39 neurons in the MPL because they receive massive input from the auditory cortex, the inferior colliculus and the periolivary area (Varga et al., 2008). In addition, we have shown that highly intense noise stimulus activates paralemniscal TIP39 neurons (Palkovits et al., 2009). Furthermore, an indirect activation of paralemniscal TIP39 neurons *via* maternal hormones cannot be excluded either.

It is particularly striking that TIP39 neurons are activated only in the PIL and MPL while TIP39 neurons in the PVG are not activated in lactating dams, which is consistent with the lack of TIP39 induction in that area. Although TIP39 disappears from the PIL earlier than from the PVG and MPL during ontogeny (Brenner et al., 2008), the adult levels are markedly reduced in all 3 brain regions. Furthermore, brain areas that receive TIP39 axons predominantly from the PVG, including the lateral septal nucleus and the medial prefrontal cortex (Dobolyi et al., 2003b; Wang et al., 2006b), also continue to possess a high PTH2 receptor level (Dobolyi et al., 2006b) suggesting that this TIP39 cell group may also be activated in response to some, so far unidentified physiological stimuli.

7.3.3. The involvement of the TIP39-PTH2 receptor system in the regulation of prolactin release

The experimental design of suckling-induced prolactin release is known to elevate plasma prolactin levels within minutes of pups return to the mothers deprived of pups for 4 h, and plasma prolactin concentrations peak 30 min after the beginning of suckling (Bodnar et al., 2004). Saline injection into the lateral ventricle or control virus injection into the hypothalamus did not influence the prolactin level elicited by suckling, which matched the expected curve. Injection of the PTH2 receptor antagonist HYWY-TIP39, however, dose-dependently blocked the elevation of plasma prolactin levels.HYWY-TIP39 binds selectively

to the PTH2 receptor (Kuo and Usdin, 2007) suggesting that HYWY-TIP39 injected into the lateral ventricle exerted its inhibitory action on the suckling-induced prolactin release *via* the PTH2 receptor. Furthermore, mediobasal hypothalamic but not preoptic injection of a virus encoding an antagonist of the PTH2 receptor markedly decreased basal serum prolactin levels and the suckling-induced prolactin release suggesting that the mediobasal hypothalamus may be the site of action of HYWY-TIP39. PTH2 receptor expressing neurons are abundant in the periventricular and arcuate nuclei of the hypothalamus (Faber et al., 2007; Wang et al., 2000). PTH2 receptors in these neurons are possible targets mediating the effect of HYWY-TIP39 on prolactin release. Dopaminergic neurons that control prolactin release from the pituitary are also located in the arcuate and periventricular hypothalamic nuclei. However, a direct effect of HYWY-TIP39 on dopaminergic neurons is not likely because the PTH2 receptor was not double-labeled with tyrosine hydroxylase (Dobolyi et al., 2006a; Usdin et al., 2003), and because close appositions between tyrosine hydroxylase neurons and fiber terminals projecting to the mediobasal hypothalamus from the PIL were not detected (Szabo et al., 2010). Therefore, HYWY-TIP39 might influence dopaminergic neurons in the mediobasal hypothalamus *via* interneurons expressing the PTH2 receptor. Dynorphin-containing neurons in the arcuate nucleus are one of the candidates because they are innervated by axon terminals derived from the PIL (Szabo et al., 2010), innervate tuberoinfundibular dopaminergic neurons (Fitzsimmons et al., 1992), and may be responsible for the effects of opioid peptides on suckling-induced prolactin release by inhibiting tuberoinfundibular dopaminergic neurons (Arbogast and Voogt, 1998; Callahan et al., 2000; Selmanoff and Gregerson, 1986). It is also a possibility that TIP39 evokes prolactin release by directly or indirectly stimulating prolactin-releasing substance-containing neurons (Andrews, 2005; Freeman et al., 2000).

7.3.4. The involvement of the TIP39-PTH2 receptor system in the regulation of maternal motivation

During the early postpartum period, pup suckling is more rewarding than cocaine (Ferris et al., 2005). The medial preoptic area has been shown to be critically important for maternal motivation (Arrati et al., 2006; Pereira and Morrell, 2011) through its projections to the nucleus accumbens and the ventral tegmental area (Numan et al., 2005). In the present study, we not only confirmed the role of the medial preoptic area in maternal motivation but also provided evidence for the involvement of the TIP39-PTH2 receptor system there. We demonstrated that fibers of TIP39 neurons projecting to the preoptic area from the PIL have a distribution similar to that of the neurons expressing expressing Fos in response to pup

exposure in areas that include the medial preoptic nucleus, other parts of the topographical medial preoptic area, and the ventral subdivision of the bed nucleus of the stria terminalis. This is a characteristic pattern in the medial preoptic region, often referred to as the medial preoptic area in which Fos-expressing neurons have been implicated in pup attachment (Lonstein et al., 1998b; Stack and Numan, 2000). In turn, we also provided morphological evidence that TIP39-containing terminals innervate the Fos-expressing neurons. Most importantly, however, the presence of the PTH2 receptor antagonist reduced the number of dams demonstrating preference for the pup-associated cage in a place preference test, and also the amount of time the dams spent in the pup-associated cage, but did not affect the time control females spent in the different cages of the test apparatus. The conditioned place preference test, used regularly in the study of addiction (Schwarz and Bilbo, 2013) and food intake regulation (Labouebe et al., 2013), is a particularly sensitive way to assess maternal motivation (Seip and Morrell, 2009). It can differentiate even between otherwise behaviorally identical postpartum maternal rats when both the number of dams demonstrating preference for the pup-associated cage and the time the dams spend in the pup-associated cage are analyzed (Mattson et al., 2003), as we also evaluated the conditioned place preference test data in this study. It is also important to note that preoptic injection of the virus expressing the PTH2 receptor antagonist did not affect plasma prolactin levels. Therefore, an indirect mechanism of action on maternal motivation *via* prolactin can be excluded even though prolactin can itself stimulate maternal behavior (Bridges et al., 1990).

7.3.5. TIP39 neurons in the PIL as relay stations of suckling information towards the hypothalamus

TIP39 neurons in the PIL are ideally positioned to receive sensory input from the nipples and transfer this information to the mediobasal hypothalamus. PIL neurons provide projections to the medial preoptic area, the arcuate nucleus and potentially to other limbic and hypothalamic areas and nuclei that might also be involved in the processing of suckling information, e.g. the release of oxytocin, the altered stress response in mothers, and lactational anoestrus (Fig. 44). In particular, we provided functional evidence that TIP39 affects prolactin release through thalamo-arcuate projections and maternal motivation through thalamo-preoptic projections. Fos expression by TIP39 neurons in the PIL in response to physical contact with the pups support that they are activated by suckling. The presence of the TIP39 in these neurons suggests the role of this neuropeptide in the regulation of maternal functions. The finding that TIP39 levels are markedly elevated in lactating mother rats provides

additional evidence for a specific maternal function of TIP39 neurons in the PIL (Cservenak et al., 2010). TIP39 expression is markedly up-regulated on the 1st, 9th and 23rd postpartum days but not on the last day of pregnancy or after weaning, which further supports the idea that elevated activity of these neurons is specific for the period of lactation. The finding that the body weight of pups is reduced in the absence of a functional TIP39 gene (Coutellier et al., 2011) and that the blockade of PTH2 receptors inhibits suckling-induced prolactin release (Cservenak et al., 2010) suggests that TIP39 plays a physiological role in the regulation of suckling-induced prolactin release. Anatomical evidence suggests that TIP39 neurons do not directly act on dopaminergic neurons in the mediobasal hypothalamus. Rather, TIP39 may excite interneurons in the arcuate nucleus, which in turn inhibit tuberoinfundibular dopamine neurons to induce prolactin release from the pituitary.

Based on previous studies on the afferent neuronal connections of the parvicellular subparafascicular nucleus in male rats, neurons in the PIL receive input from the spinal cord. These ascending inputs were implicated in the processing of sensory information related to mating and ejaculation (Coolen et al., 2004). In mothers, these afferent connections are candidates to convey suckling information from the nipples to the PIL. Using electrical microstimulations and lesions, the pathway of the suckling reflex was described to traverse from the mesencephalic lateral tegmentum towards the hypothalamus in a position ventromedial to the medial geniculate body (Tindal and Knaggs, 1971; 1977) where TIP39 neurons in the PIL are located. Destroying relay neurons in this area by local injections of ibotenic acid inhibited male ejaculation as well as the milk-ejection reflex (Hansen and Kohler, 1984). These data are consistent with the possibility that TIP39 neurons receive input related to the suckling stimulus.

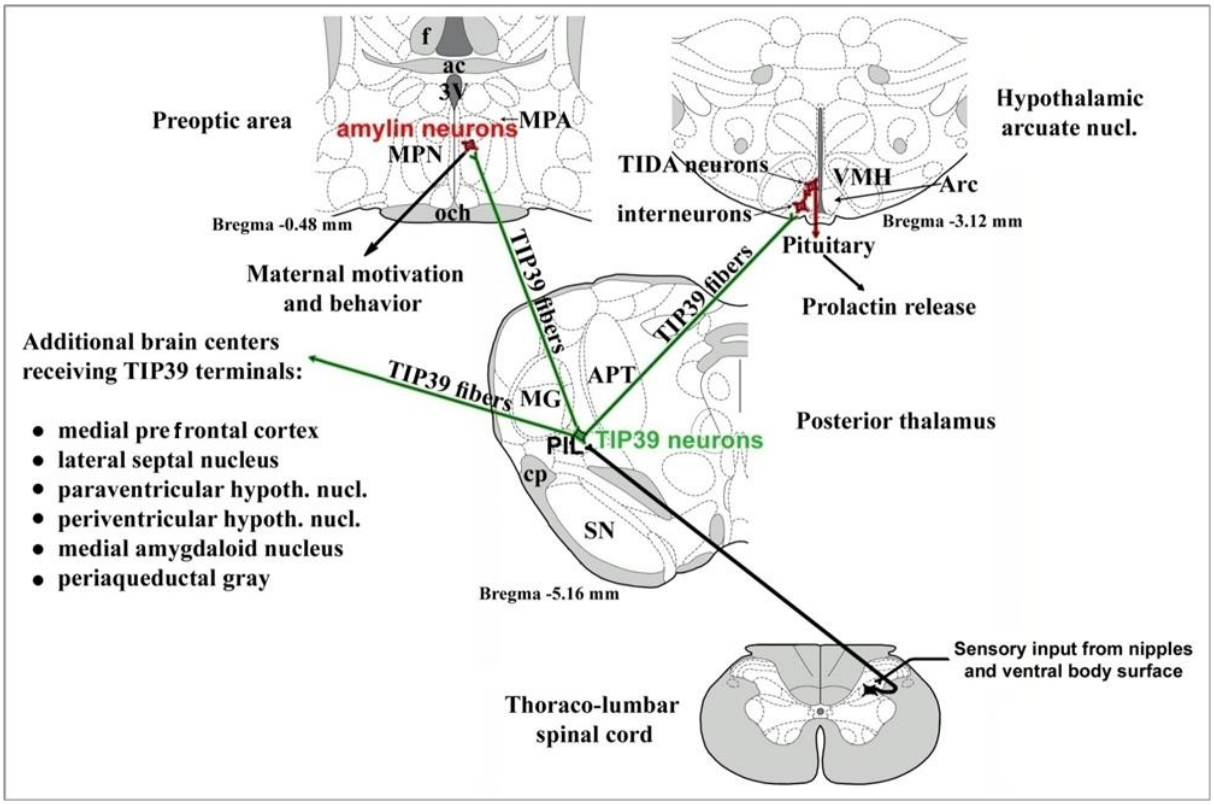

Fig. 44. TIP39 neurons in the PIL are proposed relay stations of maternal sensory information towards hypothalamic and limbic centers.

7.3.6. Additional potential functions of thalamic TIP39 neurons

Based on the distribution of the TIP39-PTH2 receptor system in the brain, its involvement in endocrine, limbic, nociceptive, and auditory functions have been hypothesized (Dobolyi et al., 2003a). It has indeed been established that the peptide neuromodulator system is involved in a variety of neuronal and neuroendocrine functions including the stress response (Dimitrov and Usdin, 2010), the anxiety level (Coutellier and Usdin, 2011; Fegley et al., 2008; LaBuda et al., 2004), thermoregulation (Dimitrov et al., 2011), and prolactin release (Cservenak et al., 2010). Some evidence is also available for a role of the TIP39-PTH2 receptor system in the regulation of arginine vasopressin (Sugimura et al., 2003) and growth hormone release (Usdin et al., 2003). Some of these actions could be part of maternal adaptations even though they are not proven yet in mothers (Dobolyi et al., 2012).

7.3.7. Potential role of TIP39 neurons of the MPL in auditory information transfer between rat mothers and pups

Limited information is available regarding the functions of the MPL and TIP39 neurons located there. The position of the MPL immediately next to the nuclei of the lateral lemniscus and its bilateral anatomical connections with auditory brain regions (Dobolyi et al., 2003b; Varga et al., 2008) suggest some auditory functions of paralemniscal TIP39 neurons. In bats, the paralemniscal area medial to the intermediate nucleus of the lateral lemniscus is activated by ultrasounds and plays a role in vocalization (Fenzl and Schuller, 2002; Metzner, 1993; 1996). In rats, paralemniscal TIP39 neurons were specifically activated by high intensity noise (Palkovits et al., 2009). Thus, specific auditory inputs may play a role in the activation of TIP39 neurons in mothers. Rat pups, when isolated, are known to vocalize in the ultrasonic range (Hofer, 1996). Pup ultrasonic vocalizations have been described to induce maternal behaviors in rats (Febo et al., 2008; Hashimoto et al., 2001; Terkel et al., 1979). Still, there are no data available at present on the anatomical pathway how ultrasonic vocalization reaches limbic and hypothalamic centers responsible for maternal behavioral and neuroendocrine changes. We hypothesize that paralemniscal TIP39 neurons may be activated in mother rats by ultrasonic vocalization of pups. In turn, paralemniscal TIP39 neurons could mediate pup ultrasonic vocalization towards higher brain centers of their mothers thereby contributing to central maternal adaptations.

Unfortunately, the projections of paralemniscal TIP39 neurons are not fully established yet. Stereotaxic lesion studies suggest projections to non-tonotopic auditory brainstem regions (Dobolyi et al., 2003a) while studies using retrograde tracers suggest that paralemniscal fibers may reach hypothalamic targets such as the hypothalamic paraventricular nucleus (Palkovits et al., 2004). Projections of paralemniscal neurons to non-tonotopic auditory brainstem regions (Dobolyi et al., 2003a) might sensitize the maternal auditory system to pup vocalization. In turn, projections to the hypothalamic paraventricular nucleus (Palkovits et al., 2004) might be involved in the altered maternal stress response.

7.4. Amylin as a novel neuropeptide

The involvement of amylin in maternal control was studied by several different approaches. In this discussion, we first compare the induction pattern of amylin obtained with different methods. Then, we discuss the activation of amylin neurons and stimuli that may activate these neurons in mothers. Next, we describe current evidence supporting the

hypothesis that amylin is neuropeptide with potential modulatory actions in postpartum dams. Finally, the possible neural functions of the brain amylin system are summarized.

7.4.1. Induction of amylin in the preoptic area

The elevated *in situ* hybridization signal of amylin during the postnatal period in rat dams suggests an elevated expression level of amylin. This was supported by the quantitative RT-PCR data, which confirmed the induction of amylin mRNA in maternally behaving rats (Dobolyi, 2009). Our data also provide information on the time course of amylin induction. Amylin mRNA is not induced 1 day before parturition but is already present one day after delivery (Szabo et al., 2012). Amylin immunoreactivity also appears in the postpartum but not in the prepartum period, which confirms the specificity of the amylin signal and suggests that the elevation of amylin mRNA is translated into an increased synthesis of amylin peptide. The number of amylin mRNA-containing and amylin-ir neurons is difficult to compare because the sections for immunoreactivity were thicker (50 *vs.* 12 μm) but the penetration of antiserum into the sections is limited. Nevertheless, the distribution of amylin mRNA-expressing and amylin-ir neurons was the same in the maternal brain (Dobolyi, 2011). Therefore, we refer to these cells as amylin neurons. The distribution of amylin neurons was widespread within some but not all parts of the preoptic area. Amylin neurons were confined to the MPN, MPA, and BNSTv, where they were relatively evenly distributed among other types of neurons. Amylin expression remained high as long as the pups were not removed from the mother, suggesting the importance of the presence of pups in amylin induction.

7.4.2. Maternal activation of preoptic amylin neurons

Fos appeared in the preoptic area of mother rats in response to pup exposure (Szabo et al., 2012). Fos-expressing neurons were abundant in the MPN, MPA, and BNSTv, and the anteroventral periventricular nucleus. This finding confirmed previously reported expression and distribution patterns of Fos in the preoptic area of mother rats (Lonstein et al., 1998b; Numan and Numan, 1997; Stack and Numan, 2000). Furthermore, double labeling of Fos with amylin mRNA and amylin immunoreactivity has demonstrated that amylin neurons are essentially all activated by pup exposure, indicating an elevated activity of amylin neurons in postpartum rat dams in this area. This finding also suggests that amylin is induced in the preoptic area of rat dams by the presence of pups. Thus, amylin represents a novel marker of neurons activated in the preoptic area of mothers (Szabo et al., 2012). Using amylin as a

marker, selective investigation of the function of these neurons will be possible using electrophysiological and gene technological procedures.

The type of pup-related stimulus that activates amylin neurons remains undetermined. The suckling stimulus, as a major driver of maternal adaptations, is a leading candidate. Recently, we provided evidence that neurons in the PIL relay the suckling information toward medial hypothalamic sites that regulate prolactin release (Cservenak et al., 2010). We also demonstrated that TIP39 fibers originating from the PIL closely appose amylin neurons there suggesting that amylin neurons are innervated by TIP39 nerve terminals. Since TIP29 neurons in the PIL are activated by the suckling stimulus, activation of amylin neurons could occur *via* posterior thalamic neurons relaying suckling information (Dobolyi, 2011). The reduced maternal induction of amylin in PTH2 receptor KO mice confirms that input by TIP39 contributes to the activation of amylin neurons. However, some degree of amylin induction was also present in PTH2 receptor KO mice suggesting additional way of activation of amylin neurons. This could be mediated by other neurotransmitters present in TIP39 neurons, non-TIP39 neurons in the PIL that also transmit suckling stimulus, or by suckling independent input from the pups such as visual, auditory, or olfactory exteroceptive stimuli. Neuronal tract tracing methods revealed a number of different brain regions, whose neurons project to the preoptic area (Simerly and Swanson, 1986). Neurons in some of the input regions of the preoptic area are activated in the presence of pups (Li et al., 1999b; Lin et al., 1998) and may convey pup-associated information towards amylin neurons.

7.4.3. Amylin as a novel neuropeptide potentially involved in maternal control

The present study provided evidence that amylin appears in the brain of maternally behaving rats, which makes amylin a neuropeptide candidate. Amylin is known to be stored and released from vesicles in the pancreas (Young, 2005). Therefore, it is likely that amylin also possesses a regulated vesicular release from terminals of preoptic neurons. Neurons in the medial preoptic nucleus, and surrounding regions activated by pup exposure project to different brain regions, including the lateral septum, the bed nucleus of the stria terminalis, the substantia innominata, the amygdala, and several different parts of the hypothalamus including the periparaventricular zone, the ventromedial and arcuate nuclei, and the lateral hypothalamic area, as well as the periaqueductal gray (Numan and Sheehan, 1997; Simerly and Swanson, 1988). Some of these projections may contain amylin in maternally behaving rats, which could activate amylin receptors present in these target areas (Becskei et al., 2004; Sexton et al., 1994; Sheward et al., 1994). Therefore, amylin, together with its receptors, is a

candidate to form a peptide neuromodulator system in the maternal brain. Thus, amylin can be considered along with a number of peptide neuromodulators recognized to be involved in aspects of maternal behaviors, including prolactin, oxytocin, vasopressin, opioids, tachykinins, and corticotropin-releasing hormone (Bosch and Neumann, 2008; Leng et al., 2008; Numan and Insel, 2003). Even though a significant increase has been reported in the average soma size of preoptic neurons during late pregnancy and lactation suggesting increased gene expressional activity (Kinsley, 2008), prolactin and vasopressin are not expressed in the preoptic area even in mothers. Nevertheless, these peptides released from fibers terminating in the preoptic area may affect maternal behaviors as recently evidenced for vasopressin (Bosch et al., 2010). Other neuropeptides, such as opioids, tachykinins, and corticotropin-releasing hormone are expressed in the preoptic area (Tohyama and Takatsuji, 1998). These peptides are, however, expressed in a number of additional brain regions, too. Thus, the restricted distribution of amylin expression in the preoptic area is unique among neuropeptides.

7.4.4. The maternal functions of amylin

The marked elevation of the level of amylin and the activation of amylin neurons in response to pup exposure suggest that amylin is involved in some aspects of maternal control. Lactation represents a heavy metabolic load for the mothers, who lose weight during this period (Augustine et al., 2008; Smith and Grove, 2002). Adiposity was suggested to be regulated by specific maternal mechanisms other than the homeostatic regulations taking place throughout the lifespan (Woodside, 2007). Because peripheral amylin, as a hormone, is involved in the termination of food intake (Lutz, 2005) and the activation of brain amylin receptors has been suggested to decrease body adiposity in rats (Rushing et al., 2001), it is conceivable that maternal amylin plays a role in the regulation of body weight in dams. However, it is likely that maternal actions of central amylin are not related to the actions of peripheral amylin because the anorectic actions of peripheral amylin are completely eliminated by lesions of the dorsal vagal complex (Lutz et al., 2001).

Bilateral lesion of the preoptic area completely eliminates maternal behaviors (Gray and Brooks, 1984; Numan, 1986) but does not considerably affects body weight, therefore, amylin induced in this region could be involved in the regulation of maternal behaviors. We found that Fos is activated in the preoptic area of these animals in response to pup exposure and that amylin neurons are among those activated in the region. Maternally activated preoptic neurons also project to brain regions involved in maternal regulations (Numan and Numan,

1997). Some of these brain regions express amylin receptors, including the bed nucleus of the stria terminalis, various hypothalamic and amygdaloid nuclei, and the periaqueductal gray (Becskei et al., 2004; Sexton et al., 1994; Sheward et al., 1994). Consequently, a likely hypothesis is that amylin plays a role in the regulation of some of the maternal behaviors that appear during the postpartum period.

In addition to metabolic and behavioral changes, endocrine and emotional adaptations take place in mothers for a limited period of time to support the offspring (Knobil and Neill, 2006). These include lactation driven by prolactin and oxytocin release (Burbach et al., 2006; Freeman et al., 2000), lactational anoestrous by the suppression of GnRH secretion (McNeilly, 2006), maternal aggression toward intruders, decreased anxiety and reduced responsiveness of the hypothalamo-pituitary-adrenal axis (Carter et al., 2001). Amylin, induced in the postpartum period, could be involved in the control of emotional and endocrine alterations in mothers. Consequently, it represents a new therapeutic direction to treat dysfunctions associated with motherhood, including postnatal depression (Mallikarjun and Oyebode, 2005).

8. SUMMARY

The scientific achievements of the Applicant described in the Dissertation can be summarized in the following points:

- A gene was identified encoding tuberoinfundibular peptide of 39 residues, and its tissue distribution of expression as well as its distribution pattern in the nervous system was described.
- Posterior intralaminar thalamic TIP39 neurons were shown to be part of an ascending system that conveys information towards the hypothalamus.
- The distribution of the receptor of TIP39, the parathyroid hormone 2 receptor (PTH2 receptor) was mapped in the brain of rat, mouse, macaque and human. The distribution of the PTH2 receptor is similar in rodents and primates.
- The expression level of TIP39 decreased during ontogenic development. However, TIP39 expression is induced in 2 of the 3 sites where TIP39 neurons are found, the posterior intralaminar complex of the thalamus, and the medial paralemniscal area. TIP39 levels remain elevated as long as the pups are weaned.
- Strong experimental evidence was provided that the endogenous TIP39 in the arcuate nucleus contributes to suckling-induced prolactin release, while TIP39 terminals in the preoptic area play a role in maternal motivation during the postpartum period.
- Using system biological tools, a novel neuropeptide, amylin, was discovered in the preoptic area of mother rats. Amylin neurons were shown to be activated in mothers in response to suckling. Amylin neurons may mediate the effect of TIP39 on maternal motivation.

In conclusion, 2 novel neuropeptides were discovered that are unique by their strong induction in the maternal brain, and play a role in suckling-induced prolactin release, and maternal motivation, respectively. These neuropeptides, TIP39 and amylin, together with their receptors are parts of new mechanisms in the central control of maternal adaptations. TIP39 neurons in the posterior intralaminar complex of the thalamus constitute a relay station in the long sought-after anatomical pathway of the suckling reflex while amylin neurons are a subgroup of neurons activated by suckling in the preoptic area, the brain region known to be the major regulator of maternal behaviors.

9. GRANT SUPPORT

As principal investigator:

2004-2005 NARSAD Young Investigator Award Grant.

2005-2007 MC-IRG 016423 Marie Curie International Reintegration Grant of the European Commission.

2007-2011 NKTH-OTKA K67646 Research Grant of the Hungarian Scientific Research Fund.

2009-2011 NFM-OTKA NNF 78219 Research Grant of the Hungarian Scientific Research Fund.

2010-2011 Pfizer Basic Research Grant.

2011-2012 OTKA NNF 85612 Research Grant of the Hungarian Scientific Research Fund.

2012-2016 OTKA K100319 Research Grant of the Hungarian Scientific Research Fund.

As senior participant:

2008-2011 OTKA NK 72929 Research Grant of the Hungarian Scientific Research Fund.

2009-2013 NKTH TECH_09_A1 Grant of the National Office for Research and Technology.

10. ADDITIONAL ACKNOWLEDGEMENTS

Previous postgraduate supervisor, Prof. Gábor Juhász, postdoctoral supervisor, Prof. Ted B. Usdin, and long-time mentor, Prof. Miklós Palkovits played pivotal roles in the scientific development of the applicant. Prof. Miklós Palkovits is specially acknowledged for making it possible for the applicant to return to Hungary after long stay in the USA and become an independent scientist with his continuous support.

Special thanks go to current and previous PhD students of the applicant who all contributed to the presented results: Tamás Varga, Éva Rebeka Szabó, Dr. Melinda Cservenák, Dr. Gabriella Pál, Dr. Csilla Vincze, and Dr. Attila G. Bagó.

The technical assistance of Jonathan Kuo, Nikolett Hanák, Viktória Dellaszéga-Lábas, Dorottya Kézdi, Frigyesné Helfferich, Magdolna Kasztner, Melitta Kiss, and Szilvia Deák is also highly appreciated.

Additional present and previous co-workers of the Neuromorphological Laboratory as well as the Department of Anatomy, Histology and Embryology, Semmelweis University, in particular, Dr. Katalin Gallatz, Dr. Zsuzsanna E. Tóth, and Prof. András Csillag are acknowledged for providing support and for the Applicant.

Long-time scientific collaborators including Dr. Katalin Adrienna Kékesi, Dr. Zsolt Kovács, Prof. Julianna Kardos, Dr. László Héja, Dr. Gábor Lovas, Prof. Zoltán Nagy és Dr. Christos Chinopoulos offered research ideas and valuable discussions for the work of the Applicant.

Finally, I have to say thank you for my family, parents Dr. Csaba and Márta Dobolyi, wife Éva Dobolyiné Renner, and our children Dániel and Zsófia as they provide the background and encouragement, without which my achievements in science would not be possible.

11. REFERENCES

Abou-Samra AB, Juppner H, Force T, Freeman MW, Kong XF, Schipani E, Urena P, Richards J, Bonventre JV, Potts JT, Jr., et al. 1992. Expression cloning of a common receptor for parathyroid hormone and parathyroid hormone-related peptide from rat osteoblast-like cells: a single receptor stimulates intracellular accumulation of both cAMP and inositol trisphosphates and increases intracellular free calcium. Proc Natl Acad Sci U S A 89:2732-2736.

Andrews ZB. 2005. Neuroendocrine regulation of prolactin secretion during late pregnancy: easing the transition into lactation. J Neuroendocrinol 17:466-473.

Andrezik JE, Beitz AJ. 1985. Reticular formation, central gray and related tegmental nuclei. In: The Rat Nervous System, Paxinos G, Ed, Vol. 2, Academic Press, New York, pp. 1-28.

Arbogast LA, Voogt JL. 1998. Endogenous opioid peptides contribute to suckling-induced prolactin release by suppressing tyrosine hydroxylase activity and messenger ribonucleic acid levels in tuberoinfundibular dopaminergic neurons. Endocrinology 139:2857-2862.

Arrati PG, Carmona C, Dominguez G, Beyer C, Rosenblatt JS. 2006. GABA receptor agonists in the medial preoptic area and maternal behavior in lactating rats. Physiol Behav 87:51-65.

Augustine RA, Ladyman SR, Grattan DR. 2008. From feeding one to feeding many: hormone-induced changes in bodyweight homeostasis during pregnancy. J Physiol 586:387-397.

Bagó AG, Dimitrov E, Saunders R, Seress L, Palkovits M, Usdin TB, Dobolyi A. 2009. Parathyroid hormone 2 receptor and its endogenous ligand tuberoinfundibular peptide of 39 residues are concentrated in endocrine, viscerosensory and auditory brain regions in macaque and human. Neuroscience 162:128-147.

Bagó AG, Palkovits M, Usdin TB, Seress L, Dobolyi A. 2008. Evidence for the expression of parathyroid hormone 2 receptor in the human brainstem. Ideggyogy Sz 61:123-126.

Baraban SC, Tallent MK. 2004. Interneuron Diversity series: Interneuronal neuropeptides--endogenous regulators of neuronal excitability. Trends Neurosci 27:135-142.

Basbaum AI, Fields HL. 1979. The origin of descending pathways in the dorsolateral funiculus of the spinal cord of the cat and rat: further studies on the anatomy of pain modulation. J Comp Neurol 187:513-531.

Baumann CR, Bassetti CL. 2005. Hypocretins (orexins): clinical impact of the discovery of a neurotransmitter. Sleep Med Rev 9:253-268.

Bean AJ, Zhang X, Hökfelt T. 1994. Peptide secretion: what do we know? FASEB J 8:630-638.

Becskei C, Riediger T, Zund D, Wookey P, Lutz TA. 2004. Immunohistochemical mapping of calcitonin receptors in the adult rat brain. Brain Res 1030:221-233.

Bodnar I, Banky Z, Nagy GM, Halasz B. 2005. Non-NMDA glutamate receptor antagonist injected into the hypothalamic paraventricular nucleus blocks the suckling stimulus-induced release of prolactin. Brain Res Bull 65:163-168.

Bodnar I, Mravec B, Kubovcakova L, Toth EB, Fulop F, Fekete MI, Kvetnansky R, Nagy GM. 2004. Stress- as well as suckling-induced prolactin release is blocked by a structural analogue of the putative hypophysiotrophic prolactin-releasing factor, salsolinol. J Neuroendocrinol 16:208-213.

Bodnar I, Olah M, Nejad KS, Nagy GM. 2009. Neuropeptides and the regulation of prolactin secretion. In: Neuropeptides and Peptide Analogs Kovacs M, Merchenthaler I, Eds, Research Signpost, Kerala.

Bosch OJ, Neumann ID. 2008. Brain vasopressin is an important regulator of maternal behavior independent of dams' trait anxiety. Proc Natl Acad Sci U S A 105:17139-17144.

Bosch OJ, Pfortsch J, Beiderbeck DI, Landgraf R, Neumann ID. 2010. Maternal behaviour is associated with vasopressin release in the medial preoptic area and bed nucleus of the stria terminalis in the rat. J Neuroendocrinol 22:420-429.

Breese McCoy SJ. 2011. Postpartum depression: an essential overview for the practitioner. South Med J 104:128-132.

Brenner D, Bago AG, Gallatz K, Palkovits M, Usdin TB, Dobolyi A. 2008. Tuberoinfundibular peptide of 39 residues in the embryonic and early postnatal rat brain. J Chem Neuroanat 36:59-68.

Bridges RS. 1996. Biochemical basis of parental behavior in the rat. Advance in the Study of Behavior. In: Parental Care: Evolution, mechanisms, and Adaptive Significance, Rosenblatt JS, Snowdon CT, Eds, Vol. 25, Academic Press, pp. 215-242.

Bridges RS, Numan M, Ronsheim PM, Mann PE, Lupini CE. 1990. Central prolactin infusions stimulate maternal behavior in steroid-treated, nulliparous female rats. Proc Natl Acad Sci U S A 87:8003-8007.

Brunton PJ, Russell JA. 2008. The expectant brain: adapting for motherhood. Nat Rev Neurosci 9:11-25.

Brunton PJ, Russell JA, Douglas AJ. 2008. Adaptive responses of the maternal hypothalamic-pituitary-adrenal axis during pregnancy and lactation. J Neuroendocrinol 20:764-776.

Bullitt E. 1990. Expression of c-fos-like protein as a marker for neuronal activity following noxious stimulation in the rat. J Comp Neurol 296:517-530.

Burbach JPH, Young LJ, Russell JA. 2006. Oxytocin: Synthesis, Secretion, and Reproductive Functions. In: Knobil and Neill´s Physiology of Reproduction, Neill JD, Ed, Academic Press, Oxford.

Callahan P, Klosterman S, Prunty D, Tompkins J, Janik J. 2000. Immunoneutralization of endogenous opioid peptides prevents the suckling-induced prolactin increase and the inhibition of tuberoinfundibular dopaminergic neurons. Neuroendocrinology 71:268-276.

Campeau S, Watson SJ, Jr. 2000. Connections of some auditory-responsive posterior thalamic nuclei putatively involved in activation of the hypothalamo-pituitary-adrenocortical axis in response to audiogenic stress in rats: an anterograde and retrograde tract tracing study combined with Fos expression. J Comp Neurol 423:474-491.

Canteras NS, Simerly RB, Swanson LW. 1995. Organization of projections from the medial nucleus of the amygdala: a PHAL study in the rat. J Comp Neurol 360:213-245.

Carlton SM, Chung JM, Leonard RB, Willis WD. 1985. Funicular trajectories of brainstem neurons projecting to the lumbar spinal cord in the monkey (Macaca fascicularis): a retrograde labeling study. J Comp Neurol 241:382-404.

Carter CS, Altemus M, Chrousos GP. 2001. Neuroendocrine and emotional changes in the post-partum period. Prog Brain Res 133:241-249.

Chen P, Smith MS. 2003. Suckling-induced activation of neuronal input to the dorsomedial nucleus of the hypothalamus: possible candidates for mediating the activation of DMH neuropeptide Y neurons during lactation. Brain Res 984:11-20.

Clopton BM, Winfield JA, Flammino FJ. 1974. Tonotopic organization: review and analysis. Brain Res 76:1-20.

Coolen LM, Allard J, Truitt WA, McKenna KE. 2004. Central regulation of ejaculation. Physiol Behav 83:203-215.

Coutellier L, Logemann A, Rusnak M, Usdin TB. 2011. Maternal absence of the parathyroid hormone 2 receptor affects postnatal pup development. J Neuroendocrinol 23:612-619.

Coutellier L, Usdin TB. 2011. Enhanced long-term fear memory and increased anxiety and depression-like behavior after exposure to an aversive event in mice lacking TIP39 signaling. Behav Brain Res 222:265-269.

Crowley WR, Ramoz G, Torto R, Keefe KA, Wang JJ, Kalra SP. 2007. Neuroendocrine actions and regulation of hypothalamic neuropeptide Y during lactation. Peptides 28:447-452.

Cservenak M, Bodnar I, Usdin TB, Palkovits M, Nagy GM, Dobolyi A. 2010. Tuberoinfundibular peptide of 39 residues is activated during lactation and participates in the suckling-induced prolactin release in rat. Endocrinology 151:5830-5840.

de Lacalle S, Saper CB. 2000. Calcitonin gene-related peptide-like immunoreactivity marks putative visceral sensory pathways in human brain. Neuroscience 100:115-130.

Del Cerro MC, Perez Izquierdo MA, Rosenblatt JS, Johnson BM, Pacheco P, Komisaruk BR. 1995. Brain 2-deoxyglucose levels related to maternal behavior-inducing stimuli in the rat. Brain Res 696:213-220.

Della Penna K, Kinose F, Sun H, Koblan KS, Wang H. 2003. Tuberoinfundibular peptide of 39 residues (TIP39): molecular structure and activity for parathyroid hormone 2 receptor. Neuropharmacology 44:141-153.

Dimitrov E, Usdin TB. 2010. Tuberoinfundibular peptide of 39 residues modulates the mouse hypothalamic-pituitary-adrenal axis via paraventricular glutamatergic neurons. J Comp Neurol 518:4375-4394.

Dimitrov EL, Kim YY, Usdin TB. 2011. Regulation of hypothalamic signaling by tuberoinfundibular peptide of 39 residues is critical for the response to cold: a novel peptidergic mechanism of thermoregulation. J Neurosci 31:18166-18179.

Dimitrov EL, Kuo J, Kohno K, Usdin TB. 2013. Neuropathic and inflammatory pain are modulated by tuberoinfundibular peptide of 39 residues. Proc Natl Acad Sci U S A.

Dobolyi A. 2009. Central amylin expression and its induction in rat dams. J Neurochem 111:1490-1500.

Dobolyi A. 2011. Novel potential regulators of maternal adaptations during lactation: tuberoinfundibular peptide 39 and amylin. J Neuroendocrinol 23:1002-1008.

Dobolyi A, Dimitrov E, Palkovits M, Usdin TB. 2012. The neuroendocrine functions of the parathyroid hormone 2 receptor. Front Endocrinol (Lausanne) 3:121.

Dobolyi A, Irwin S, Makara G, Usdin TB, Palkovits M. 2005. Calcitonin gene-related peptide-containing pathways in the rat forebrain. J Comp Neurol 489:92-119.

Dobolyi A, Irwin S, Wang J, Usdin TB. 2006a. The distribution and neurochemistry of the parathyroid hormone 2 receptor in the rat hypothalamus. Neurochem Res 31:227-236.

Dobolyi A, Palkovits M, Bodnar I, Usdin TB. 2003a. Neurons containing tuberoinfundibular peptide of 39 residues project to limbic, endocrine, auditory and spinal areas in rat. Neuroscience 122:1093-1105.

Dobolyi A, Palkovits M, Usdin TB. 2003b. Expression and distribution of tuberoinfundibular peptide of 39 residues in the rat central nervous system. J Comp Neurol 455:547-566.

Dobolyi A, Palkovits M, Usdin TB. 2010. The TIP39-PTH2 receptor system: unique peptidergic cell groups in the brainstem and their interactions with central regulatory mechanisms. Prog Neurobiol 90:29-59.

Dobolyi A, Ueda H, Uchida H, Palkovits M, Usdin TB. 2002. Anatomical and physiological evidence for involvement of tuberoinfundibular peptide of 39 residues in nociception. Proc Natl Acad Sci U S A 99:1651-1656.

Dobolyi A, Wang J, Irwin S, Usdin TB. 2006b. Postnatal development and gender-dependent expression of TIP39 in the rat brain. J Comp Neurol 498:375-389.

Dubois-Dauphin M, Armstrong WE, Tribollet E, Dreifuss JJ. 1985. Somatosensory systems and the milk-ejection reflex in the rat. II. The effects of lesions in the ventroposterior thalamic complex, dorsal columns and lateral cervical nucleus-dorsolateral funiculus. Neuroscience 15:1131-1140.

Eichinger A, Fiaschi-Taesch N, Massfelder T, Fritsch S, Barthelmebs M, Helwig JJ. 2002. Transcript expression of the tuberoinfundibular peptide (TIP)39/PTH2 receptor system and non-PTH1 receptor-mediated tonic effects of TIP39 and other PTH2 receptor ligands in renal vessels. Endocrinology 143:3036-3043.

Faber CA, Dobolyi A, Sleeman M, Usdin TB. 2007. Distribution of tuberoinfundibular peptide of 39 residues and its receptor, parathyroid hormone 2 receptor, in the mouse brain. J Comp Neurol 502:563-583.

Febo M, Numan M, Ferris CF. 2005. Functional magnetic resonance imaging shows oxytocin activates brain regions associated with mother-pup bonding during suckling. J Neurosci 25:11637-11644.

Febo M, Stolberg TL, Numan M, Bridges RS, Kulkarni P, Ferris CF. 2008. Nursing stimulation is more than tactile sensation: It is a multisensory experience. Horm Behav 54:330-339.

Fegley DB, Holmes A, Riordan T, Faber CA, Weiss JR, Ma S, Batkai S, Pacher P, Dobolyi A, Murphy A, Sleeman MW, Usdin TB. 2008. Increased fear- and stress-related anxiety-like behavior in mice lacking tuberoinfundibular peptide of 39 residues. Genes Brain Behav 7:933-942.

Fenzl T, Schuller G. 2002. Periaqueductal gray and the region of the paralemniscal area have different functions in the control of vocalization in the neotropical bat, Phyllostomus discolor. Eur J Neurosci 16:1974-1986.

Fenzl T, Schuller G. 2007. Dissimilarities in the vocal control over communication and echolocation calls in bats. Behav Brain Res 182:173-179.

Ferris CF, Kulkarni P, Sullivan JM, Jr., Harder JA, Messenger TL, Febo M. 2005. Pup suckling is more rewarding than cocaine: evidence from functional magnetic resonance imaging and three-dimensional computational analysis. J Neurosci 25:149-156.

Fitzsimmons MD, Olschowka JA, Wiegand SJ, Hoffman GE. 1992. Interaction of opioid peptide-containing terminals with dopaminergic perikarya in the rat hypothalamus. Brain Res 581:10-18.

Fjeldheim AK, Hovring PI, Loseth OP, Johansen PW, Glover JC, Matre V, Olstad OK, Reppe S, Gordeladze JO, Walaas SI, Gautvik KM. 2005. Thyrotrophin-releasing hormone receptor 1 and prothyrotrophin-releasing hormone mRNA expression in the central nervous system are regulated by suckling in lactating rats. Eur J Endocrinol 152:791-803.

Fleming AS, Rosenblatt JS. 1974. Maternal behavior in the virgin and lactating rat. J Comp Physiol Psychol 86:957-972.

Franklin KBJ, Paxinos G. 1997. The mouse brain in stereotaxic coordinates. Academic Press, San Diego.

Fredholm BB, Hökfelt T, Milligan G. 2007. G-protein-coupled receptors: an update. Acta Physiol (Oxf) 190:3-7.

Freeman ME, Kanyicska B, Lerant A, Nagy G. 2000. Prolactin: structure, function, and regulation of secretion. Physiol Rev 80:1523-1631.

Fuse G. 1926. Vergleichend-anatomische Beobachtungen am Hirnstamme der Saugetiere. VIII.: Eine weitere Bemerkung über den Nucleus ventralis accessorius lemnisci lateralis bei einigen Karnivoren (Katze, Hund, Fuchs, Dachs, Meler anakuma). Arb. Anat. Inst. Sendai 12:39-44.

Gebre-Medhin S, Mulder H, Zhang Y, Sundler F, Betsholtz C. 1998. Reduced nociceptive behavior in islet amyloid polypeptide (amylin) knockout mice. Brain Res Mol Brain Res 63:180-183.

Gensure RC, Gardella TJ, Juppner H. 2005. Parathyroid hormone and parathyroid hormone-related peptide, and their receptors. Biochem Biophys Res Commun 328:666-678.

Gensure RC, Ponugoti B, Gunes Y, Papasani MR, Lanske B, Bastepe M, Rubin DA, Juppner H. 2004. Identification and characterization of two parathyroid hormone-like molecules in zebrafish. Endocrinology 145:1634-1639.

Gillespie MT, Martin TJ. 1994. The parathyroid hormone-related protein gene and its expression. Mol Cell Endocrinol 100:143-147.

Goold CP, Usdin TB, Hoare SR. 2001. Regions in rat and human parathyroid hormone (PTH) 2 receptors controlling receptor interaction with PTH and with antagonist ligands. J Pharmacol Exp Ther 299:678-690.

Grattan DR, Kokay IC. 2008. Prolactin: a pleiotropic neuroendocrine hormone. J Neuroendocrinol 20:752-763.

Gray P, Brooks PJ. 1984. Effect of lesion location within the medial preoptic-anterior hypothalamic continuum on maternal and male sexual behaviors in female rats. Behav Neurosci 98:703-711.

Hage SR, Jurgens U. 2006. On the role of the pontine brainstem in vocal pattern generation: a telemetric single-unit recording study in the squirrel monkey. J Neurosci 26:7105-7115.

Hannig S, Jurgens U. 2006. Projections of the ventrolateral pontine vocalization area in the squirrel monkey. Exp Brain Res 169:92-105.

Hansen S, Kohler C. 1984. The importance of the peripeduncular nucleus in the neuroendocrine control of sexual behavior and milk ejection in the rat. Neuroendocrinology 39:563-572.

Hardy SG, Haigler HJ, Leichnetz GR. 1983. Paralemniscal reticular formation: response of cells to a noxious stimulus. Brain Res 267:217-223.

Hashimoto H, Saito TR, Furudate S, Takahashi KW. 2001. Prolactin levels and maternal behavior induced by ultrasonic vocalizations of the rat pup. Exp Anim 50:307-312.

Haws CM, Williamson AM, Fields HL. 1989. Putative nociceptive modulatory neurons in the dorsolateral pontomesencephalic reticular formation. Brain Res 483:272-282.

Hay DL, Christopoulos G, Christopoulos A, Sexton PM. 2004. Amylin receptors: molecular composition and pharmacology. Biochem Soc Trans 32:865-867.

Henkel CK, Edwards SB. 1978. The superior colliculus control of pinna movements in the cat: possible anatomical connections. J Comp Neurol 182:763-776.

Herbert H, Klepper A, Ostwald J. 1997. Afferent and efferent connections of the ventrolateral tegmental area in the rat. Anat Embryol (Berl) 196:235-259.

Herdegen T, Leah JD. 1998. Inducible and constitutive transcription factors in the mammalian nervous system: control of gene expression by Jun, Fos and Krox, and CREB/ATF proteins. Brain Res Brain Res Rev 28:370-490.

Herman JP, Cullinan WE. 1997. Neurocircuitry of stress: central control of the hypothalamo-pituitary-adrenocortical axis. Trends Neurosci 20:78-84.

Herman JP, Tasker JG, Ziegler DR, Cullinan WE. 2002. Local circuit regulation of paraventricular nucleus stress integration: glutamate-GABA connections. Pharmacol Biochem Behav 71:457-468.

Hoare SR, Bonner TI, Usdin TB. 1999a. Comparison of rat and human parathyroid hormone 2 (PTH2) receptor activation: PTH is a low potency partial agonist at the rat PTH2 receptor. Endocrinology 140:4419-4425.

Hoare SR, de Vries G, Usdin TB. 1999b. Measurement of agonist and antagonist ligand-binding parameters at the human parathyroid hormone type 1 receptor: evaluation of receptor states and modulation by guanine nucleotide. J Pharmacol Exp Ther 289:1323-1333.

Hofer MA. 1996. Multiple regulators of ultrasonic vocalization in the infant rat. Psychoneuroendocrinology 21:203-217.

Hökfelt T, Bean A, Ceccatelli S, Dagerlind A, Elde RP, Goldstein M, Meister B, Melander T, Nicholas AP, Pelto-Huikko M, et al. 1992. Neuropeptides and classical transmitters. Localization and interaction. Arzneimittelforschung 42:196-201.

Hökfelt T, Broberger C, Xu ZQ, Sergeyev V, Ubink R, Diez M. 2000. Neuropeptides--an overview. Neuropharmacology 39:1337-1356.

Hökfelt T, Millhorn D, Seroogy K, Tsuruo Y, Ceccatelli S, Lindh B, Meister B, Melander T, Schalling M, Bartfai T, et al. 1987. Coexistence of peptides with classical neurotransmitters. Experientia 43:768-780.

Holstege G, Kuypers HG. 1982. The anatomy of brain stem pathways to the spinal cord in cat. A labeled amino acid tracing study. Prog Brain Res 57:145-175.

Hunyady B, Krempels K, Harta G, Mezey E. 1996. Immunohistochemical signal amplification by catalyzed reporter deposition and its application in double immunostaining. J Histochem Cytochem 44:1353-1362.

Hurwitz S. 1996. Homeostatic control of plasma calcium concentration. Crit Rev Biochem Mol Biol 31:41-100.

Jacoby E, Bouhelal R, Gerspacher M, Seuwen K. 2006. The 7 TM G-protein-coupled receptor target family. ChemMedChem 1:761-782.

Juss TS, Wakerley JB. 1981. Mesencephalic areas controlling pulsatile oxytocin release in the suckled rat. J Endocrinol 91:233-244.

Kim EM, Kotz CM, Welch CC, Grace MK, Billington CJ, Levine AS. 1997. Lactation decreases mRNA levels of opioid peptides in the arcuate nucleus of the rat. Brain Res 769:303-308.

Kinsley CH. 2008. The neuroplastic maternal brain. Horm Behav 54:1-4.

Knobil E, Neill JD. 2006. Knobil and Neill's Physiology of Reproduction. Academic Press, San Diego.

Kostich WA, Grzanna R, Lu NZ, Largent BL. 2004. Immunohistochemical visualization of corticotropin-releasing factor type 1 (CRF1) receptors in monkey brain. J Comp Neurol 478:111-125.

Kuo J, Usdin TB. 2007. Development of a rat parathyroid hormone 2 receptor antagonist. Peptides 28:887-892.

Kutner RH, Zhang XY, Reiser J. 2009. Production, concentration and titration of pseudotyped HIV-1-based lentiviral vectors. Nat Protoc 4:495-505.

Labouebe G, Liu S, Dias C, Zou H, Wong JC, Karunakaran S, Clee SM, Phillips AG, Boutrel B, Borgland SL. 2013. Insulin induces long-term depression of ventral tegmental area dopamine neurons via endocannabinoids. Nat Neurosci.

LaBuda CJ, Dobolyi A, Usdin TB. 2004. Tuberoinfundibular peptide of 39 residues produces anxiolytic and antidepressant actions. Neuroreport 15:881-885.

Ladyman SR, Augustine RA, Grattan DR. 2010. Hormone interactions regulating energy balance during pregnancy. J Neuroendocrinol 22:805-817.

Lamming GE. 1994. Marshall's Physiology of Reproduction, Vol. 3, Chapman & Hall, London.

Law F, Ferrari S, Rizzoli R, Bonjour JP. 1994. Parathyroid hormone-related protein: physiology and pathophysiology. Adv Nephrol Necker Hosp 23:281-294.

LeDoux JE, Farb C, Ruggiero DA. 1990. Topographic organization of neurons in the acoustic thalamus that project to the amygdala. J Neurosci 10:1043-1054.

Leffert JD, Newgard CB, Okamoto H, Milburn JL, Luskey KL. 1989. Rat amylin: cloning and tissue-specific expression in pancreatic islets. Proc Natl Acad Sci U S A 86:3127-3130.

Lehman MN, Merkley CM, Coolen LM, Goodman RL. 2010. Anatomy of the kisspeptin neural network in mammals. Brain Res 1364:90-102.

Leichnetz GR, Watkins L, Griffin G, Murfin I, Mayer DJ. 1978. The projection from the nucleus raphe magnus and other brainstem nuclei to the spinal cord in the rat: a study using the HRP blue-reaction. Neurosci Lett 8:119-124.

Leng G, Meddle SL, Douglas AJ. 2008. Oxytocin and the maternal brain. Curr Opin Pharmacol 8:731-734.

Li C, Chen P, Smith MS. 1999a. Identification of neuronal input to the arcuate nucleus (ARH) activated during lactation: implications in the activation of neuropeptide Y neurons. Brain Res 824:267-276.

Li C, Chen P, Smith MS. 1999b. Neural populations in the rat forebrain and brainstem activated by the suckling stimulus as demonstrated by cFos expression. Neuroscience 94:117-129.

Lin SH, Miyata S, Matsunaga W, Kawarabayashi T, Nakashima T, Kiyohara T. 1998. Metabolic mapping of the brain in pregnant, parturient and lactating rats using fos immunohistochemistry. Brain Res 787:226-236.

Lois C, Hong EJ, Pease S, Brown EJ, Baltimore D. 2002. Germline transmission and tissue-specific expression of transgenes delivered by lentiviral vectors. Science 295:868-872.

Lonstein JS, Simmons DA, Stern JM. 1998a. Functions of the caudal periaqueductal gray in lactating rats: kyphosis, lordosis, maternal aggression, and fearfulness. Behav Neurosci 112:1502-1518.

Lonstein JS, Simmons DA, Swann JM, Stern JM. 1998b. Forebrain expression of c-fos due to active maternal behaviour in lactating rats. Neuroscience 82:267-281.

Lutz TA. 2005. Pancreatic amylin as a centrally acting satiating hormone. Curr Drug Targets 6:181-189.

Lutz TA. 2006. Amylinergic control of food intake. Physiol Behav 89:465-471.

Lutz TA. 2010. The role of amylin in the control of energy homeostasis. Am J Physiol Regul Integr Comp Physiol 298:R1475-1484.

Lutz TA, Mollet A, Rushing PA, Riediger T, Scharrer E. 2001. The anorectic effect of a chronic peripheral infusion of amylin is abolished in area postrema/nucleus of the solitary tract (AP/NTS) lesioned rats. Int J Obes Relat Metab Disord 25:1005-1011.

Lyons DJ, Horjales-Araujo E, Broberger C. 2010. Synchronized network oscillations in rat tuberoinfundibular dopamine neurons: switch to tonic discharge by thyrotropin-releasing hormone. Neuron 65:217-229.

Ma S, Gundlach AL. 2007. Relaxin-family peptide and receptor systems in brain: insights from recent anatomical and functional studies. Adv Exp Med Biol 612:119-137.

Mai JK, Assheuer J, Paxinos G. 1997. Atlas of the human brain. Academic Press, San Diego.

Mallikarjun PK, Oyebode F. 2005. Prevention of postnatal depression. J R Soc Health 125:221-226.

Martin TJ, Moseley JM, Gillespie MT. 1991. Parathyroid hormone-related protein: biochemistry and molecular biology. Crit Rev Biochem Mol Biol 26:377-395.

Martin TJ, Moseley JM, Williams ED. 1997. Parathyroid hormone-related protein: hormone and cytokine. J Endocrinol 154 Suppl:S23-37.

Mattson BJ, Williams SE, Rosenblatt JS, Morrell JI. 2003. Preferences for cocaine- or pup-associated chambers differentiates otherwise behaviorally identical postpartum maternal rats. Psychopharmacology (Berl) 167:1-8.

McIlmoyl M. 1965. Two neurological staining techniques utlizing the dye luxol fast blue. Can J Med Technol. 27:118-123.

McNeilly AS. 2006. Suckling and the Control of Gonadotropin Secretion. In: Knobil and Neill´s Physiology of Reproduction, Neill JD, Ed, Academic Press, Oxford.

Meister B. 2007. Neurotransmitters in key neurons of the hypothalamus that regulate feeding behavior and body weight. Physiol Behav 92:263-271.

Metzner W. 1993. An audio-vocal interface in echolocating horseshoe bats. J Neurosci 13:1899-1915.

Metzner W. 1996. Anatomical basis for audio-vocal integration in echolocating horseshoe bats. J Comp Neurol 368:252-269.

Mikkelsen JD, Simonneaux V. 2009. The neuroanatomy of the kisspeptin system in the mammalian brain. Peptides 30:26-33.

Moga MM, Weis RP, Moore RY. 1995. Efferent projections of the paraventricular thalamic nucleus in the rat. J Comp Neurol 359:221-238.

Morgan HD, Watchus JA, Fleming AS. 1997. The effects of electrical stimulation of the medial preoptic area and the medial amygdala on maternal responsiveness in female rats. Ann N Y Acad Sci 807:602-605.

Morgan JI, Curran T. 1991. Stimulus-transcription coupling in the nervous system: involvement of the inducible proto-oncogenes fos and jun. Annu Rev Neurosci 14:421-451.

Muff R, Born W, Kaufmann M, Fischer JA. 1994. Parathyroid hormone and parathyroid hormone-related protein receptor update. Mol Cell Endocrinol 100:35-38.

Mulder H, Leckstrom A, Uddman R, Ekblad E, Westermark P, Sundler F. 1995. Islet amyloid polypeptide (amylin) is expressed in sensory neurons. J Neurosci 15:7625-7632.

Neumann ID. 2001. Alterations in behavioral and neuroendocrine stress coping strategies in pregnant, parturient and lactating rats. Prog Brain Res 133:143-152.

Neumann ID. 2003. Brain mechanisms underlying emotional alterations in the peripartum period in rats. Depress Anxiety 17:111-121.

Neumann ID. 2008. Brain oxytocin: a key regulator of emotional and social behaviours in both females and males. J Neuroendocrinol 20:858-865.

Neville MC. 2006. Lactation and Its Hormonal Control. In: Physiology of Reproduction, Neill JD, Ed, Academic Press, Amsterdam, pp. 2993-3054.

Numan M. 1986. The role of the medial preoptic area in the regulation of maternal behavior in the rat. Ann N Y Acad Sci 474:226-233.

Numan M. 2006. Hypothalamic neural circuits regulating maternal responsiveness toward infants. Behav Cogn Neurosci Rev 5:163-190.

Numan M, Insel TR. 2003. The Neurobiology of Parental Behavior. Springer, New York.

Numan M, Numan MJ. 1997. Projection sites of medial preoptic area and ventral bed nucleus of the stria terminalis neurons that express Fos during maternal behavior in female rats. J Neuroendocrinol 9:369-384.

Numan M, Numan MJ, Schwarz JM, Neuner CM, Flood TF, Smith CD. 2005. Medial preoptic area interactions with the nucleus accumbens-ventral pallidum circuit and maternal behavior in rats. Behav Brain Res 158:53-68.

Numan M, Sheehan TP. 1997. Neuroanatomical circuitry for mammalian maternal behavior. Ann N Y Acad Sci 807:101-125.

Numan M, Woodside B. 2010. Maternity: neural mechanisms, motivational processes, and physiological adaptations. Behav Neurosci 124:715-741.

Oakley AE, Clifton DK, Steiner RA. 2009. Kisspeptin signaling in the brain. Endocr Rev 30:713-743.

Oliver KR, Kane SA, Salvatore CA, Mallee JJ, Kinsey AM, Koblan KS, Keyvan-Fouladi N, Heavens RP, Wainwright A, Jacobson M, Dickerson IM, Hill RG. 2001. Cloning, characterization and central nervous system distribution of receptor activity modifying proteins in the rat. Eur J Neurosci 14:618-628.

Olszewski J, Baxter D. 1982. Cytoarchitecture of the Human Brain Stem. Karger, New York.

Osto M, Wielinga PY, Alder B, Walser N, Lutz TA. 2007. Modulation of the satiating effect of amylin by central ghrelin, leptin and insulin. Physiol Behav 91:566-572.

Palkovits M. 1973. Isolated removal of hypothalamic or other brain nuclei of the rat. Brain Res 59:449-450.

Palkovits M. 2003. Hypothalamic regulation of food intake. Clin Neurosci 56:288-302.

Palkovits M, Dobolyi A, Helfferich F, Usdin TB. 2004. Localization and chemical characterization of the audiogenic stress pathway. Ann N Y Acad Sci 1018:16-24.

Palkovits M, Dobolyi A, Helfferich F, Usdin TB. 2009. Acute loud noise activates TIP39-immunoreactive neurons in the rat brain. Brain Structure and Function Submitted.

Palkovits M, Harvey-White J, Liu J, Kovacs ZS, Bobest M, Lovas G, Bago AG, Kunos G. 2008. Regional distribution and effects of postmortal delay on endocannabinoid content of the human brain. Neuroscience 152:1032-1039.

Palkovits M, Usdin TB, Makara GB, Dobolyi A. 2010. Tuberoinfundibular peptide of 39 residues- immunoreactive fibers in the zona incerta and the supraoptic decussations terminate in the neuroendocrine hypothalamus. Neurochem Res 35:2078-2085.

Pan W, Kastin AJ. 2008. Urocortin and the brain. Prog Neurobiol 84:148-156.

Papez JW. 1926. Reticulo-spinal tracts in the cat. Marchi method. J Comp Neurol 41:365-399.

Paxinos G, Butcher LL. 1985. Organizational principles of the brain as revealed by choline acetyltransferase and acetylcholinesterase distribution and projections. In: The rat nervous system, Paxinos G, Ed, Vol. 1: Forebrain and Midbrain, Academic Press, Sydney, pp. 487–521.

Paxinos G, Huang X. 1995. Atlas of the human brainstem. Academic Press, Sydney.

Paxinos G, Törk I, Tecott LH, Valentino KL. 1991. Atlas of the developing rat brain. Academic Press, San Diego.

Paxinos G, Watson C. 1997. The rat brain in stereotaxic coordinates. Academic Press, Sidney.

Paxinos G, Watson C. 1998. The rat brain in stereotaxic coordinates. Academic Press, San Diego.

Paxinos G, Watson C. 2005. The rat brain in stereotaxic coordinates. Academic Press, San Diego.

Paxinos G, Watson C. 2007. The rat brain in stereotaxic coordinates. Academic Press, San Diego.

Pereira M, Morrell JI. 2009. The changing role of the medial preoptic area in the regulation of maternal behavior across the postpartum period: facilitation followed by inhibition. Behav Brain Res 205:238-248.

Pereira M, Morrell JI. 2011. Functional mapping of the neural circuitry of rat maternal motivation: effects of site-specific transient neural inactivation. J Neuroendocrinol 23:1020-1035.

Pineda R, Aguilar E, Pinilla L, Tena-Sempere M. 2011. Physiological roles of the kisspeptin/GPR54 system in the neuroendocrine control of reproduction. Prog Brain Res 181:55-77.

Piserchio A, Usdin T, Mierke DF. 2000. Structure of tuberoinfundibular peptide of 39 residues. J Biol Chem 275:27284-27290.

Potes CS, Lutz TA. 2010. Brainstem mechanisms of amylin-induced anorexia. Physiol Behav 100:511-518.

Poyner DR, Sexton PM, Marshall I, Smith DM, Quirion R, Born W, Muff R, Fischer JA, Foord SM. 2002. International Union of Pharmacology. XXXII. The mammalian calcitonin gene-related peptides, adrenomedullin, amylin, and calcitonin receptors. Pharmacol Rev 54:233-246.

Pralong FP. 2010. Insulin and NPY pathways and the control of GnRH function and puberty onset. Mol Cell Endocrinol 324:82-86.

Risold PY, Swanson LW. 1997. Connections of the rat lateral septal complex. Brain Res Brain Res Rev 24:115-195.

Rizzoli R, Ferrari SL, Pizurki L, Caverzasio J, Bonjour JP. 1992. Actions of parathyroid hormone and parathyroid hormone-related protein. J Endocrinol Invest 15:51-56.

Roger M, Arnault P. 1989. Anatomical study of the connections of the primary auditory area in the rat. J Comp Neurol 287:339-356.

Roland BL, Sutton SW, Wilson SJ, Luo L, Pyati J, Huvar R, Erlander MG, Lovenberg TW. 1999. Anatomical distribution of prolactin-releasing peptide and its receptor suggests

additional functions in the central nervous system and periphery. Endocrinology 140:5736-5745.

Rondini TA, Donato J, Jr., Rodrigues Bde C, Bittencourt JC, Elias CF. 2010. Chemical identity and connections of medial preoptic area neurons expressing melanin-concentrating hormone during lactation. J Chem Neuroanat 39:51-62.

Rosenblatt JS. 1967. Nonhormonal basis of maternal behavior in the rat. Science 156:1512-1514.

Ross G, Engel P, Abdallah Y, Kummer W, Schluter KD. 2005. Tuberoinfundibular peptide of 39 residues: a new mediator of cardiac function via nitric oxide production in the rat heart. Endocrinology 146:2221-2228.

Ross G, Heinemann MP, Schluter KD. 2007. Vasodilatory effect of tuberoinfundibular peptide (TIP39): requirement of receptor desensitization and its beneficial effect in the post-ischemic heart. Peptides 28:878-886.

Rushing PA, Hagan MM, Seeley RJ, Lutz TA, D'Alessio DA, Air EL, Woods SC. 2001. Inhibition of central amylin signaling increases food intake and body adiposity in rats. Endocrinology 142:5035.

Rushing PA, Hagan MM, Seeley RJ, Lutz TA, Woods SC. 2000. Amylin: a novel action in the brain to reduce body weight. Endocrinology 141:850-853.

Russell JA, Douglas AJ, Ingram CD. 2001. Brain preparations for maternity--adaptive changes in behavioral and neuroendocrine systems during pregnancy and lactation. An overview. Prog Brain Res 133:1-38.

Schuller G, Radtke-Schuller S. 1990. Neural control of vocalization in bats: mapping of brainstem areas with electrical microstimulation eliciting species-specific echolocation calls in the rufous horseshoe bat. Exp Brain Res 79:192-206.

Schwarz JM, Bilbo SD. 2013. Adolescent morphine exposure affects long-term microglial function and later-life relapse liability in a model of addiction. J Neurosci 33:961-971.

Seip KM, Morrell JI. 2009. Transient inactivation of the ventral tegmental area selectively disrupts the expression of conditioned place preference for pup- but not cocaine-paired contexts. Behav Neurosci 123:1325-1338.

Selmanoff M, Gregerson KA. 1986. Suckling-induced prolactin release is suppressed by naloxone and simulated by beta-endorphin. Neuroendocrinology 42:255-259.

Sexton PM, Paxinos G, Kenney MA, Wookey PJ, Beaumont K. 1994. In vitro autoradiographic localization of amylin binding sites in rat brain. Neuroscience 62:553-567.

Sheward WJ, Lutz EM, Harmar AJ. 1994. The expression of the calcitonin receptor gene in the brain and pituitary gland of the rat. Neurosci Lett 181:31-34.

Siegel HI. 1986. Hormonal basis of maternal behavior in the rat. Ann N Y Acad Sci 474:202-215.

Simerly RB, Swanson LW. 1986. The organization of neural inputs to the medial preoptic nucleus of the rat. J Comp Neurol 246:312-342.

Simerly RB, Swanson LW. 1988. Projections of the medial preoptic nucleus: a Phaseolus vulgaris leucoagglutinin anterograde tract-tracing study in the rat. J Comp Neurol 270:209-242.

Slattery DA, Neumann ID. 2008. No stress please! Mechanisms of stress hyporesponsiveness of the maternal brain. J Physiol 586:377-385.

Smith MS, Grove KL. 2002. Integration of the regulation of reproductive function and energy balance: lactation as a model. Front Neuroendocrinol 23:225-256.

Smith MS, True C, Grove KL. 2010. The neuroendocrine basis of lactation-induced suppression of GnRH: role of kisspeptin and leptin. Brain Res 1364:139-152.

Stack EC, Numan M. 2000. The temporal course of expression of c-Fos and Fos B within the medial preoptic area and other brain regions of postpartum female rats during prolonged mother--young interactions. Behav Neurosci 114:609-622.

Stern JM. 1989. Maternal Behavior: Sensory, Hormonal and Neural Determinants. In: Psychoendocrinology, Brush FR, Levine AS, Eds, Academic Press, San Diego, pp. 103-226.

Sugimura Y, Murase T, Ishizaki S, Tachikawa K, Arima H, Miura Y, Usdin TB, Oiso Y. 2003. Centrally administered tuberoinfundibular peptide of 39 residues inhibits arginine vasopressin release in conscious rats. Endocrinology 144:2791-2796.

Szabo ER, Cservenak M, Dobolyi A. 2012. Amylin is a novel neuropeptide with potential maternal functions in the rat. FASEB J 26:272-281.

Szabo FK, Snyder N, Usdin TB, Hoffman GE. 2010. A direct neuronal connection between the subparafascicular and ventrolateral arcuate nuclei in non-lactating female rats. Could this pathway play a role in the suckling-induced prolactin release? Endocrine 37:62-70.

Taber E. 1961. The cytoarchitecture of the brain stem of the cat. I. Brain stem nuclei of cat. J Comp Neurol 116:27-69.

Tavakoli-Nezhad M, Arbogast LA. 2010. Mu and kappa opioid receptor expression in the mediobasal hypothalamus and effectiveness of selective antagonists on prolactin release during lactation. Neuroscience 166:359-367.

Terenzi MG, Ingram CD. 2005. Oxytocin-induced excitation of neurones in the rat central and medial amygdaloid nuclei. Neuroscience 134:345-354.

Terkel J, Damassa DA, Sawyer CH. 1979. Ultrasonic cries from infant rats stimulate prolactin release in lactating mothers. Horm Behav 12:95-102.

Tindal JS, Knaggs GS. 1971. Determination of the detailed hypothalamic route of the milk-ejection reflex in the guinea-pig. J Endocrinol 50:135-152.

Tindal JS, Knaggs GS. 1977. Pathways in the forebrain of the rat concerned with the release of prolactin. Brain Res 119:211-221.

Tohyama M, Takatsuji K. 1998. Atlas of Neuroactive Substances and Their Receptors in the Rat. Oxford University Press, Oxford.

Topaloglu AK, Kotan LD, Yuksel B. 2010. Neurokinin B signalling in human puberty. J Neuroendocrinol 22:765-770.

Tsukamura H, Maeda K. 2001. Non-metabolic and metabolic factors causing lactational anestrus: rat models uncovering the neuroendocrine mechanism underlying the suckling-induced changes in the mother. Prog Brain Res 133:187-205.

Usdin TB. 2000. The PTH2 receptor and TIP39: a new peptide-receptor system. Trends Pharmacol Sci 21:128-130.

Usdin TB, Bonner TI, Harta G, Mezey E. 1996. Distribution of parathyroid hormone-2 receptor messenger ribonucleic acid in rat. Endocrinology 137:4285-4297.

Usdin TB, Bonner TI, Hoare SR. 2002. The parathyroid hormone 2 (PTH2) receptor. Receptors Channels 8:211-218.

Usdin TB, Dobolyi A, Ueda H, Palkovits M. 2003. Emerging functions for tuberoinfundibular peptide of 39 residues. Trends Endocrinol Metab 14:14-19.

Usdin TB, Gruber C, Bonner TI. 1995. Identification and functional expression of a receptor selectively recognizing parathyroid hormone, the PTH2 receptor. J Biol Chem 270:15455-15458.

Usdin TB, Hilton J, Vertesi T, Harta G, Segre G, Mezey E. 1999a. Distribution of the parathyroid hormone 2 receptor in rat: immunolocalization reveals expression by several endocrine cells. Endocrinology 140:3363-3371.

Usdin TB, Hoare SR, Wang T, Mezey E, Kowalak JA. 1999b. TIP39: a new neuropeptide and PTH2-receptor agonist from hypothalamus. Nat Neurosci 2:941-943.

Usdin TB, Paciga M, Riordan T, Kuo J, Parmelee A, Petukova G, Camerini-Otero RD, Mezey E. 2008. Tuberoinfundibular Peptide of 39 residues is required for germ cell development. Endocrinology 149:4292-4300.

Valenzuela DM, Murphy AJ, Frendewey D, Gale NW, Economides AN, Auerbach W, Poueymirou WT, Adams NC, Rojas J, Yasenchak J, Chernomorsky R, Boucher M, Elsasser AL, Esau L, Zheng J, Griffiths JA, Wang X, Su H, Xue Y, Dominguez MG, Noguera I, Torres R, Macdonald LE, Stewart AF, DeChiara TM, Yancopoulos GD.

2003. High-throughput engineering of the mouse genome coupled with high-resolution expression analysis. Nat Biotechnol 21:652-659.

van den Pol AN. 2012. Neuropeptide transmission in brain circuits. Neuron 76:98-115.

van Rossum D, Hanisch UK, Quirion R. 1997. Neuroanatomical localization, pharmacological characterization and functions of CGRP, related peptides and their receptors. Neurosci Biobehav Rev 21:649-678.

Varga T, Mogyorodi B, Bago AG, Cservenak M, Domokos D, Renner E, Gallatz K, Usdin TB, Palkovits M, Dobolyi A. 2012. Paralemniscal TIP39 is induced in rat dams and may participate in maternal functions. Brain Struct Funct 217:323-335.

Varga T, Palkovits M, Usdin TB, Dobolyi A. 2008. The medial paralemniscal nucleus and its afferent neuronal connections in rat. J Comp Neurol 511:221-237.

Wakerley JB, O'Neill DS, ter Haar MB. 1978. Relationship between the suckling-induced release of oxytocin and prolactin in the urethane-anaesthetized lactating rat. J Endocrinol 76:493-500.

Walker CD, Lightman SL, Steele MK, Dallman MF. 1992. Suckling is a persistent stimulus to the adrenocortical system of the rat. Endocrinology 130:115-125.

Wang J, Palkovits M, Usdin TB, Dobolyi A. 2006a. Afferent connections of the subparafascicular area in rat. Neuroscience 138:197-220.

Wang J, Palkovits M, Usdin TB, Dobolyi A. 2006b. Forebrain projections of tuberoinfundibular peptide of 39 residues (TIP39)-containing subparafascicular neurons. Neuroscience 138:1245-1263.

Wang T, Palkovits M, Rusnak M, Mezey E, Usdin TB. 2000. Distribution of parathyroid hormone-2 receptor-like immunoreactivity and messenger RNA in the rat nervous system. Neuroscience 100:629-649.

Webster WR. 1977. Central neural mechanisms of hearing. Proc Aust Physiol Pharmacol Soc 8:1-7.

Wimalawansa SJ. 1997. Amylin, calcitonin gene-related peptide, calcitonin, and adrenomedullin: a peptide superfamily. Crit Rev Neurobiol 11:167-239.

Wojcik-Gladysz A, Polkowska J. 2006. Neuropeptide Y--a neuromodulatory link between nutrition and reproduction at the central nervous system level. Reprod Biol 6 Suppl 2:21-28.

Woodside B. 2007. Prolactin and the hyperphagia of lactation. Physiol Behav 91:375-382.

Wünscher W, Shober W, Werner L. 1965. Architectonisher Atlas vom Hirnstamm der Ratte. S. Hirzel, Leipzig.

Xu J, Kirigiti MA, Grove KL, Smith MS. 2009. Regulation of food intake and gonadotropin-releasing hormone/luteinizing hormone during lactation: role of insulin and leptin. Endocrinology 150:4231-4240.

Yamada M, Shibusawa N, Ishii S, Horiguchi K, Umezawa R, Hashimoto K, Monden T, Satoh T, Hirato J, Mori M. 2006. Prolactin secretion in mice with thyrotropin-releasing hormone deficiency. Endocrinology 147:2591-2596.

Yamada S, Uenoyama Y, Kinoshita M, Iwata K, Takase K, Matsui H, Adachi S, Inoue K, Maeda KI, Tsukamura H. 2007. Inhibition of metastin (kisspeptin-54)-GPR54 signaling in the arcuate nucleus-median eminence region during lactation in rats. Endocrinology 148:2226-2232.

Yasui Y, Nakano K, Mizuno N. 1992. Descending projections from the subparafascicular thalamic nucleus to the lower brain stem in the rat. Exp Brain Res 90:508-518.

Young A. 2005. Tissue expression and secretion of amylin. Adv Pharmacol 52:19-45.

Zilles K, Wree A. 1985. Cortex: areal and laminar structure. In: The Rat Nervous System, Paxinos G, Ed, Vol. 1, Academic press, Sydney, pp. 375-415.